

# The Effect of Variability on the Estimation of Quasar Black Hole Masses

Brian C. Wilhite<sup>1,2</sup>, Robert J. Brunner<sup>1,2</sup>, Donald P. Schneider<sup>3</sup>, and Daniel E. Vanden Berk<sup>3</sup>

## ABSTRACT

We investigate the time-dependent variations of ultraviolet (UV) black hole mass estimates of quasars in the Sloan Digital Sky Survey (SDSS). From SDSS spectra of 615 high-redshift ( $1.69 < z < 4.75$ ) quasars with spectra from two epochs, we estimate black hole masses, using a single-epoch technique which employs an additional, automated night-sky-line removal, and relies on UV continuum luminosity and C IV  $\lambda 1549$  emission line dispersion. Mass estimates show variations between epochs at about the 30% level for the sample as a whole. We determine that, for our full sample, measurement error in the line dispersion likely plays a larger role than the inherent variability, in terms of contributing to variations in mass estimates between epochs. However, we use the variations in quasars with  $r$ -band spectral signal-to-noise ratio greater than 15 to estimate that the contribution to these variations from inherent variability is roughly 20%. We conclude that these differences in black hole mass estimates between epochs indicate variability is not a large contributor to the current factor of two scatter between mass estimates derived from low- and high-ionization emission lines.

*Subject headings:* galaxies: active — quasars: general — techniques: spectroscopic

## 1. Introduction

In active galactic nuclei (AGN) and quasars, it is now generally accepted that for low-ionization broad emission lines, such as  $H\beta$ , the line width is mostly controlled by gravity,

---

<sup>1</sup>The University of Illinois, Department of Astronomy, 1002 W. Green St., Urbana, IL 61801

<sup>2</sup>National Center for Supercomputing Applications, MC-257, 1205 W. Clark Street, Urbana, IL 61801

<sup>3</sup>The Pennsylvania State University, Department of Astronomy and Astrophysics, 525 Davey Lab, University Park, PA 16802

and thus closely related to the mass of the quasar central black hole (Osterbrock & Shuder 1982; Peterson & Wandel 1999, 2000; Onken & Peterson 2002; Kollatschny 2003). However, there is some debate as to the physical processes responsible for producing the observed profile of higher ionization lines, such as C IV  $\lambda 1549$ . The C IV line has been observed to be both blueshifted (see, e.g. Wilkes 1984; Richards et al. 2002b) and asymmetric (Wilkes 1984; Vanden Berk et al. 2001) hinting that physical processes other than gravity may be at least partially responsible for the C IV profile. Recently, Baskin & Laor (2005) demonstrated that, due to these differences in line profile, black hole mass estimates involving C IV line width may be less accurate than previously believed, or even biased, perhaps with systematic over or underestimates of mass by a factor of a few.

If one does assume that the width of a given quasar broad emission line can be related to the velocity of gas in orbit around the central black hole, a black hole mass can be computed via the virial equation:

$$M_{BH} = f \frac{R(\Delta v)^2}{G}, \quad (1)$$

where  $f$  is a scale factor of order unity that depends on the geometry of the broad line region (BLR),  $R$  is the distance from the black hole to the specific portion of the BLR which contains the emitting gas in question (a distance which likely differs for each species), and  $\Delta v$  is the velocity width of the broad emission line itself. While line width is easily determined from a single-epoch spectrum, determining the BLR size is less straightforward. Reverberation mapping techniques have proven very successful in estimating BLR sizes, and by extension, determining the masses of the black holes at the centers of a few dozen active galactic nuclei (e.g., Wandel, Peterson, & Malkan 1999; Peterson et al. 2004). These radii are found by measuring the response time of variations in emission line flux to changes in continuum flux. Though simple in principle, measuring these response times requires constant spectral monitoring, and is observationally taxing. However, Wandel, Peterson, & Malkan (1999) and Kaspi et al. (2000), and later Kaspi et al. (2005), demonstrated that a simple scaling relationship exists between BLR size and continuum luminosity ( $R \propto L^\alpha$ ). Kaspi et al. (2005) determined that the size of the H $\beta$  BLR scales with both optical and UV continua, allowing for the use of continuum luminosity in both of these wavelength ranges as a proxy for BLR size and paving the way for reliable, single-epoch black hole mass estimates.

Single-epoch estimates have been calibrated using the H $\beta$  (Wandel, Peterson, & Malkan 1999) and Mg II  $\lambda 2798$  (McLure & Jarvis 2002) emission lines. Vestergaard (2002) developed a method of estimating black hole masses derived from C IV FWHM and  $\lambda L_\lambda(1350 \text{ \AA})$  (abbreviated  $L_{1350}$ ), calibrated by the corresponding reverberation-mapping masses, utilizing the scaling relationship determined by Kaspi et al. (2000). Namely,  $R_{CIV} \propto L_{1350}^{0.70}$ .

More recently, Peterson et al. (2004) reanalyzed a large amount of reverberation mapping data, removing lower-quality data and re-establishing the scaling relationships used for calibration of single-epoch mass estimates. Subsequently, Kaspi et al. (2005) used these revised relationships to update the BLR size-continuum luminosity relationships, and Bentz et al. (2006) made additional corrections after correcting for luminosity contributions from host galaxies’ starlight. These developments led to a re-calibration of UV black hole masses in Vestergaard & Peterson (2006), who utilized an empirically determined radius-luminosity relationship more consistent with photoionization theory:  $R_{\text{CIV}} \propto L_{1350}^{0.53}$ . Early results of a monitoring campaign to apply reverberation mapping to  $z \sim 3$  quasars indicate that, over 7 orders of magnitude in luminosity, the C IV BLR size-UV luminosity relationship has a slope similar to that of the H $\beta$  BLR size-UV luminosity relationship (Kaspi et al. 2007), confirming the assumptions made by Vestergaard & Peterson (2006).

Additionally, Vestergaard & Peterson (2006) calibrated an estimate for black hole mass which relies upon the dispersion of the C IV line ( $\sigma_{\text{CIV}}$ , the second moment about the mean), and the luminosity density at 1450Å:

$$\log M_{\text{BH}}(\text{C IV}) = \log \left[ \left( \frac{\sigma_{\text{CIV}}}{1000 \text{ km s}^{-1}} \right)^2 \left( \frac{\lambda L_{\lambda}(1450\text{\AA})}{10^{44} \text{ erg s}^{-1}} \right)^{0.53} \right] + (6.73 \pm 0.01). \quad (2)$$

Based on comparisons with reverberation mapping masses, Vestergaard & Peterson (2006) state that these masses are likely good to within a factor of 3.

One potential problem in estimating black hole masses from single-epoch spectra is the inherent variability of quasars. This variability is key to reverberation mapping techniques, but will necessarily inject uncertainties into single-epoch mass estimates. The optical and ultraviolet portions of quasar continua have long been known to vary in luminosity on the order of 10% – 20% on time scales from weeks to years (e.g., Smith & Hoeffleit 1963; Uomoto, Wills, & Wills 1976; Hook, McMahon, Boyle, & Irwin 1994; Giveon et al. 1999; de Vries, Becker, 2003). Vanden Berk et al. (2004), using a sample of  $\sim 25000$  quasars, confirmed known correlations, and parameterized relationships, between variability and rest-frame time lag, luminosity, rest-frame wavelength and redshift. Additionally, Wilhite et al. (2005, hereafter Paper I) completed the first study of the detailed dependence of variability upon wavelength, demonstrating that that variability increased with decreasing wavelength, but only at wavelengths less than 2500Å. Increased variability at shorter wavelengths, such as that seen in Paper I, and earlier (e.g., Cutri et al. 1985; Collier et al. 2001; Vanden Berk et al. 2004), can impact black hole mass estimates that rely on rest-frame UV luminosity.

In addition, the fluxes and profiles of quasar emission lines are known to vary with

time (e.g., Peterson 1993; Wanders & Peterson 1996; Wandel, Peterson, & Malkan 1999; Sergeev et al. 2001), mostly in response to fluctuations in continuum luminosity. C IV has been closely monitored in a relatively small number of low-redshift, low-luminosity objects like NGC 5548 (Clavel et al. 1991; Korista et al. 1995) and NGC 4151 (Crenshaw et al. 1996), as well as in a few high-redshift quasars (Kaspi et al. 2007). Recently, Wilhite et al. (2006, hereafter Paper II) studied C IV variability in an ensemble of  $\sim 100$  SDSS quasars with multiple-epoch spectroscopy, finding that the width of an individual C IV line increases with line flux, and varies by as much as 30%, on rest-frame time scales of weeks to months. Paper I focused on the variability of the quasar continuum, while Paper II centered on variability of the C IV line. Given the interest in black hole mass estimates, we feel there is a definite need to re-examine UV variability in the context of mass estimators, and to attempt to quantify the effect (or lack thereof) of variability on determining black hole masses.

We briefly describe the quasar sample and the additional, necessary spectrophotometric calibrations in §2. We describe the process used to estimate black hole masses, including the continuum- and line-fitting techniques used, in §3. The epoch-to-epoch black hole mass estimate differences are examined in §4. The results are discussed in §5, and we conclude in §6.

For consistency with Papers I and II, we assume a flat, cosmological-constant-dominated cosmology with parameter values  $\Omega_\Lambda = 0.7$ ,  $\Omega_M = 0.3$ , and  $H_0 = 70 \text{ km s}^{-1} \text{ Mpc}^{-1}$  to calculate luminosity distances. Though these parameter values differ slightly from recent measurements (e.g., Spergel et al. 2007), this should have little effect on results, as we are chiefly concerned with the effect of variability between epochs.

## 2. The Quasar Dataset

### 2.1. The Sloan Digital Sky Survey

The Sloan Digital Sky Survey (York et al. 2000), using a dedicated 2.5-meter telescope (Gunn et al. 2006) at the Apache Point Observatory in the Sacramento Mountains of New Mexico, has, through Summer 2005, acquired imaging and spectroscopic data for  $\sim 8000 \text{ deg}^2$ , mostly centered on the Northern Galactic Cap. A 54-chip drift-scan camera (Gunn et al. 1998) acquires imaging data which are reduced and calibrated by using the astrometric (Pier et al. 2003) and photometric (Lupton et al. 2001) software pipelines. The photometric system is normalized such that SDSS  $u, g, r, i$  and  $z$  magnitudes (Fukugita et al. 1996) are on the AB system (Smith et al. 2002). A 0.5-meter telescope monitors site photometric quality and extinction (Hogg, Finkbeiner, Schlegel, & Gunn 2001; Ivezić et al. 2004; Tucker et al.

2006).

After image processing, selected objects are targeted for spectroscopy (Strauss et al. 2002; Eisenstein et al. 2001; Richards et al. 2002a; Stoughton et al. 2002) and grouped in 3-degree diameter tiles (Blanton et al. 2003). For each tile, an aluminum plate is drilled with 640 holes reserved for roughly 500 galaxies, 50 quasars and 50 stars (40 calibration spectra—32 sky fibers and 8 reddening standards—are also taken with each plate). Plates are placed in the imaging plane of the telescope and the holes plugged with optical fibers running from the telescope to twin spectrographs.

SDSS spectra are obtained in three or four consecutive 15-minute observations and cover the observer-frame optical and near infrared, from 3900Å–9100Å. The `Spectro2d` pipeline flat-fields and flux calibrates spectra, and `Spectro1d` identifies spectral features and classifies objects by spectral type (Stoughton et al. 2002). Extragalactic objects with broad emission lines ( $\text{FWHM} \gtrsim 1000 \text{km s}^{-1}$ ) are defined to be quasars.

As we are interested in variations in spectroscopic mass-estimation techniques, we focus here on those quasars that have multiple spectroscopic observations. Through June 2004, objects on 181 different plates had been observed at least twice, with time lags between observations ranging from days to years. Fifty-three of these plates (containing roughly 2200 quasars) have observations more than 50 days apart, indicating that spectra from these observations have not been co-added and are, therefore, appropriate for variability studies (see Paper I for a lengthier discussion of these data). 52 of these 53 plate pairs are contained in the Fourth Data Release (DR4; Adelman-McCarthy et al. 2006).

## 2.2. Refinement of Spectroscopic Calibration

It was demonstrated in both Vanden Berk et al. (2004) and Paper I that additional spectrophotometric calibration beyond the standard SDSS processing is required for variability studies. Paper I contains a complete discussion of those calibration methods; we briefly summarize the salient points here. The `Spectro1d` pipeline determines three signal-to-noise (S/N) ratios for each spectrum by calculating the median S/N ratio per pixel in the sections of the spectrum corresponding to the SDSS  $g$ ,  $r$  and  $i$  filter transmission curves. Hereafter, we use the phrase “high-S/N epoch” to refer to the observation with the higher median  $r$ -band signal-to-noise ratio and “low-S/N epoch” to refer to the observation with the lower median  $r$ -band signal-to-noise ratio. Although most objects follow the plate-wide trend, this does not address the relative S/N values for any given individual object, nor does it correspond to an object’s relative line or continuum flux at a given epoch. The stars on a plate are used to

resolve calibration differences between the high- and low-S/N epochs, under the assumption that the majority of stars are non-variable (obviously variable stars are removed from this re-calibration). For each pair of observations, we create a re-calibration spectrum, equal to the ratio of the median stellar high-S/N epoch flux to the median stellar low-S/N flux, as a function of wavelength. This re-calibration spectrum is fitted with a 5th-order polynomial to preserve real wavelength dependences, but remove pixel-to-pixel noise (see Figure 5 of Paper I), leaving a smooth, relatively featureless curve as a function of wavelength. All low-S/N epoch spectra are rescaled by this “correction” spectrum.

In Papers I and II, we studied only those objects that had been shown to vary significantly between epochs. Here we measure C IV line width, and estimate the central black hole mass, for all objects in which the entire C IV line and the 1450Å luminosity are observed. (As discussed in § 3.3, this corresponds to objects with  $1.69 < z < 4.75$ .) Out of the main sample of 2210 quasars, 702 are at a redshift where C IV measurements can be made in the SDSS spectra. Of these, 87 (13%) are noted in ? for showing evidence of broad absorption near the C IV emission line. Because of the difficulties broad absorption lines (BALs) can create in estimating the continuum flux and fitting the C IV emission line these BAL quasars are removed, leaving 615 objects to comprise the main sample studied below. Table 1 gives a summary of the observations used in this paper, including the names and redshifts of the quasars observed, as well as the Modified Julian Dates (MJDs) and signal-to-noise ratios of the individual observations.

The distributions of the  $r$ -band spectral signal-to-noise ratio at both epochs are shown as histograms in Figure 1. The mean  $S/N_r$  at the high-S/N epoch ( $S/N_{r,\text{HSN}}$ ) is 12.0, while the mean  $S/N_{r,\text{LSN}} = 9.9$ .

Figure 2 shows  $S/N_{r,\text{HSN}}$  versus  $S/N_{r,\text{LSN}}$ . As mentioned above, “high-S/N” or “low-S/N” epoch is a plate-wide designation; thus a few individual objects actually have greater  $S/N_{r,\text{LSN}}$  than  $S/N_{r,\text{HSN}}$ . For the vast majority of objects, however  $S/N_{r,\text{HSN}} > S/N_{r,\text{LSN}}$ . In addition, most objects have  $S/N_r$  at the two epochs such that they lie near the line  $S/N_{r,\text{HSN}} = S/N_{r,\text{LSN}}$ . Therefore, when examining the effects of spectral signal-to-noise ratio upon variations in black hole mass estimates between epochs, we will rely upon  $S/N_{r,\text{HSN}}$ .

### 2.3. Sample Spectra

Figure 3 shows observed-frame spectra at both epochs for three quasars from the sample to demonstrate how spectral  $r$ -band signal-to-noise ratio relates to overall spectral quality. These three quasars, SDSS J150104.94–010727.9 (Quasar 149 in Table 1;  $S/N_{r,\text{HSN}}=4.9$ ),

SDSS J101416.97+484816.1 (Quasar 551;  $S/N_{r,\text{HSN}}=12.1$ ) and SDSS J 030449.86–000813.4 (Quasar 259;  $S/N_{r,\text{HSN}}=30.8$ ) were chosen to represent a range of  $S/N_{r,\text{HSN}}$  values. Only the region of the spectrum used in the estimation of black hole mass (corresponding to the rest-frame interval [1440Å,1710Å]; see §3) is shown.

### 3. Calculating Black Hole Mass Estimates

This paper uses the Vestergaard & Peterson (2006) UV black hole mass estimator, seen in Equation 2, which requires measuring the continuum flux at a wavelength blueward of the C IV line, as well as the dispersion of the C IV line itself. The measurements of these two quantities are described below.

#### 3.1. Sky Subtraction

It was determined in Paper II that occasional errors in the SDSS night-sky removal pipeline could lead to errors in continuum and line fitting. In a small fraction (less than 5%) of objects, night sky lines are significantly under- or over-subtracted. In Paper II, spectra were visually inspected for signs of poor night sky subtraction. For this work, with over 600 C IV emission lines to fit (and for future work with larger samples of SDSS quasars), night sky subtraction has been automated. The night sky lines for which the algorithm searches are OI  $\lambda 5577$ , Na  $\lambda 5890$ , OI  $\lambda 6300$  and the well-known atmospheric O<sub>2</sub> Fraunhofer A and B bands (covering the [7594Å, 7621Å] and [6867Å, 6884Å] intervals, respectively). If any of these known night sky lines lies in the part of the spectrum corresponding to the rest-frame interval [1440Å, 1700Å] (the interval used to measure continuum luminosity and line dispersion; see §§3.2–3.3), the algorithm tests to ensure that the pipeline night sky subtraction was done properly. The average flux in a 10Å region centered on the night sky line position (37Å and 27Å regions are used for the wider A and B bands, respectively) is compared to the average flux of the 25Å range on either side of the 10Å region. If the night sky region flux is more than 3 standard deviations larger or smaller than the average flux of the surrounding region, then the flux in the night sky region is estimated using a linear interpolation based upon the pixels in the surrounding continuum region. If the 25Å range overlaps with the C IV emission line (corresponding to the rest-frame interval [1496Å, 1596Å]), the region is truncated to include only known continuum flux. The flux density uncertainties in the individual pixels are not altered, however. This may lead to a slight overestimation of the errors in the given quantities, but it not likely to have a large effect.

### 3.2. 1450Å Continuum Luminosity

After the night sky subtraction errors have been corrected, the 1450Å flux density,  $f_{\lambda}(1450)$ , is calculated by taking the mean of the flux density in the pixels corresponding to the rest-frame interval [1445Å, 1455Å]. This is translated to a luminosity density by calculating the luminosity distance analytically from the redshift, and then to luminosity by multiplying by wavelength:  $L_{1450} = 1450\text{Å} \times L_{\lambda}(1450)$ . Figure 4 shows the distribution of 1450Å luminosities,  $L_{1450}$  at both epochs. Values for  $L_{1450}$  range from 10 to roughly  $500 \times 10^{44} \text{ erg s}^{-1}$ , with a median at the high-S/N epoch of  $93.1 \times 10^{44} \text{ erg s}^{-1}$  and  $92.6 \times 10^{44} \text{ erg s}^{-1}$  at the low-S/N epoch.

The distribution of estimated uncertainties in  $L_{1450}$ , calculated through standard error propagation, with the standard deviation in flux in the [1445Å, 1455Å] interval used as the uncertainty in  $f_{\lambda}(1450)$ , is shown for both epochs in Figure 4. These uncertainties are roughly an order of magnitude smaller than the luminosities themselves, with a median of  $11.6 \times 10^{44} \text{ erg s}^{-1}$  at the high-S/N epoch and  $13.9 \times 10^{44} \text{ erg s}^{-1}$  at the low-S/N epoch.

### 3.3. C IV Line Dispersion

The dispersion of the C IV line is calculated in the same manner as in Paper II. We briefly describe that procedure here; for a full description, see §3 of that paper.

To avoid contamination from unidentified emission just redward of the C IV emission line (see, e.g., Wilkes 1984; Boyle 1990; Laor et al. 1994; Vanden Berk et al. 2001), as well as known emission from He II, O III], Al II] and Fe II, the red side of the continuum is fit over the rest-frame interval [1685Å, 1700Å]. The blue continuum is fit over the interval [1472Å, 1487Å]. Then, using all pixels corresponding to either of these wavelength ranges, the continuum is fit with a linear least squares algorithm (POLY\_FIT in IDL). Once the fit has been performed, the continuum fit is subtracted from the entire region of interest.

To measure the line profile, we integrate over the interval [1496Å, 1596Å]. This allows us to exclude potentially contaminating flux blueward of the line profile. For reasons of stability, we opt to use the line median, rather than the mean, in measuring the line center, as the mean is too easily affected by noisy pixels in the line wings. The median is simply the midpoint of the line flux, the wavelength which evenly divides the continuum-subtracted flux in the line profile.

We then calculate the line profile dispersion, the second moment about the median wavelength:



$$\sigma^2 = \frac{\int_{\text{CIV}} (\lambda - \lambda_{\text{median}})^2 F_\lambda d\lambda}{\int_{\text{CIV}} F_\lambda d\lambda}, \quad (3)$$

where C IV in the integrals simply means we are integrating over the [1496Å, 1596Å] interval containing the entire line profile. Line widths range from 1000 to 5000 km s<sup>-1</sup>, with median values of 3541 km s<sup>-1</sup> and 3531 km s<sup>-1</sup> at the high- and low-S/N epochs, respectively. A histogram of measured line widths for both epochs is shown in Figure 5.

To determine the uncertainties in these quantities, we use a Monte Carlo method. Noise is added to each pixel in the region of interest by assigning a random number drawn from a Gaussian distribution with mean equal to the measured flux in that pixel and standard deviation equal to the measured error in that pixel. The continuum is fit, and the line median and standard deviation calculated; this is done 1000 times per quasar. The standard deviation of the distribution of resulting values is assigned to be the error in that quantity. The uncertainties in the line width (as seen in Figure 5) are, for the most part, less than 500 km s<sup>-1</sup>, with a median uncertainty of 159 km s<sup>-1</sup> at the high-S/N epoch and 202 km s<sup>-1</sup> at the low-S/N epoch—like with L<sub>1450</sub>, the uncertainties are roughly an order of magnitude lower than the values themselves.

### 3.4. Single-Epoch Mass Estimates

Once the continuum luminosity (L<sub>1450</sub>) and emission line dispersion ( $\sigma_{\text{CIV}}$ ) have been calculated, it is straightforward to estimate the quasar’s black hole mass from Equation 2. This is done at both the high- and low-S/N epochs for all 615 objects in the main sample. The distributions of high- and low-S/N-epoch black hole masses are shown in Figure 6. The majority of objects are estimated to have high-S/N black hole masses in the range from 10<sup>8.5</sup> M<sub>⊙</sub> to 10<sup>9.5</sup> M<sub>⊙</sub>. The median high-S/N and low-S/N-epoch masses are 10<sup>8.88</sup> M<sub>⊙</sub> and 10<sup>8.87</sup> M<sub>⊙</sub>, respectively. The distributions of uncertainties in M<sub>BH</sub> (calculated by propagating measurement errors in L<sub>1450</sub> and  $\sigma_{\text{CIV}}$ ) at each epoch are shown in Figure 6. The median uncertainty at the high-S/N epoch is 10<sup>7.97</sup> M<sub>⊙</sub>; at the low-S/N epoch it is 10<sup>8.04</sup> M<sub>⊙</sub>.

Figure 7 shows the fractional uncertainty in L<sub>1450</sub>,  $\sigma_{\text{CIV}}$ , and M<sub>BH</sub> as a function of S/N<sub>r</sub> at the high-S/N epoch. (The low-S/N versions of these plots are very similar and, therefore, not shown.) The uncertainty in the 1450Å luminosity appears to dominate the M<sub>BH</sub> measurement error. It should also be noted that for virtually all quasars with a signal-to-noise ratio greater than 15, our estimate of the measurement uncertainty for M<sub>BH</sub> is less than 10%.

Table 2 contains the relevant quantities in the estimation of black hole mass at both epochs, including the masses themselves, and the measured luminosities and line dispersions.

## 4. Measuring the Consistency of Estimates of $M_{BH}$

### 4.1. Variations in Luminosity and Line Dispersion

Figure 8 shows the high-S/N epoch values versus low-S/N epoch values for 1450Å luminosity and C IV. The width of these distributions is due to a combination of the intrinsic variability of the quasars and the uncertainty in the measurement of those quantities.

To measure the relative change in a quantity, we will use the fractional change with respect to the average over the two epochs observed. The fractional change in 1450Å luminosity is given by Equation 4:

$$\Delta L_{1450} = 2(L_{1450,HSN} - L_{1450,LSN}) / (L_{1450,HSN} + L_{1450,LSN}) \quad (4)$$

$\Delta\sigma_{CIV}$  and  $\Delta M_{BH}$  are defined similarly.

The two panels of Figure 9 show the distribution of values of  $\Delta L_{1450}$  and  $\Delta\sigma_{CIV}$ . The sample standard deviation for the  $\Delta L_{1450}$  distribution is 0.161, corresponding to a change in continuum luminosity of roughly 16% between epochs. The sample standard deviation of the  $\sigma_{CIV}$  distribution is 0.108, which corresponds to a change in line width of  $\sim 11\%$  between epochs. It should come as no surprise that the continuum luminosity exhibits larger variations between epochs than the line dispersion. Much of this variation is due to the intrinsic variability of the quasars themselves, and it is well known that quasars' continua are more variable than their emission lines (see, e.g., Paper I, Figure 13).

Figure 10 shows the fractional changes in  $L_{1450}$  and  $\sigma_{CIV}$  as a function of high-S/N epoch signal-to-noise ratio. The average variations are clearly, and unsurprisingly, larger for quasars with low spectral signal-to-noise ratios ( $S/N_{r,HSN} \lesssim 15$ ) than for quasars with high values ( $(S/N_{r,HSN} \gtrsim 15)$ ). However, the variations are nonzero for quasars with the highest spectral signal-to-noise ratios, an indication that intrinsic variability does play a role in these variations.

The fractional changes in continuum luminosity and C IV line dispersion are shown as a function of rest-frame time lag between epochs ( $\Delta\tau$ ) in Figure 11. To test the role of variability in these, we divide the quasars into two bins in  $\Delta\tau$ , as suggested by the distribution of observations in Figure 11: one bin for quasars with  $\Delta\tau < 50$  days, and another for quasars with  $\Delta\tau > 50$  days. In intrinsically time-variable populations, one would expect the variations in these quantities to show a time dependence, as seen in structure functions (di Clemente et al. 1996; de Vries et al. 2005).  $\Delta L_{1450}$  shows such a dependence. The mean  $\Delta L_{1450}$  in the low- $\Delta\tau$  bin is 0.11; in the high- $\Delta\tau$  bin, it is 0.18. However there is no such dependence for  $\Delta\sigma_{CIV}$ . The mean values of  $\Delta\sigma_{CIV}$  are 0.099 and 0.092 for the low- and

high- $\Delta\tau$  bins, respectively.

This indicates that the intrinsic variability of the quasars themselves plays a larger role in the variations seen in  $L_{1450}$  than in those seen in  $\sigma_{CIV}$ . The fact that there appears to be little difference in the size of the  $\sigma_{CIV}$  variations between the low- $\Delta\tau$  and high- $\Delta\tau$  bins indicates that these variations are likely dominated by measurement uncertainty, not by intrinsic variability in the width of these lines. This also suggests that the measurement errors quoted in §3.3 and Table 2 may be underestimated.

#### 4.2. Variations in Estimated Black Hole Mass

The estimate for black hole masses at the high-S/N epoch is plotted against the mass estimate from the low-S/N epoch in Figure 12. Most quasars do lie near the  $M_{BH,HSN} = M_{BH,LSN}$  line, indicating good general agreement in estimated mass measurements between the two epochs.

Figure 13 shows the distribution in fractional change in the estimate of black hole mass between epochs,  $\Delta M_{BH}$ . The standard deviation is 0.301, corresponding to a roughly 30% change in the estimate between epochs. This scatter represents total inter-epoch variation in the mass estimate, due to variations in either  $L_{1450}$ ,  $\sigma_{CIV}$ , or both. Some of this change is simply due to random error in the measurements. The rest of this scatter is due to the intrinsic variability of the quasars’ luminosities and line dispersions between epochs.

Figure 15 shows the fractional change in estimated black hole mass as a function of the fractional change in luminosity and  $\sigma_{CIV}$  line dispersion. Here it is quite clear that the line dispersion variations dominate the variations in black hole mass. This obviously follows from Equation 2, as the mass estimate is more strongly dependent on line dispersion than continuum luminosity. In fact, there appears to be a roughly linear relationship, with a slope of roughly 2, equal to the exponent for  $\sigma_{CIV}$ . However, it did not have to be the case that the line dispersion dominates the variations in black hole mass—if the variations in luminosity were much larger than those of the line dispersion, then Figure 15 might look quite different.

In fact, given that the time delays between observations for our sample are only of the order of weeks or months in the quasars’ rest frames, one would expect that the continuum luminosity variations would play a larger role in samples with longer time baselines, as structure function studies (di Clemente et al. 1996; de Vries et al. 2005) demonstrate that longer time baselines lead to larger average variations between observations.

For now, we adopt  $\sim 30\%$  as the contribution of inter-epoch variations to the uncer-

tainty in the estimation of black hole masses from SDSS spectra, using the  $\sigma_{\text{CIV}}$  line and nearby continuum. Given the apparent dominance of measurement uncertainty in the inter-epoch variations in the measured line dispersion, and the line dispersion’s dominance of the variations in black hole mass estimate, it is not clear that we are able to set a lower limit on the effect of variability that lies below 30%.

Figure 14 shows the fractional change in  $M_{\text{BH}}$  as a function of the  $r$ -band spectral signal-to-noise ratio. As was the case with  $\Delta L_{1450}$  and  $\Delta\sigma_{\text{CIV}}$ , the width of the  $\Delta M_{\text{BH}}$  distribution decreases with increasing  $S/N_{r,\text{HSN}}$ . However, though the distribution narrows, it does not appear to be approaching zero width.

Though some of the scatter is a result of measurement uncertainties, the width of the  $\Delta M_{\text{BH}}$  distribution for high ( $S/N_{r,\text{HSN}} > 15$ ) signal-to-noise ratio objects does give some sense for the magnitude of the variations due to inherent quasar variability. Thus, though it is only a rough estimate, we adopt the standard deviation of the  $\Delta M_{\text{BH}}$  distribution as a rough estimate for the size of the inter-epoch variations in estimated back hole mass. For the 148 quasars with  $S/N_{r,\text{HSN}} > 15$ , the standard deviation is 0.219, corresponding to a roughly 20% change. This is decidedly larger than the  $M_{\text{BH}}$  measurement uncertainty of less than 10% for virtually all quasars, as seen in Figure 7 and discussed in § 3.4

## 5. Discussion

Mass estimates of objects in the main sample are consistent between epochs at the 30% level. Given that the mass estimate is a function of the line width squared, but only the square root of the luminosity, it should not come as a surprise that the the variations in mass estimates are more strongly dependent on  $\Delta\sigma_{\text{CIV}}$  than on  $\Delta L_{1450}$ .

Even with the re-calibrated UV black hole masses, Vestergaard & Peterson (2006) find a scatter of a factor of about 2 between the UV and optical mass estimates. Variability of the quasar continuum luminosity and line width was thought to be a possible source for this scatter. However, this scatter is much larger than the differences in mass estimates seen between epochs in either our full sample or the quasars with signal-to-noise ratio greater than 15. This suggests that variability is not a likely cause for the majority of this scatter.

That said, if improvements in UV techniques are possible, variability will set an ultimate limit on the precision of these techniques; it is unlikely that any estimate that relies solely on the C IV emission line could do better than the 20% uncertainty in  $M_{\text{BH}}$  that comes solely from the inherent variability of the continuum luminosity and C IV line dispersion, as suggested by those quasars with  $S/N_{r,\text{HSN}} > 15$ .

## 6. Conclusions

We have explored the effect of continuum and C IV emission line variability on single-epoch estimators of quasar black hole mass.

1) Quasar black hole mass estimates determined from SDSS spectra of the rest-frame ultraviolet show inter-epoch variations at the 30% level, due to the combination of the intrinsic variability of quasars and uncertainty in the measurement of continuum luminosity and C IV emission line width.

2) For our full sample, measurement error and inherent quasar variability contribute roughly equally to the inconsistencies between epochs in the estimation of  $M_{\text{BH}}$ .

3) The  $\sim 20\%$  uncertainty in  $M_{\text{BH}}$  due to inherent variability, as suggested by the quasars with  $S/N_{r,\text{HSN}} > 15$ , sets a lower limit on the reproducibility of future UV black hole mass estimates.

4) Current UV black hole mass estimates for high-redshift quasars are believed to only be accurate to a factor of two, based on correlations seen with low-ionization-line mass estimates, but the smaller scatter seen here between epochs (30% for the full sample) seems to indicate that much of this scatter is yet to be understood.

B.C.W. and R.J.B. would like to acknowledge support from NASA through grants NAG5-12578 and NAG5-12580, as well as support through the NSF PACI Project. The authors made extensive use of the storage and computing facilities at the National Center for Supercomputing Applications and would like to thank the technical staff for their assistance in enabling this work.

Funding for the SDSS and SDSS-II has been provided by the Alfred P. Sloan Foundation, the Participating Institutions, the National Science Foundation, the U.S. Department of Energy, the National Aeronautics and Space Administration, the Japanese Monbukagakusho, the Max Planck Society, and the Higher Education Funding Council for England. The SDSS Web Site is <http://www.sdss.org/>.

The SDSS is managed by the Astrophysical Research Consortium for the Participating Institutions. The Participating Institutions are the American Museum of Natural History, Astrophysical Institute Potsdam, University of Basel, Cambridge University, Case Western Reserve University, University of Chicago, Drexel University, Fermilab, the Institute for Advanced Study, the Japan Participation Group, Johns Hopkins University, the Joint Institute for Nuclear Astrophysics, the Kavli Institute for Particle Astrophysics and Cosmology, the Korean Scientist Group, the Chinese Academy of Sciences (LAMOST), Los Alamos National Laboratory, the Max-Planck-Institute for Astronomy (MPIA), the Max-Planck-Institute for

Astrophysics (MPA), New Mexico State University, Ohio State University, University of Pittsburgh, University of Portsmouth, Princeton University, the United States Naval Observatory, and the University of Washington.

## REFERENCES

- Adelman-McCarthy, J. K., et al. 2006, *ApJS*, 162, 38
- Baskin, A., & Laor, A. 2005, *MNRAS*, 356, 1029
- Bentz, M. C., Peterson, B. M., Pogge, R. W., Vestergaard, M., & Onken, C. A. 2006, *ApJ*, 644, 133
- Blanton, M. R., Lin, H., Lupton, R. H., Maley, F. M., Young, N., Zehavi, I., & Loveday, J. 2003, *AJ*, 125, 2276
- Boyle, B. J. 1990, *MNRAS*, 243, 231
- Cannon, R. D., Penston, M. V., & Brett, R. A. 1971, *MNRAS*, 152, 79
- Clavel, J., et al. 1991, *ApJ*, 366, 64
- Collier, S., et al. 2001, *ApJ*, 561, 146
- Crenshaw, D. M., et al. 1996, *ApJ*, 470, 322
- Cristiani, S., Trentini, S., La Franca, F., & Andreani, P. 1997, *A&A*, 321, 123
- Cutri, R. M., Wisniewski, W. Z., Rieke, G. H., & Lebofsky, M. J. 1985, *ApJ*, 296, 423
- de Vries, W. H., Becker, R. H., & White, R. L. 2003, *AJ*, 126, 1217
- de Vries, W. H., Becker, R. H., White, R. L., & Loomis, C. 2005, *AJ*, 129, 615
- di Clemente, A., Giallongo, E., Natali, G., Trevese, D., & Vagnetti, F. 1996, *ApJ*, 463, 466
- Eisenstein, D. J. et al. 2001, *AJ*, 122, 2267
- Espey, B. R., Carswell, R. F., Bailey, J. A., Smith, M. G., & Ward, M. J. 1989, *ApJ*, 342, 666
- Ferrarese, L., Pogge, R. W., Peterson, B. M., Merritt, D., Wandel, A., & Joseph, C. L. 2001, *ApJ*, 555, L79

- Fukugita, M., Ichikawa, T., Gunn, J. E., Doi, M., Shimasaku, K., & Schneider, D. P. 1996, *AJ*, 111, 1748
- Gebhardt, K., et al. 2000, *ApJ*, 543, L5
- Giveon, U., Maoz, D., Kaspi, S., Netzer, H., & Smith, P. S. 1999, *MNRAS*, 306, 637
- Gunn, J. E. et al. 1998, *AJ*, 116, 3040
- Gunn, J. E., et al. 2006, *AJ*, 131, 2332
- Hawkins, M. R. S. 2002, *MNRAS*, 329, 76
- Helfand, D. J., Stone, R. P. S., Willman, B., White, R. L., Becker, R. H., Price, T., Gregg, M. D., & McMahon, R. G. 2001, *AJ*, 121, 1872
- Hogg, D. W., Finkbeiner, D. P., Schlegel, D. J., & Gunn, J. E. 2001, *AJ*, 122, 2129
- Hook, I. M., McMahon, R. G., Boyle, B. J., & Irwin, M. J. 1994, *MNRAS*, 268, 305
- Ivezić, Z., et al. 2004, *AGN Physics with the Sloan Digital Sky Survey*, Proceedings of a conference held in Princeton, NJ, USA, 27-31 July 2003, Edited by Gordon T. Richards and Patrick B. Hall, ASP Conference Series, Volume 311. San Francisco: Astronomical Society of the Pacific, 2004., p.437, 437
- Jester, S. 2005, *ApJ*, 625, 667
- Kaspi, S., Smith, P. S., Netzer, H., Maoz, D., Jannuzi, B. T., & Giveon, U. 2000, *ApJ*, 533, 631
- Kaspi, S., Maoz, D., Netzer, H., Peterson, B. M., Vestergaard, M., & Jannuzi, B. T. 2005, *ApJ*, 629, 61
- Kaspi, S., Brandt, W. N., Maoz, D., Netzer, H., Schneider, D. P., & Shemmer, O. 2007, *ApJ*, 659, 997
- Kollatschny, W. 2003, *A&A*, 407, 461
- Korista, K. T., et al. 1995, *ApJS*, 97, 285
- Laor, A., Bahcall, J. N., Jannuzi, B. T., Schneider, D. P., Green, R. F., & Hartig, G. F. 1994, *ApJ*, 420, 110
- Laor, A. 1998, *ApJ*, 505, L83

- Lundgren, B. F., Wilhite, B. C., Brunner, R. J., Hall, P. B., Schneider, D. P., York, D. G., Vanden Berk, D. E., & Brinkmann, J. 2007, *ApJ*, 656, 73
- Lupton, R., Gunn, J. E., Ivezić, Z., Knapp, G. R., Kent, S., & Yasuda, N. 2001, in *ASP Conf. Ser. 238, Astronomical Data Analysis Software and Systems X*, ed. F. R. Harnden, Jr., F. A. Primini, and H. E. Payne (San Francisco: Astr. Soc. Pac.), p. 269, astro-ph[0101420]
- McLure, R. J., & Jarvis, M. J. 2002, *MNRAS*, 337, 109
- Oke, J. B. 1967, *ApJ*, 150, L5
- Onken, C. A., & Peterson, B. M. 2002, *ApJ*, 572, 746
- Osterbrock, D. E., & Shuder, J. M. 1982, *ApJS*, 49, 149
- Peterson, B. M. 1993, *PASP*, 105, 247
- Peterson, B. M., & Wandel, A. 1999, *ApJ*, 521, L95
- Peterson, B. M., & Wandel, A. 2000, *ApJ*, 540, L13
- Peterson, B. M., et al. 2004, *ApJ*, 613, 682
- Peterson, B. M., et al. 2005, *ApJ*, 632, 799
- Pier, J. R., et al. 2003, *AJ*, 125, 1559
- Rengstorf, A. W., Brunner, R. J., & Wilhite, B. C. 2006, *AJ*, 131, 1923
- Richards, G. T. et al. 2002, *AJ*, 123, 2945
- Richards, G. T., Vanden Berk, D. E., Reichard, T. A., Hall, P. B., Schneider, D. P., SubbaRao, M., Thakar, A. R., & York, D. G. 2002, *AJ*, 124, 1
- Sergeev, V. I., Pronik, S. G., & Sergeeva, E. A. 2001, *ApJ*, 554, 245
- Smith, H. J., & Hoeffleit, D. 1963, *Nature*, 198, 650
- Smith, J. A. et al. 2002, *AJ*, 123, 2121
- Spergel, D. N. et al. 2007, *ApJ*, In Press
- Stoughton, C. et al. 2002, *AJ*, 123, 485
- Strauss, M. A. et al. 2002, *AJ*, 124, 1810



- Trèvese, D., Kron, R. G., & Bunone, A. 2001, *ApJ*, 551, 103
- Trèvese, D. & Vagnetti, F. 2002, *ApJ*, 564, 624
- Tucker, D. L., et al. 2006, *AN*, 327, 821
- Uomoto, A. K., Wills, B. J., & Wills, D. 1976, *AJ*, 81, 905
- Vanden Berk, D. E. et al. 2001, *AJ*, 122, 549
- Vanden Berk, D. E., et al. 2004, *ApJ*, 601, 692
- Vestergaard, M. 2002, *ApJ*, 571, 733
- Vestergaard, M., & Peterson, B. M. 2006, *ApJ*, 641, 689
- Wandel, A., Peterson, B. M., & Malkan, M. A. 1999, *ApJ*, 526, 579
- Wanders, I., & Peterson, B. M. 1996, *ApJ*, 466, 174
- Wilhite, B. C., Vanden Berk, D. E., Kron, R. G., Schneider, D. P., Pereyra, N., Brunner, R. J., Richards, G. T., & Brinkmann, J. V. 2005, *ApJ*, 633, 638
- Wilhite, B. C., Vanden Berk, D. E., Brunner, R. J., & Brinkmann, J. V. 2006, *ApJ*, 641, 78
- Wilkes, B. J. 1984, *MNRAS*, 207, 73
- York, D. G. et al. 2000, *AJ*, 120, 1579

Table 1. Variable Quasar Sample. HSN and LSN indicate the high- and low-S/N ratio epochs, respectively.

Number	SDSS J	MJD		HSN	$z$	LSN	$S/N_r$	
		HSN	LSN				HSN	LSN
1	100543.42–005559.9	51910	51581	$1.712 \pm 0.002$	$1.717 \pm 0.002$	8.4	7.0	
2	100356.15–005940.4	51910	51581	$2.108 \pm 0.002$	$2.108 \pm 0.001$	16.9	15.3	
3	100013.37+011203.2	51910	51581	$1.801 \pm 0.003$	$1.805 \pm 0.001$	12.3	11.4	
4	100246.85+002104.0	51910	51581	$2.172 \pm 0.002$	$2.169 \pm 0.002$	19.4	17.5	
5	100412.88+001257.5	51910	51581	$2.240 \pm 0.002$	$2.243 \pm 0.002$	11.1	9.5	
6	100428.43+001825.6	51910	51581	$3.045 \pm 0.001$	$2.989 \pm 0.046$	16.3	11.2	
7	100623.58+004141.1	51910	51581	$1.919 \pm 0.001$	$1.916 \pm 0.001$	9.3	7.6	
8	100715.53+004258.3	51910	51581	$1.676 \pm 0.001$	$1.677 \pm 0.002$	9.7	9.4	
9	111603.99–011412.1	51984	51608	$2.174 \pm 0.002$	$2.177 \pm 0.002$	16.1	15.0	
10	111502.65–002344.0	51984	51608	$1.960 \pm 0.002$	$1.959 \pm 0.002$	12.9	9.5	
11	111201.25–011324.4	51984	51608	$2.237 \pm 0.002$	$2.240 \pm 0.002$	20.6	13.1	
12	111319.93+010508.9	51984	51608	$1.855 \pm 0.002$	$1.854 \pm 0.003$	13.8	8.7	
13	111642.34+000557.3	51984	51608	$2.151 \pm 0.002$	$2.155 \pm 0.002$	10.4	7.9	
14	111858.55+000654.8	51984	51608	$2.436 \pm 0.004$	$2.457 \pm 0.001$	20.8	16.2	
15	114745.57–005609.5	51959	51584	$1.941 \pm 0.002$	$1.946 \pm 0.003$	18.2	14.5	
16	114646.40–010554.3	51959	51584	$2.119 \pm 0.001$	$2.119 \pm 0.002$	10.4	6.6	
17	114534.51–004338.7	51959	51584	$1.750 \pm 0.002$	$1.747 \pm 0.002$	12.0	7.4	
18	114547.54–003106.7	51959	51584	$2.043 \pm 0.002$	$2.029 \pm 0.004$	17.1	11.1	
19	114530.42–001159.3	51959	51584	$1.751 \pm 0.002$	$1.751 \pm 0.002$	8.2	6.2	
20	114311.23–002133.0	51959	51584	$1.920 \pm 0.001$	$1.911 \pm 0.002$	11.6	7.5	
21	114220.26–001216.3	51959	51584	$2.486 \pm 0.007$	$2.490 \pm 0.005$	15.4	9.5	
22	114211.59–005344.2	51959	51584	$1.919 \pm 0.002$	$1.919 \pm 0.002$	22.7	16.4	
23	114201.24–004442.1	51959	51584	$1.725 \pm 0.002$	$1.720 \pm 0.002$	7.6	4.6	
24	114104.35+010526.2	51959	51584	$1.692 \pm 0.002$	$1.691 \pm 0.002$	10.4	6.6	
25	114410.13+001813.7	51959	51584	$1.792 \pm 0.002$	$1.792 \pm 0.002$	16.9	8.4	
26	114752.67+010430.7	51959	51584	$2.072 \pm 0.001$	$2.072 \pm 0.002$	13.5	7.7	
27	114948.81+000855.8	51959	51584	$1.970 \pm 0.001$	$1.968 \pm 0.004$	12.9	10.9	
28	115554.11–010340.8	51943	51662	$1.969 \pm 0.003$	$1.954 \pm 0.004$	10.8	8.6	
29	115154.83–005904.6	51943	51662	$1.928 \pm 0.002$	$1.930 \pm 0.001$	12.9	7.6	

Table 1—Continued

Number	SDSS J	MJD		HSN	$z$	LSN	$S/N_r$	
		HSN	LSN				HSN	LSN
30	115238.98–004606.1	51943	51662	1.762 ± 0.002	1.766 ± 0.001	18.3	12.6	
31	115157.05–001412.6	51943	51662	1.654 ± 0.002	1.654 ± 0.001	11.9	9.0	
32	115043.87–002354.0	51943	51662	1.976 ± 0.001	1.975 ± 0.001	40.0	27.2	
33	115105.33+002928.3	51943	51662	1.769 ± 0.001	1.772 ± 0.002	12.9	8.3	
34	115058.73+005504.4	51943	51662	1.753 ± 0.002	1.755 ± 0.001	10.9	7.7	
35	115115.38+003827.0	51943	51662	1.880 ± 0.002	1.886 ± 0.002	23.7	15.0	
36	115213.55+001946.7	51943	51662	1.834 ± 0.002	1.834 ± 0.001	8.0	7.3	
37	120142.24–001639.9	51930	51663	1.993 ± 0.002	1.982 ± 0.001	27.6	15.2	
38	115826.94–000701.4	51930	51663	1.808 ± 0.002	1.809 ± 0.002	11.4	6.3	
39	115254.79+002010.5	51930	51663	2.359 ± 0.002	2.365 ± 0.002	13.0	5.4	
40	115723.76+005419.6	51930	51663	1.841 ± 0.003	1.843 ± 0.002	20.0	8.9	
41	124524.59–000937.9	51928	51660	2.084 ± 0.002	2.084 ± 0.002	29.7	20.8	
42	124540.99–002744.7	51928	51660	1.693 ± 0.002	1.692 ± 0.002	18.0	16.3	
43	124356.22–000021.8	51928	51660	1.837 ± 0.002	1.836 ± 0.002	9.8	7.2	
44	124310.79–003640.7	51928	51660	2.039 ± 0.001	2.040 ± 0.000	9.6	8.7	
45	124242.11+001157.9	51928	51660	2.159 ± 0.002	2.158 ± 0.002	14.2	9.4	
46	124551.44+010505.0	51928	51660	2.809 ± 0.001	2.809 ± 0.001	19.1	17.8	
47	130242.61–000728.1	51689	51994	1.721 ± 0.001	1.720 ± 0.002	25.1	23.0	
48	130157.36–001532.5	51689	51994	1.975 ± 0.002	1.971 ± 0.002	14.5	11.6	
49	130033.29–000652.5	51689	51994	2.078 ± 0.001	1.507 ± 0.003	4.4	4.6	
50	125818.59–004631.0	51689	51994	1.831 ± 0.002	1.830 ± 0.002	10.8	8.8	
51	125928.80–002730.0	51689	51994	1.907 ± 0.001	1.905 ± 0.002	9.4	7.4	
52	125710.91–002641.2	51689	51994	1.783 ± 0.002	1.785 ± 0.002	16.8	16.1	
53	125532.99–001642.6	51689	51994	2.033 ± 0.001	2.036 ± 0.002	11.9	10.4	
54	125617.52–001918.2	51689	51994	1.769 ± 0.002	1.770 ± 0.002	7.9	5.5	
55	125359.69–003227.4	51689	51994	1.692 ± 0.001	1.686 ± 0.002	10.7	10.7	
56	125359.62–000540.7	51689	51994	1.977 ± 0.002	1.982 ± 0.002	9.7	8.2	
57	125254.53–000555.7	51689	51994	1.859 ± 0.001	1.863 ± 0.001	3.6	3.3	
58	125329.98+000730.1	51689	51994	2.669 ± 0.003	2.694 ± 0.001	6.2	6.3	

Table 1—Continued

Number	SDSS J	MJD		HSN	$z$	LSN	$S/N_r$	
		HSN	LSN				HSN	LSN
59	125810.14+005535.4	51689	51994	2.128 ± 0.001	2.126 ± 0.002	2.6	2.6	
60	125743.93+005733.5	51689	51994	1.805 ± 0.000	1.811 ± 0.002	22.0	22.5	
61	125818.26+010613.8	51689	51994	1.728 ± 0.001	1.730 ± 0.002	13.1	13.9	
62	125656.19+002121.1	51689	51994	2.016 ± 0.001	2.003 ± 0.002	3.8	3.3	
63	130029.02+004637.2	51689	51994	1.868 ± 0.001	1.865 ± 0.002	18.0	18.4	
64	130019.99+002641.4	51689	51994	1.754 ± 0.002	1.752 ± 0.002	17.1	16.6	
65	130132.67+003801.8	51689	51994	1.828 ± 0.002	1.830 ± 0.002	5.1	5.7	
66	130127.19+001849.0	51689	51994	2.117 ± 0.001	2.119 ± 0.002	7.2	7.3	
67	131549.26−004314.1	51985	51585	1.960 ± 0.002	1.964 ± 0.002	9.2	11.4	
68	131052.51−005533.2	51985	51585	4.159 ± 0.005	4.160 ± 0.001	11.9	12.1	
69	131128.35+004929.6	51985	51585	2.809 ± 0.002	2.807 ± 0.001	13.4	10.6	
70	131540.48−000633.3	51985	51585	2.107 ± 0.002	2.107 ± 0.001	11.8	10.3	
71	131426.44+010545.3	51985	51585	1.838 ± 0.002	1.837 ± 0.003	10.8	7.4	
72	131630.46+005125.5	51985	51585	2.403 ± 0.002	2.405 ± 0.001	18.3	11.7	
73	131840.95+003103.9	51984	51665	1.773 ± 0.002	1.780 ± 0.001	8.2	6.7	
74	131913.99+005251.9	51984	51665	1.827 ± 0.002	1.829 ± 0.001	9.3	5.8	
75	132009.10+002336.7	51984	51665	1.713 ± 0.002	1.709 ± 0.001	14.8	12.0	
76	132314.50+003250.7	51984	51665	1.960 ± 0.001	1.961 ± 0.001	8.8	6.3	
77	132333.04+004750.3	51984	51665	1.779 ± 0.002	1.775 ± 0.001	26.4	19.5	
78	133018.00−010238.5	51959	51663	2.126 ± 0.002	2.127 ± 0.002	10.5	7.2	
79	132750.93−000340.0	51959	51663	1.794 ± 0.002	1.794 ± 0.001	10.3	7.1	
80	132410.46−011243.7	51959	51663	1.836 ± 0.002	1.835 ± 0.002	6.6	5.2	
81	132214.82+005419.9	51959	51663	2.145 ± 0.002	2.148 ± 0.002	19.6	15.0	
82	132555.11+011423.6	51959	51663	1.960 ± 0.002	1.953 ± 0.003	7.5	5.8	
83	132812.09+005643.2	51959	51663	2.024 ± 0.002	2.024 ± 0.002	19.5	15.2	
84	133513.43−004641.1	51955	51662	2.027 ± 0.004	2.039 ± 0.001	10.0	6.8	
85	133037.05−004529.4	51955	51662	2.108 ± 0.002	2.106 ± 0.001	16.2	10.1	
86	132944.35+004004.6	51955	51662	2.312 ± 0.002	2.311 ± 0.002	22.0	17.1	
87	133138.50+004221.1	51955	51662	2.429 ± 0.004	2.438 ± 0.002	16.2	13.2	

Table 1—Continued

Number	SDSS J	MJD		HSN	$z$	LSN	$S/N_r$	
		HSN	LSN				HSN	LSN
88	133125.93+004414.0	51955	51662	2.022 ± 0.002	2.023 ± 0.002	15.2	12.9	
89	133241.02+010237.6	51955	51662	1.752 ± 0.002	1.755 ± 0.001	13.5	10.6	
90	133823.04+001611.8	51955	51662	2.162 ± 0.002	2.163 ± 0.002	17.3	10.8	
91	133939.01+001021.6	51955	51662	2.126 ± 0.002	2.129 ± 0.001	10.4	4.6	
92	134636.52+011155.2	51943	51666	1.673 ± 0.001	1.677 ± 0.002	6.7	8.6	
93	134755.67+003935.1	51943	51666	3.813 ± 0.001	3.816 ± 0.001	6.2	7.6	
94	134834.97+010626.2	51943	51666	1.926 ± 0.002	1.929 ± 0.002	20.2	19.6	
95	135048.91+001522.0	51943	51666	1.834 ± 0.002	1.834 ± 0.002	8.3	8.3	
96	140344.06−003359.3	51942	51641	1.744 ± 0.002	1.740 ± 0.001	9.7	7.0	
97	140323.39−000606.9	51942	51641	2.460 ± 0.001	2.454 ± 0.002	27.7	22.3	
98	140114.28−004537.1	51942	51641	2.522 ± 0.001	2.504 ± 0.008	14.2	12.8	
99	135951.09−004250.4	51942	51641	2.063 ± 0.001	2.063 ± 0.001	15.5	12.8	
100	135735.01−004648.9	51942	51641	1.771 ± 0.002	1.770 ± 0.002	27.1	25.2	
101	135844.57−011055.1	51942	51641	1.961 ± 0.002	1.961 ± 0.001	16.7	18.0	
102	135603.51−010421.9	51942	51641	1.933 ± 0.001	1.932 ± 0.002	14.2	14.1	
103	135605.41−010024.4	51942	51641	1.886 ± 0.002	1.877 ± 0.002	12.6	8.9	
104	135534.38−000841.7	51942	51641	1.789 ± 0.002	1.792 ± 0.002	9.6	7.7	
105	135247.96−002351.6	51942	51641	1.670 ± 0.003	1.669 ± 0.002	6.3	4.5	
106	135623.29+004427.2	51942	51641	1.977 ± 0.002	1.981 ± 0.002	10.7	10.7	
107	135445.66+002050.3	51942	51641	2.503 ± 0.001	2.508 ± 0.002	23.0	22.5	
108	135514.61+001157.4	51942	51641	1.806 ± 0.002	1.808 ± 0.003	15.2	14.2	
109	135721.77+005501.2	51942	51641	1.997 ± 0.001	1.996 ± 0.001	22.2	19.8	
110	135828.74+005811.5	51942	51641	3.922 ± 0.001	3.931 ± 0.001	9.5	7.1	
111	140253.25+002921.2	51942	51641	1.939 ± 0.002	1.936 ± 0.002	11.6	10.5	
112	140224.15+003002.2	51942	51641	2.418 ± 0.002	2.418 ± 0.003	18.4	13.7	
113	142033.25−003233.3	51609	51957	2.676 ± 0.007	2.682 ± 0.008	11.2	10.9	
114	141951.60−004605.9	51609	51957	1.937 ± 0.001	1.933 ± 0.003	6.6	7.2	
115	141734.28+005730.1	51609	51957	2.407 ± 0.001	2.403 ± 0.002	5.0	4.8	
116	141822.91−000054.5	51609	51957	2.045 ± 0.002	2.048 ± 0.002	16.0	15.8	

Table 1—Continued

Number	SDSS J	MJD		HSN	$z$	LSN	$S/N_r$	
		HSN	LSN				HSN	LSN
117	141937.59–000132.4	51609	51957	1.837 ± 0.002	1.839 ± 0.002	10.3	9.0	
118	142045.98–000517.9	51609	51957	2.196 ± 0.002	2.193 ± 0.002	9.7	10.8	
119	141956.96+010652.6	51609	51957	2.206 ± 0.003	2.207 ± 0.002	9.3	9.5	
120	142205.10–000120.7	51609	51957	1.860 ± 0.002	1.863 ± 0.002	13.5	11.2	
121	142205.56+004143.2	51609	51957	2.155 ± 0.002	2.157 ± 0.002	8.7	8.0	
122	143628.46–003840.2	51637	51690	2.052 ± 0.002	2.048 ± 0.001	20.1	16.5	
123	143229.24–010616.1	51637	51690	2.085 ± 0.002	2.086 ± 0.002	28.8	26.9	
124	143255.35–003109.2	51637	51690	2.071 ± 0.002	2.069 ± 0.001	12.3	14.6	
125	143116.86–004637.7	51637	51690	2.211 ± 0.002	2.211 ± 0.001	12.8	12.0	
126	142954.48+002327.5	51637	51690	1.992 ± 0.001	2.000 ± 0.001	10.6	9.8	
127	143124.03+002302.7	51637	51690	1.947 ± 0.002	1.941 ± 0.000	9.2	9.0	
128	143307.40+003319.1	51637	51690	2.743 ± 0.001	2.744 ± 0.001	11.4	11.3	
129	143436.51+010522.2	51637	51690	2.202 ± 0.002	2.200 ± 0.001	10.7	11.1	
130	143601.58+002041.9	51637	51690	1.787 ± 0.001	1.267 ± 0.001	12.8	21.5	
131	145817.52–004115.7	51994	51666	2.618 ± 0.001	2.615 ± 0.001	12.1	10.9	
132	145903.25–002256.4	51994	51666	2.012 ± 0.001	1.999 ± 0.004	12.1	8.9	
133	145722.70–010800.9	51994	51666	2.232 ± 0.002	2.232 ± 0.002	27.5	21.4	
134	145613.19–003652.9	51994	51666	1.760 ± 0.002	1.760 ± 0.002	6.1	4.1	
135	145555.00–003713.4	51994	51666	1.948 ± 0.002	1.945 ± 0.002	9.3	5.5	
136	145302.09–010524.4	51994	51666	1.808 ± 0.002	1.806 ± 0.002	27.6	17.9	
137	145128.92–005655.7	51994	51666	2.114 ± 0.002	2.114 ± 0.002	18.2	15.7	
138	145246.52+003450.5	51994	51666	2.542 ± 0.001	2.546 ± 0.002	2.8	4.0	
139	145155.24+000521.9	51994	51666	2.018 ± 0.002	2.021 ± 0.002	13.1	11.4	
140	145317.44+003441.1	51994	51666	2.164 ± 0.002	2.164 ± 0.002	17.1	12.4	
141	145337.98+002010.6	51994	51666	1.862 ± 0.002	1.861 ± 0.002	10.3	6.4	
142	145429.65+004121.2	51994	51666	2.659 ± 0.001	2.638 ± 0.005	14.1	9.7	
143	145447.70+003436.3	51994	51666	1.914 ± 0.001	1.910 ± 0.002	14.1	10.9	
144	145633.42+000555.4	51994	51666	1.836 ± 0.002	1.839 ± 0.001	6.4	5.6	
145	145815.22+003908.6	51994	51666	2.022 ± 0.002	2.013 ± 0.003	10.4	8.5	

Table 1—Continued

Number	SDSS J	MJD		HSN	$z$	LSN	$S/N_r$	
		HSN	LSN				HSN	LSN
146	145754.05+003638.9	51994	51666	$2.760 \pm 0.001$		$2.760 \pm 0.001$	12.7	11.3
147	150826.49–003026.9	51990	51614	$1.650 \pm 0.002$		$1.648 \pm 0.000$	10.0	6.4
148	150314.57–000905.8	51990	51614	$1.701 \pm 0.003$		$1.703 \pm 0.002$	9.3	7.8
149	150104.94–010727.9	51990	51614	$2.134 \pm 0.001$		$2.138 \pm 0.001$	4.9	3.2
150	145943.03+010601.5	51990	51614	$2.094 \pm 0.002$		$2.097 \pm 0.001$	19.1	15.1
151	145901.28+002123.7	51990	51614	$1.985 \pm 0.002$		$1.990 \pm 0.002$	15.3	12.4
152	145838.04+002418.0	51990	51614	$1.887 \pm 0.002$		$1.882 \pm 0.001$	12.8	9.8
153	145907.19+002401.3	51990	51614	$3.011 \pm 0.001$		$3.012 \pm 0.001$	16.7	12.8
154	145914.50+000648.7	51990	51614	$1.899 \pm 0.002$		$1.898 \pm 0.001$	9.7	7.0
155	150046.92+000427.3	51990	51614	$1.688 \pm 0.002$		$1.688 \pm 0.001$	12.9	6.6
156	150123.45+001940.0	51990	51614	$1.929 \pm 0.002$		$1.929 \pm 0.002$	20.6	17.5
157	150353.21+005837.9	51990	51614	$2.089 \pm 0.002$		$2.091 \pm 0.002$	19.7	15.1
158	150548.40+010801.2	51990	51614	$1.699 \pm 0.002$		$1.697 \pm 0.002$	16.2	12.6
159	150613.10+002854.8	51990	51614	$3.369 \pm 0.001$		$3.359 \pm 0.001$	13.5	10.3
160	150631.75+000518.1	51990	51614	$1.692 \pm 0.003$		$1.691 \pm 0.002$	23.5	16.8
161	150611.23+001823.6	51990	51614	$2.838 \pm 0.001$		$2.806 \pm 0.015$	11.5	9.2
162	131559.71–031852.7	51691	51990	$1.726 \pm 0.002$		$1.731 \pm 0.003$	22.3	17.3
163	131728.74–024759.4	51691	51990	$3.377 \pm 0.001$		$1.430 \pm 0.001$	8.5	9.1
164	131435.50–033035.9	51691	51990	$1.897 \pm 0.001$		$1.895 \pm 0.002$	18.5	17.4
165	131228.04–032308.7	51691	51990	$2.194 \pm 0.002$		$2.195 \pm 0.002$	13.4	13.2
166	130751.67–014119.9	51691	51990	$1.743 \pm 0.002$		$1.738 \pm 0.002$	9.2	9.6
167	131623.99–015834.9	51691	51990	$2.996 \pm 0.003$		$3.004 \pm 0.001$	11.3	10.8
168	171143.95+603634.6	51695	51780	$2.129 \pm 0.002$		$2.131 \pm 0.002$	8.8	9.7
169	171212.37+605328.9	51695	51780	$1.682 \pm 0.003$		$1.684 \pm 0.000$	10.0	10.2
170	171304.62+611945.4	51695	51780	$1.782 \pm 0.002$		$1.783 \pm 0.002$	9.2	9.0
171	171424.68+612404.6	51695	51780	$2.036 \pm 0.001$		$2.042 \pm 0.001$	11.5	11.3
172	171300.19+612354.4	51695	51780	$1.847 \pm 0.001$		$1.845 \pm 0.002$	9.5	9.7
173	170611.38+610052.7	51695	51780	$2.069 \pm 0.002$		$2.055 \pm 0.001$	11.4	10.9
174	170144.60+603300.6	51695	51780	$1.820 \pm 0.002$		$1.821 \pm 0.002$	15.1	13.6

Table 1—Continued

Number	SDSS J	MJD		HSN	$z$	LSN	$S/N_r$	
		HSN	LSN				HSN	LSN
175	170102.17+612300.9	51695	51780	2.287 ± 0.002	2.287 ± 0.002	23.2	23.3	
176	165755.53+604002.5	51695	51780	2.332 ± 0.010	2.355 ± 0.001	16.6	14.1	
177	170306.09+615244.3	51695	51780	1.916 ± 0.003	1.919 ± 0.002	29.1	28.0	
178	170954.32+615817.5	51695	51780	1.847 ± 0.004	1.857 ± 0.004	10.1	9.9	
179	172909.92+624519.7	51694	51789	1.748 ± 0.003	1.754 ± 0.003	10.7	8.2	
180	172047.64+624638.3	51694	51789	1.831 ± 0.002	1.823 ± 0.003	8.9	10.7	
181	171633.36+621625.4	51694	51789	2.118 ± 0.001	2.120 ± 0.002	12.7	14.7	
182	171731.04+621912.1	51694	51789	2.119 ± 0.001	2.118 ± 0.002	10.8	12.3	
183	171420.59+630020.2	51694	51789	1.709 ± 0.002	1.712 ± 0.002	10.7	11.2	
184	171015.71+634806.1	51694	51789	1.786 ± 0.002	1.789 ± 0.002	9.2	8.3	
185	171535.96+632336.0	51694	51789	2.182 ± 0.002	2.182 ± 0.002	17.3	16.6	
186	172026.24+633517.3	51694	51789	2.149 ± 0.002	2.150 ± 0.002	18.3	16.8	
187	171712.86+640344.7	51694	51789	2.105 ± 0.001	2.103 ± 0.001	13.4	11.3	
188	234336.14–003955.4	51877	51783	1.781 ± 0.002	1.782 ± 0.002	18.6	13.4	
189	234033.71–005637.0	51877	51783	3.650 ± 0.001	3.652 ± 0.001	8.7	7.7	
190	234002.76–005242.1	51877	51783	2.256 ± 0.002	2.257 ± 0.002	17.1	13.7	
191	233838.71+011448.3	51877	51783	2.078 ± 0.002	2.073 ± 0.002	7.3	6.2	
192	233930.00+003017.2	51877	51783	3.052 ± 0.001	3.003 ± 0.028	18.4	14.7	
193	234340.34+011254.4	51877	51783	1.952 ± 0.002	1.949 ± 0.001	10.1	10.9	
194	234500.91+004156.1	51877	51783	2.193 ± 0.002	2.192 ± 0.002	11.6	11.4	
195	002609.07–003749.3	51900	51816	2.382 ± 0.000	2.379 ± 0.003	12.4	8.8	
196	002322.70–004829.2	51900	51816	2.251 ± 0.002	2.250 ± 0.003	14.6	9.5	
197	002139.30–003154.5	51900	51816	2.157 ± 0.002	2.155 ± 0.002	23.8	15.2	
198	002146.71–004847.9	51900	51816	2.502 ± 0.002	2.501 ± 0.002	19.6	12.0	
199	002028.34–002915.0	51900	51816	1.927 ± 0.002	1.927 ± 0.002	16.6	9.9	
200	001950.05–004040.7	51900	51816	4.327 ± 0.001	4.351 ± 0.001	7.5	4.9	
201	001657.00+005532.0	51900	51816	1.756 ± 0.002	1.755 ± 0.001	14.7	8.8	
202	002143.30+010840.2	51900	51816	1.901 ± 0.002	1.905 ± 0.002	10.7	7.7	
203	005102.42–010244.4	51876	51812	1.874 ± 0.004	1.878 ± 0.002	28.6	29.7	



Table 1—Continued

Number	SDSS J	MJD		HSN	$z$	LSN	$S/N_r$	
		HSN	LSN				HSN	LSN
204	005128.60–002453.9	51876	51812	1.939 ± 0.003	1.937 ± 0.002	15.3	13.5	
205	005013.78–002446.4	51876	51812	2.032 ± 0.001	2.020 ± 0.003	9.3	9.0	
206	004806.06–010321.5	51876	51812	2.528 ± 0.001	2.526 ± 0.002	20.6	23.4	
207	004806.06+004623.4	51876	51812	2.362 ± 0.001	2.333 ± 0.016	10.4	9.5	
208	004856.35+005648.1	51876	51812	2.327 ± 0.002	2.328 ± 0.002	22.5	20.3	
209	004639.85+000732.1	51876	51812	2.128 ± 0.002	2.123 ± 0.002	15.7	15.0	
210	004918.97+002609.4	51876	51812	1.946 ± 0.001	1.945 ± 0.002	24.4	19.4	
211	005001.81+002620.1	51876	51812	1.940 ± 0.001	1.930 ± 0.003	10.8	10.3	
212	005157.24+000354.8	51876	51812	1.956 ± 0.002	1.955 ± 0.002	30.6	28.0	
213	005202.40+010129.2	51876	51812	2.270 ± 0.002	2.271 ± 0.002	35.8	33.3	
214	020505.81+011415.9	51812	51877	2.232 ± 0.002	2.233 ± 0.002	11.5	12.1	
215	020646.30+010505.5	51812	51877	2.270 ± 0.002	2.269 ± 0.003	14.2	11.9	
216	020646.97+001800.5	51812	51877	1.679 ± 0.002	1.681 ± 0.002	13.2	11.8	
217	020953.16+005511.0	51812	51877	2.191 ± 0.002	2.193 ± 0.002	14.9	9.6	
218	020845.53+002236.0	51812	51877	1.885 ± 0.002	1.885 ± 0.002	32.9	33.8	
219	022534.09+000347.9	51817	52238	1.736 ± 0.001	1.734 ± 0.002	4.0	2.8	
220	022430.15–004131.1	51817	52238	1.667 ± 0.002	1.665 ± 0.001	10.9	10.7	
221	022152.95–003226.1	51817	52238	1.712 ± 0.001	1.714 ± 0.002	9.3	7.7	
222	022143.18–001803.8	51817	52238	2.640 ± 0.001	2.645 ± 0.001	14.2	12.0	
223	022346.42–003908.2	51817	52238	1.675 ± 0.002	1.678 ± 0.002	11.9	15.3	
224	022326.60–010406.7	51817	52238	1.933 ± 0.001	1.929 ± 0.002	9.4	8.2	
225	022050.25–002534.5	51817	52238	1.705 ± 0.002	1.703 ± 0.002	4.4	3.4	
226	022058.10–002946.8	51817	52238	1.708 ± 0.001	1.714 ± 0.001	6.1	4.3	
227	021954.57–000304.5	51817	52238	1.776 ± 0.001	1.781 ± 0.002	3.3	2.5	
228	021754.80+000234.0	51817	52238	2.044 ± 0.002	2.031 ± 0.001	5.5	8.4	
229	022259.69+011028.3	51817	52238	1.838 ± 0.002	1.836 ± 0.002	8.6	8.0	
230	022128.26+002056.1	51817	52238	2.039 ± 0.001	2.039 ± 0.001	10.4	10.3	
231	022414.65+011341.8	51817	52238	1.785 ± 0.001	1.787 ± 0.001	4.3	3.5	
232	022230.28+001844.5	51817	52238	2.189 ± 0.002	2.189 ± 0.001	9.1	8.5	

Table 1—Continued

Number	SDSS J	MJD		HSN	$z$	LSN	$S/N_r$	
		HSN	LSN				HSN	LSN
233	022526.15+010124.0	51817	52238	$1.875 \pm 0.002$		$1.870 \pm 0.001$	6.3	3.7
234	022540.44+005720.9	51817	52238	$2.010 \pm 0.002$		$2.011 \pm 0.002$	10.3	9.6
235	022553.60+005130.9	51817	52238	$1.813 \pm 0.002$		$1.814 \pm 0.002$	13.4	12.3
236	022647.42+001254.4	51817	52238	$2.138 \pm 0.001$		$2.156 \pm 0.001$	9.4	8.4
237	022656.06+002248.0	51817	52238	$1.869 \pm 0.001$		$1.863 \pm 0.001$	4.2	4.1
238	030002.70–001219.2	51816	51877	$1.680 \pm 0.002$		$1.676 \pm 0.001$	5.3	5.7
239	025933.72–002517.6	51816	51877	$1.759 \pm 0.001$		$1.760 \pm 0.001$	13.3	13.3
240	025713.07–010157.6	51816	51877	$1.868 \pm 0.002$		$1.872 \pm 0.001$	7.5	6.9
241	025819.32–000806.1	51816	51877	$2.110 \pm 0.002$		$2.108 \pm 0.002$	7.0	6.7
242	025510.55–000712.9	51816	51877	$1.686 \pm 0.002$		$1.692 \pm 0.006$	5.5	5.4
243	025513.03+000639.4	51816	51877	$1.882 \pm 0.000$		$1.880 \pm 0.002$	8.3	8.0
244	025356.07+001057.4	51816	51877	$1.699 \pm 0.002$		$1.700 \pm 0.002$	8.7	8.0
245	025429.74–004334.0	51816	51877	$1.739 \pm 0.002$		$1.742 \pm 0.001$	4.2	3.7
246	025345.20–004706.0	51816	51877	$2.451 \pm 0.001$		$2.431 \pm 0.012$	16.1	15.5
247	025447.40–004111.2	51816	51877	$2.009 \pm 0.003$		$0.678 \pm 0.004$	5.9	5.3
248	025340.94+001110.0	51816	51877	$1.687 \pm 0.001$		$1.687 \pm 0.000$	22.0	19.2
249	025209.80+000548.9	51816	51877	$2.111 \pm 0.002$		$2.114 \pm 0.001$	4.4	4.0
250	025038.67–004739.1	51816	51877	$1.841 \pm 0.001$		$1.841 \pm 0.002$	15.4	17.3
251	025151.27+005739.0	51816	51877	$1.828 \pm 0.003$		$1.829 \pm 0.001$	6.2	6.3
252	025229.76+010049.0	51816	51877	$2.020 \pm 0.002$		$2.009 \pm 0.003$	5.6	5.6
253	025019.27+003100.7	51816	51877	$2.027 \pm 0.002$		$2.014 \pm 0.002$	5.5	4.7
254	025401.44+002916.1	51816	51877	$2.008 \pm 0.002$		$2.010 \pm 0.002$	11.4	11.4
255	025516.88+011134.5	51816	51877	$2.839 \pm 0.003$		$2.848 \pm 0.001$	7.7	7.8
256	025518.58+004847.6	51816	51877	$3.989 \pm 0.003$		$3.987 \pm 0.001$	12.1	10.5
257	025828.99+001526.2	51816	51877	$2.063 \pm 0.002$		$2.053 \pm 0.000$	4.3	4.8
258	025922.63+005829.3	51816	51877	$1.858 \pm 0.002$		$1.861 \pm 0.002$	11.0	12.6
259	030449.86–000813.4	51817	51873	$3.295 \pm 0.002$		$3.295 \pm 0.001$	30.8	30.2
260	030341.04–002321.8	51817	51873	$3.231 \pm 0.001$		$3.232 \pm 0.001$	27.7	27.2
261	030027.11–004848.7	51817	51873	$2.017 \pm 0.001$		$2.017 \pm 0.002$	12.9	12.0

Table 1—Continued

Number	SDSS J	MJD		HSN	$z$	LSN	$S/N_r$	
		HSN	LSN				HSN	LSN
262	025928.52–001959.9	51817	51873	2.001 ± 0.002	2.001 ± 0.002	32.5	31.5	
263	030045.25+001656.7	51817	51873	1.742 ± 0.002	1.744 ± 0.003	11.6	11.3	
264	025905.64+001121.8	51817	51873	3.365 ± 0.002	3.365 ± 0.001	25.9	24.8	
265	030404.46+010327.5	51817	51873	1.833 ± 0.002	1.835 ± 0.001	13.6	13.1	
266	030600.41+010145.4	51817	51873	2.191 ± 0.001	2.190 ± 0.001	14.6	10.8	
267	030725.90+003709.4	51817	51873	2.114 ± 0.002	2.122 ± 0.001	10.7	7.9	
268	031348.33–010433.0	51931	52254	2.467 ± 0.002	2.469 ± 0.001	10.8	10.4	
269	031404.43–003947.2	51931	52254	2.103 ± 0.002	2.105 ± 0.002	15.6	15.2	
270	031003.01–004645.7	51931	52254	2.113 ± 0.002	2.114 ± 0.001	26.4	24.3	
271	031028.87–005326.2	51931	52254	2.462 ± 0.001	2.469 ± 0.001	19.7	18.4	
272	030719.92+004538.7	51931	52254	1.906 ± 0.001	1.904 ± 0.002	9.8	7.9	
273	031127.55+005357.3	51931	52254	1.758 ± 0.002	1.762 ± 0.001	11.4	8.9	
274	031237.57+004511.2	51931	52254	1.823 ± 0.001	1.823 ± 0.002	8.4	8.0	
275	032158.90–010037.6	51929	51821	1.761 ± 0.001	1.763 ± 0.002	6.3	5.3	
276	032253.09–001121.6	51929	51821	1.879 ± 0.002	1.875 ± 0.002	2.9	3.7	
277	032158.40–001102.6	51929	51821	2.153 ± 0.002	2.152 ± 0.002	12.4	12.0	
278	032028.36–003255.4	51929	51821	1.799 ± 0.002	1.794 ± 0.002	2.4	2.3	
279	031845.17–001845.3	51929	51821	3.223 ± 0.002	3.231 ± 0.003	13.5	12.1	
280	031441.46–000319.7	51929	51821	2.123 ± 0.002	2.121 ± 0.002	16.6	14.0	
281	031609.84+004043.2	51929	51821	2.920 ± 0.001	2.917 ± 0.001	15.3	13.0	
282	031544.54+004220.9	51929	51821	1.880 ± 0.001	1.883 ± 0.002	10.4	7.8	
283	031731.99+001010.4	51929	51821	1.959 ± 0.002	1.951 ± 0.002	7.4	8.3	
284	031805.30+001735.9	51929	51821	1.777 ± 0.002	1.776 ± 0.002	4.2	4.7	
285	032022.76+004108.3	51929	51821	1.787 ± 0.002	1.784 ± 0.002	20.5	22.0	
286	031949.59+005520.5	51929	51821	2.039 ± 0.001	2.042 ± 0.002	9.5	11.3	
287	033931.23–002458.7	51810	51879	1.667 ± 0.002	1.664 ± 0.002	12.3	10.2	
288	033335.03–004926.9	51810	51879	1.774 ± 0.001	1.777 ± 0.001	11.2	10.2	
289	033523.31–002203.9	51810	51879	1.768 ± 0.002	1.769 ± 0.002	22.5	20.6	
290	033356.92–003122.9	51810	51879	1.866 ± 0.001	1.867 ± 0.001	12.9	11.4	

Table 1—Continued

Number	SDSS J	MJD		HSN	$z$	LSN	$S/N_r$	
		HSN	LSN				HSN	LSN
291	033334.73–001621.4	51810	51879	1.826 ± 0.002	1.822 ± 0.002	5.3	5.0	
292	033201.41–004310.2	51810	51879	1.744 ± 0.002	1.742 ± 0.001	7.9	7.8	
293	033131.17–005704.2	51810	51879	1.805 ± 0.002	1.805 ± 0.002	15.4	14.2	
294	032933.97–004801.1	51810	51879	1.878 ± 0.000	1.880 ± 0.001	12.9	11.5	
295	032941.12–002246.6	51810	51879	2.416 ± 0.001	2.413 ± 0.001	4.8	4.4	
296	033004.34+000901.6	51810	51879	1.797 ± 0.001	1.799 ± 0.002	8.9	8.4	
297	033351.52+002341.6	51810	51879	1.814 ± 0.001	1.814 ± 0.001	10.7	10.3	
298	033310.29+000321.6	51810	51879	1.727 ± 0.002	1.728 ± 0.001	5.0	4.1	
299	033546.44+011622.4	51810	51879	2.092 ± 0.002	2.092 ± 0.002	8.5	7.1	
300	033515.59+002900.8	51810	51879	2.241 ± 0.002	2.238 ± 0.001	19.2	18.8	
301	033934.74+002302.8	51810	51879	1.732 ± 0.002	1.730 ± 0.002	9.0	7.7	
302	034435.96–001527.5	51811	51885	2.345 ± 0.002	2.344 ± 0.002	10.9	9.3	
303	034329.63–010838.9	51811	51885	1.726 ± 0.002	1.727 ± 0.002	18.5	16.8	
304	034318.37–004447.9	51811	51885	1.748 ± 0.002	1.752 ± 0.002	2.9	1.5	
305	034247.24–004129.6	51811	51885	2.226 ± 0.001	2.224 ± 0.002	5.5	3.7	
306	033954.26–002055.0	51811	51885	2.320 ± 0.001	2.319 ± 0.001	10.2	9.2	
307	034002.84–000627.9	51811	51885	1.720 ± 0.002	1.719 ± 0.001	8.1	7.0	
308	033854.77–000520.9	51811	51885	3.050 ± 0.002	3.051 ± 0.001	16.6	19.0	
309	033931.23–002458.7	51811	51885	1.669 ± 0.002	1.669 ± 0.001	13.6	12.0	
310	033708.45–000614.3	51811	51885	1.660 ± 0.001	1.658 ± 0.002	10.5	8.1	
311	033832.65+004518.5	51811	51885	1.839 ± 0.002	1.836 ± 0.001	8.8	8.1	
312	033639.50+002535.3	51811	51885	1.679 ± 0.003	1.682 ± 0.002	7.1	6.0	
313	034111.09+011617.9	51811	51885	1.840 ± 0.005	1.835 ± 0.002	7.6	5.7	
314	034119.57+010136.2	51811	51885	2.081 ± 0.002	1.503 ± 0.002	5.4	3.9	
315	034023.49+003111.9	51811	51885	1.910 ± 0.001	1.904 ± 0.001	6.7	5.9	
316	034027.31+003441.6	51811	51885	1.875 ± 0.001	1.875 ± 0.002	31.5	33.4	
317	033934.74+002302.8	51811	51885	1.732 ± 0.001	1.733 ± 0.004	10.5	8.8	
318	034143.88+000355.6	51811	51885	1.697 ± 0.001	1.692 ± 0.002	7.8	6.3	
319	034403.48+003426.9	51811	51885	2.046 ± 0.001	2.041 ± 0.000	9.8	7.4	

Table 1—Continued

Number	SDSS J	MJD		HSN	$z$	LSN	$S/N_r$	
		HSN	LSN				HSN	LSN
320	034501.37+000638.9	51811	51885	1.670 ± 0.002	1.667 ± 0.002	13.6	11.4	
321	004023.76+140807.4	51817	51884	1.870 ± 0.001	1.869 ± 0.002	38.4	50.4	
322	003453.74+141856.1	51817	51884	1.679 ± 0.001	1.679 ± 0.001	4.4	4.3	
323	003418.65+145102.8	51817	51884	2.114 ± 0.002	2.113 ± 0.001	8.5	7.8	
324	003520.91+143730.2	51817	51884	1.857 ± 0.002	1.860 ± 0.001	4.8	3.2	
325	003240.57+143951.9	51817	51884	1.864 ± 0.002	1.865 ± 0.001	4.0	3.0	
326	003230.37+145248.0	51817	51884	1.688 ± 0.001	1.681 ± 0.001	7.8	6.6	
327	005010.32+142947.4	51868	51812	2.042 ± 0.001	2.042 ± 0.002	7.2	6.3	
328	004721.96+140706.3	51868	51812	1.741 ± 0.001	1.737 ± 0.002	7.8	6.5	
329	004833.54+142056.8	51868	51812	1.819 ± 0.002	1.816 ± 0.001	10.7	10.3	
330	004710.84+145715.5	51868	51812	2.298 ± 0.010	2.296 ± 0.001	4.9	5.4	
331	004736.10+145256.4	51868	51812	1.845 ± 0.003	1.846 ± 0.002	7.4	6.8	
332	004455.68+134831.4	51868	51812	2.225 ± 0.002	2.226 ± 0.002	5.8	5.5	
333	004516.62+141811.4	51868	51812	2.122 ± 0.002	2.119 ± 0.001	7.9	7.8	
334	004238.23+135054.8	51868	51812	1.771 ± 0.001	1.773 ± 0.002	6.2	4.8	
335	004241.29+134241.1	51868	51812	1.786 ± 0.002	1.785 ± 0.002	12.0	10.8	
336	004103.71+144518.9	51868	51812	1.767 ± 0.002	1.765 ± 0.001	6.9	6.2	
337	004112.64+140534.0	51868	51812	2.093 ± 0.001	2.108 ± 0.001	3.7	3.0	
338	003955.81+153357.3	51868	51812	1.770 ± 0.002	1.770 ± 0.002	11.7	11.6	
339	004105.97+150512.4	51868	51812	2.281 ± 0.003	2.283 ± 0.002	4.7	3.9	
340	004403.47+151200.0	51868	51812	1.781 ± 0.002	1.780 ± 0.002	13.2	13.1	
341	004417.55+153257.1	51868	51812	2.065 ± 0.002	2.062 ± 0.002	9.8	9.8	
342	004609.30+160335.1	51868	51812	1.829 ± 0.004	1.829 ± 0.001	3.2	3.6	
343	004637.04+154652.4	51868	51812	1.767 ± 0.002	1.765 ± 0.002	3.3	3.5	
344	004742.39+155937.5	51868	51812	1.832 ± 0.001	1.835 ± 0.002	7.2	7.2	
345	004928.39+152859.1	51868	51812	2.201 ± 0.003	2.198 ± 0.003	6.9	6.7	
346	010838.82+140428.4	51811	51878	1.706 ± 0.002	1.700 ± 0.001	17.7	16.9	
347	010826.27+142939.6	51811	51878	1.755 ± 0.001	1.755 ± 0.002	11.4	10.9	
348	010823.77+141450.0	51811	51878	2.258 ± 0.001	2.259 ± 0.002	14.4	13.7	

Table 1—Continued

Number	SDSS J	MJD		HSN	$z$	LSN	$S/N_r$	
		HSN	LSN				HSN	LSN
349	010531.94+135548.8	51811	51878	1.791 ± 0.002	1.788 ± 0.002	13.4	11.6	
350	010725.09+153900.0	51811	51878	1.763 ± 0.001	1.761 ± 0.001	9.6	14.1	
351	010931.40+144729.1	51811	51878	2.066 ± 0.002	2.064 ± 0.001	14.7	13.7	
352	011036.55+145737.6	51811	51878	1.693 ± 0.002	1.694 ± 0.002	13.4	12.6	
353	011309.05+153553.7	51811	51878	1.807 ± 0.002	1.807 ± 0.002	19.5	19.3	
354	094012.22–004627.1	52314	52027	2.343 ± 0.003	2.328 ± 0.006	9.8	6.9	
355	093759.81–004051.3	52314	52027	2.066 ± 0.002	2.067 ± 0.001	4.8	4.6	
356	093805.41–000637.5	52314	52027	2.098 ± 0.002	2.104 ± 0.002	7.7	6.4	
357	093622.06–004555.4	52314	52027	1.776 ± 0.002	1.778 ± 0.002	3.3	2.7	
358	093736.74–000732.1	52314	52027	1.789 ± 0.002	1.791 ± 0.002	8.3	5.1	
359	093715.35–002106.7	52314	52027	3.125 ± 0.002	3.114 ± 0.001	2.6	1.9	
360	093547.44–001541.4	52314	52027	1.949 ± 0.002	0.648 ± 0.002	3.1	2.9	
361	093355.09–004109.8	52314	52027	1.677 ± 0.001	1.679 ± 0.002	5.9	5.1	
362	093423.78–003015.3	52314	52027	1.941 ± 0.002	1.937 ± 0.002	10.3	10.5	
363	093233.65–003441.9	52314	52027	1.836 ± 0.002	1.838 ± 0.002	4.1	2.8	
364	093308.64–000834.1	52314	52027	2.543 ± 0.002	2.550 ± 0.001	8.6	7.0	
365	093150.57–001935.2	52314	52027	1.839 ± 0.002	1.836 ± 0.002	8.8	8.3	
366	093129.00+000825.2	52314	52027	2.020 ± 0.002	2.003 ± 0.005	6.6	5.7	
367	093411.51+002952.1	52314	52027	1.907 ± 0.002	1.916 ± 0.002	14.7	12.0	
368	093450.69+004716.0	52314	52027	2.210 ± 0.002	2.211 ± 0.002	14.1	12.9	
369	093551.20+002333.0	52314	52027	1.758 ± 0.002	1.756 ± 0.002	3.6	3.0	
370	093556.91+002255.6	52314	52027	3.750 ± 0.001	3.754 ± 0.001	15.2	12.5	
371	093716.63+001824.4	52314	52027	1.673 ± 0.002	1.680 ± 0.002	7.4	6.3	
372	093846.09+010130.1	52314	52027	1.896 ± 0.002	1.909 ± 0.001	5.9	5.1	
373	094026.17–000131.7	52314	52027	1.983 ± 0.002	1.014 ± 0.002	7.7	7.5	
374	094149.60+003254.3	52314	52027	2.003 ± 0.002	2.003 ± 0.003	3.1	3.5	
375	131615.03+012449.0	52295	52029	1.734 ± 0.000	1.732 ± 0.001	8.4	6.9	
376	131712.01+020225.0	52295	52029	2.155 ± 0.002	2.159 ± 0.002	7.6	6.5	
377	131545.73+020505.1	52295	52029	2.247 ± 0.002	2.247 ± 0.002	12.3	9.3	

Table 1—Continued

Number	SDSS J	MJD		HSN	$z$	LSN	$S/N_r$	
		HSN	LSN				HSN	LSN
378	131349.47+012051.2	52295	52029	1.940 ± 0.003	1.941 ± 0.002	18.0	13.1	
379	131439.23+021214.9	52295	52029	1.776 ± 0.001	1.776 ± 0.002	6.3	5.7	
380	131215.80+021432.1	52295	52029	1.674 ± 0.002	1.678 ± 0.003	11.1	7.6	
381	131040.74+020127.0	52295	52029	1.827 ± 0.002	1.828 ± 0.002	12.5	7.8	
382	130754.43+021820.2	52295	52029	1.868 ± 0.002	1.862 ± 0.002	7.9	4.4	
383	130855.25+030614.2	52295	52029	1.785 ± 0.002	1.783 ± 0.002	9.8	7.7	
384	130848.84+024308.9	52295	52029	2.100 ± 0.002	2.101 ± 0.002	8.5	5.6	
385	130825.64+025736.0	52295	52029	1.754 ± 0.002	1.755 ± 0.002	10.9	4.3	
386	131228.34+033758.6	52295	52029	2.014 ± 0.004	2.003 ± 0.003	8.9	6.3	
387	131404.91+024959.1	52295	52029	1.948 ± 0.003	1.948 ± 0.001	11.9	8.3	
388	082050.72+431146.1	52207	51959	2.496 ± 0.002	2.497 ± 0.001	10.0	7.2	
389	082033.97+432751.8	52207	51959	2.407 ± 0.003	2.404 ± 0.002	22.2	14.4	
390	081647.23+432921.8	52207	51959	1.851 ± 0.002	1.848 ± 0.002	6.1	4.9	
391	081152.56+434051.2	52207	51959	2.184 ± 0.003	2.187 ± 0.002	12.7	8.4	
392	081348.96+440901.9	52207	51959	2.280 ± 0.002	2.275 ± 0.002	8.6	7.5	
393	081349.02+441517.7	52207	51959	2.215 ± 0.002	2.210 ± 0.002	13.6	11.4	
394	081241.12+442129.0	52207	51959	4.350 ± 0.001	4.353 ± 0.001	7.7	6.1	
395	081752.07+450728.6	52207	51959	2.037 ± 0.002	2.039 ± 0.002	16.6	13.6	
396	081743.90+444931.7	52207	51959	1.663 ± 0.002	1.660 ± 0.002	17.0	14.0	
397	081810.03+443148.8	52207	51959	3.877 ± 0.001	3.863 ± 0.001	11.6	8.8	
398	081614.97+435640.2	52207	51959	1.958 ± 0.100	1.957 ± 0.002	5.2	4.8	
399	081926.52+445759.9	52207	51959	1.713 ± 0.002	1.708 ± 0.002	9.3	6.8	
400	081931.48+450801.5	52207	51959	1.872 ± 0.001	1.871 ± 0.002	18.0	14.9	
401	081845.12+441211.2	52207	51959	2.282 ± 0.000	2.282 ± 0.002	10.0	7.4	
402	082049.80+440736.3	52207	51959	1.850 ± 0.002	1.854 ± 0.002	12.0	9.6	
403	082059.16+442820.4	52207	51959	1.931 ± 0.001	1.932 ± 0.002	8.0	6.2	
404	082310.94+442048.1	52207	51959	1.780 ± 0.002	1.781 ± 0.002	13.9	12.6	
405	082140.54+445609.3	52207	51959	2.115 ± 0.002	2.114 ± 0.004	12.6	10.3	
406	082418.40+441256.9	52207	51959	1.673 ± 0.002	1.674 ± 0.002	8.5	7.6	

Table 1—Continued

Number	SDSS J	MJD		HSN	$z$	LSN	$S/N_r$	
		HSN	LSN				HSN	LSN
407	082501.99+435338.4	52207	51959	1.903 ± 0.002	1.903 ± 0.002	12.8	14.1	
408	154400.16+531903.3	52374	52442	2.975 ± 0.001	2.945 ± 0.006	23.6	17.6	
409	154358.50+532125.6	52374	52442	1.656 ± 0.002	1.662 ± 0.002	13.0	9.4	
410	154401.17+534049.3	52374	52442	2.290 ± 0.002	2.294 ± 0.002	8.9	7.8	
411	154359.44+535903.1	52374	52442	2.370 ± 0.002	2.350 ± 0.014	33.7	32.9	
412	154125.46+534812.9	52374	52442	2.543 ± 0.002	2.526 ± 0.006	12.4	10.6	
413	154025.43+535129.9	52374	52442	1.831 ± 0.002	1.835 ± 0.002	11.2	9.9	
414	154012.56+531145.7	52374	52442	1.757 ± 0.001	1.763 ± 0.002	6.8	4.8	
415	154102.52+530048.1	52374	52442	2.565 ± 0.001	2.565 ± 0.001	17.3	12.0	
416	153925.02+532439.5	52374	52442	3.168 ± 0.002	3.187 ± 0.001	4.0	2.8	
417	153527.89+534014.4	52374	52442	1.650 ± 0.002	1.646 ± 0.002	7.5	6.0	
418	153501.74+534626.5	52374	52442	1.796 ± 0.001	1.793 ± 0.002	17.1	15.5	
419	153727.20+531619.7	52374	52442	1.885 ± 0.002	1.885 ± 0.002	10.2	6.5	
420	153215.89+535416.4	52374	52442	1.795 ± 0.002	1.797 ± 0.002	15.1	11.3	
421	153001.69+540452.3	52374	52442	1.721 ± 0.001	1.719 ± 0.002	13.7	8.7	
422	153658.76+550040.3	52374	52442	1.940 ± 0.002	1.940 ± 0.002	16.6	11.2	
423	153417.95+541252.5	52374	52442	3.136 ± 0.002	3.135 ± 0.001	9.6	7.6	
424	153737.59+541228.5	52374	52442	1.661 ± 0.002	1.658 ± 0.002	9.2	7.9	
425	153943.87+543546.9	52374	52442	1.659 ± 0.002	1.657 ± 0.002	12.1	10.0	
426	154052.43+551104.7	52374	52442	1.924 ± 0.002	1.924 ± 0.001	12.1	9.1	
427	154253.86+551225.1	52374	52442	2.188 ± 0.002	2.190 ± 0.002	12.5	9.2	
428	160127.66+505807.0	52375	52081	2.383 ± 0.001	2.409 ± 0.002	9.8	4.9	
429	160202.11+495904.3	52375	52081	2.024 ± 0.001	2.020 ± 0.002	17.6	9.1	
430	160252.65+493914.5	52375	52081	1.795 ± 0.001	1.790 ± 0.002	13.6	7.9	
431	155502.30+502531.3	52375	52081	1.794 ± 0.001	1.793 ± 0.002	15.1	8.5	
432	155623.63+502255.0	52375	52081	1.776 ± 0.002	1.772 ± 0.002	6.8	3.9	
433	155640.99+502139.4	52375	52081	1.865 ± 0.001	1.855 ± 0.001	11.3	5.4	
434	155818.88+514536.0	52375	52081	2.318 ± 0.002	2.329 ± 0.002	13.2	5.7	
435	155704.97+514435.4	52375	52081	3.757 ± 0.001	3.754 ± 0.001	4.0	2.3	



Table 1—Continued

Number	SDSS J	MJD		HSN	$z$	LSN	$S/N_r$	
		HSN	LSN				HSN	LSN
436	155917.35+520244.9	52375	52081	$3.042 \pm 0.002$		$3.042 \pm 0.001$	10.5	4.9
437	155922.10+515104.5	52375	52081	$1.860 \pm 0.003$		$1.862 \pm 0.002$	13.0	5.3
438	160126.32+511038.1	52375	52081	$1.844 \pm 0.002$		$1.847 \pm 0.002$	9.5	3.7
439	160547.59+511330.2	52375	52081	$1.785 \pm 0.002$		$1.782 \pm 0.001$	8.0	3.6
440	160247.40+514417.9	52375	52081	$1.948 \pm 0.001$		$1.939 \pm 0.005$	8.7	4.6
441	160529.50+515900.6	52375	52081	$1.656 \pm 0.002$		$1.658 \pm 0.002$	11.4	4.8
442	231040.97–010823.0	52884	52534	$2.065 \pm 0.001$		$2.066 \pm 0.001$	8.7	7.2
443	231209.93–005658.7	52884	52534	$2.989 \pm 0.001$		$2.990 \pm 0.001$	6.3	4.5
444	231242.98–005244.5	52884	52534	$2.192 \pm 0.002$		$2.189 \pm 0.002$	6.6	4.9
445	231312.07–001657.9	52884	52534	$3.791 \pm 0.002$		$3.825 \pm 0.000$	4.4	2.7
446	230952.29–003138.9	52884	52534	$3.975 \pm 0.003$		$3.975 \pm 0.000$	6.7	4.5
447	230745.01–005122.8	52884	52534	$1.841 \pm 0.005$		$1.838 \pm 0.001$	5.1	3.4
448	230745.15–004542.6	52884	52534	$1.841 \pm 0.001$		$1.838 \pm 0.003$	11.4	8.1
449	230638.25–010700.2	52884	52534	$2.313 \pm 0.001$		$2.296 \pm 0.005$	11.3	9.1
450	230504.46–010451.3	52884	52534	$2.023 \pm 0.001$		$1.052 \pm 0.003$	6.0	3.9
451	230437.65–005703.3	52884	52534	$2.492 \pm 0.001$		$2.503 \pm 0.001$	5.8	4.5
452	230402.78–003855.4	52884	52534	$2.773 \pm 0.001$		$2.771 \pm 0.001$	3.3	2.4
453	230424.87–010140.8	52884	52534	$1.890 \pm 0.001$		$1.886 \pm 0.000$	3.0	2.6
454	230228.94+002249.1	52884	52534	$1.694 \pm 0.002$		$1.694 \pm 0.002$	14.2	11.6
455	230239.68+002702.5	52884	52534	$1.864 \pm 0.001$		$1.857 \pm 0.004$	3.1	3.1
456	230524.46+005209.7	52884	52534	$1.846 \pm 0.002$		$1.844 \pm 0.001$	6.5	2.7
457	230323.77+001615.1	52884	52534	$3.691 \pm 0.001$		$3.688 \pm 0.001$	4.3	3.6
458	230435.93+003001.5	52884	52534	$2.002 \pm 0.001$		$0.676 \pm 0.003$	3.4	2.8
459	230441.51+003307.2	52884	52534	$3.326 \pm 0.002$		$3.323 \pm 0.001$	6.1	3.8
460	230603.79+000319.7	52884	52534	$1.813 \pm 0.002$		$1.811 \pm 0.002$	3.8	2.9
461	230524.30+003034.0	52884	52534	$1.755 \pm 0.002$		$1.756 \pm 0.001$	15.0	9.7
462	230724.97+000957.8	52884	52534	$1.898 \pm 0.001$		$1.897 \pm 0.001$	9.0	6.7
463	230839.94+010548.4	52884	52534	$1.745 \pm 0.002$		$1.745 \pm 0.002$	6.2	4.5
464	230936.87+005215.5	52884	52534	$2.221 \pm 0.001$		$2.221 \pm 0.002$	9.0	7.0

Table 1—Continued

Number	SDSS J	MJD		HSN	$z$	LSN	$S/N_r$	
		HSN	LSN				HSN	LSN
465	230959.52+005537.4	52884	52534	2.401 ± 0.001	2.400 ± 0.004	18.0	14.3	
466	230957.65−000127.2	52884	52534	2.110 ± 0.002	2.117 ± 0.002	5.0	3.7	
467	231055.32+004817.2	52884	52534	2.994 ± 0.002	2.994 ± 0.001	14.1	8.4	
468	231121.98+004959.7	52884	52534	2.063 ± 0.002	2.063 ± 0.001	10.4	5.6	
469	231147.89+002941.9	52884	52534	1.901 ± 0.001	1.901 ± 0.001	9.5	7.1	
470	231241.77+002450.3	52884	52534	1.893 ± 0.002	1.885 ± 0.004	15.9	7.7	
471	224408.50+123315.5	52520	52264	2.145 ± 0.001	2.148 ± 0.001	18.7	7.3	
472	224145.11+122557.1	52520	52264	2.630 ± 0.003	2.614 ± 0.006	24.5	11.3	
473	223619.19+132620.3	52520	52264	3.296 ± 0.003	3.280 ± 0.005	18.2	6.8	
474	223536.42+125724.8	52520	52264	2.066 ± 0.001	2.054 ± 0.002	8.1	3.0	
475	223809.92+140409.9	52520	52264	2.223 ± 0.002	2.221 ± 0.002	13.5	5.5	
476	223848.23+133926.8	52520	52264	2.228 ± 0.002	2.227 ± 0.002	12.2	5.2	
477	223843.99+140226.9	52520	52264	2.003 ± 0.001	1.990 ± 0.003	11.8	3.8	
478	224005.09+143147.8	52520	52264	3.491 ± 0.002	3.508 ± 0.000	4.7	1.1	
479	224101.41+144334.5	52520	52264	1.699 ± 0.002	1.701 ± 0.002	13.3	4.5	
480	075153.67+331319.8	52237	52577	1.928 ± 0.003	1.932 ± 0.002	13.9	7.6	
481	075217.23+335524.5	52237	52577	1.683 ± 0.003	1.682 ± 0.001	5.8	5.1	
482	075225.59+334310.0	52237	52577	1.728 ± 0.005	1.725 ± 0.002	12.0	13.2	
483	075118.29+323704.3	52237	52577	2.152 ± 0.002	2.155 ± 0.002	9.3	10.2	
484	075149.83+335517.2	52237	52577	2.054 ± 0.001	2.065 ± 0.002	3.5	4.1	
485	075044.04+340658.4	52237	52577	2.145 ± 3.900	2.146 ± 0.002	24.6	22.0	
486	074902.48+340108.2	52237	52577	1.763 ± 0.001	1.758 ± 0.002	10.5	10.0	
487	074758.66+335432.5	52237	52577	1.689 ± 0.002	1.700 ± 0.001	6.3	9.2	
488	074823.86+332051.2	52237	52577	2.988 ± 0.002	2.989 ± 0.001	6.3	9.1	
489	074701.96+332213.1	52237	52577	2.167 ± 0.001	2.164 ± 0.001	7.8	8.4	
490	074851.16+343359.1	52237	52577	3.312 ± 0.002	3.330 ± 0.001	13.4	13.4	
491	075133.67+341906.0	52237	52577	1.942 ± 0.001	1.939 ± 0.002	17.8	17.6	
492	075218.49+352815.5	52237	52577	1.727 ± 0.002	1.727 ± 0.002	12.0	11.3	
493	075412.60+343625.7	52237	52577	1.754 ± 0.001	1.757 ± 0.001	9.7	9.3	

Table 1—Continued

Number	SDSS J	MJD		HSN	$z$	LSN	$S/N_r$	
		HSN	LSN				HSN	LSN
494	075321.93+350733.6	52237	52577	$1.895 \pm 0.002$		$1.907 \pm 0.001$	3.8	5.0
495	075524.11+342134.5	52237	52577	$2.125 \pm 0.001$		$2.126 \pm 0.002$	33.4	29.8
496	075430.58+345521.8	52237	52577	$1.777 \pm 0.002$		$1.778 \pm 0.002$	9.1	9.6
497	075813.28+343828.6	52237	52577	$2.258 \pm 0.001$		$2.257 \pm 0.002$	13.5	13.5
498	075639.17+350315.9	52237	52577	$2.051 \pm 0.002$		$2.040 \pm 0.001$	5.7	4.3
499	144405.65+571444.8	52346	52433	$1.800 \pm 0.002$		$1.793 \pm 0.002$	16.1	11.1
500	144439.83+573119.7	52346	52433	$1.994 \pm 0.002$		$0.671 \pm 0.001$	6.5	3.4
501	143934.15+570110.1	52346	52433	$2.035 \pm 0.002$		$2.041 \pm 0.001$	8.5	5.9
502	143959.46+572717.1	52346	52433	$1.786 \pm 0.001$		$1.785 \pm 0.002$	5.8	4.9
503	144013.62+573336.3	52346	52433	$1.713 \pm 0.001$		$1.717 \pm 0.003$	9.1	7.1
504	144059.16+573724.3	52346	52433	$2.041 \pm 0.002$		$2.040 \pm 0.002$	6.0	5.7
505	143624.07+564909.2	52346	52433	$2.106 \pm 0.002$		$2.110 \pm 0.001$	17.0	14.5
506	143124.31+572803.5	52346	52433	$2.066 \pm 0.002$		$2.066 \pm 0.001$	16.3	14.3
507	143118.11+572428.6	52346	52433	$3.243 \pm 0.008$		$3.253 \pm 0.001$	13.1	11.7
508	143252.46+564847.7	52346	52433	$2.034 \pm 0.001$		$2.037 \pm 0.001$	14.8	12.4
509	143125.24+565858.5	52346	52433	$2.044 \pm 0.001$		$2.062 \pm 0.000$	6.8	5.5
510	143200.72+570526.0	52346	52433	$2.192 \pm 0.001$		$2.192 \pm 0.002$	6.9	4.9
511	142451.40+574540.6	52346	52433	$2.811 \pm 0.002$		$2.815 \pm 0.001$	11.1	8.2
512	143325.24+583455.3	52346	52433	$1.833 \pm 0.007$		$1.834 \pm 0.002$	7.7	6.0
513	143602.15+591459.4	52346	52433	$1.767 \pm 0.000$		$1.763 \pm 0.002$	11.9	10.8
514	143807.63+580701.0	52346	52433	$1.999 \pm 0.001$		$1.989 \pm 0.002$	8.8	5.9
515	143848.90+584909.4	52346	52433	$1.792 \pm 0.002$		$1.796 \pm 0.002$	4.9	3.9
516	143838.86+584004.1	52346	52433	$1.996 \pm 0.000$		$1.996 \pm 0.002$	8.5	6.5
517	144034.18+580351.7	52346	52433	$1.680 \pm 0.001$		$1.679 \pm 0.001$	14.7	9.4
518	145316.61+560750.8	52347	52435	$1.847 \pm 0.001$		$1.842 \pm 0.001$	2.6	2.5
519	145158.79+560515.1	52347	52435	$2.225 \pm 0.001$		$2.225 \pm 0.002$	8.9	9.9
520	145028.76+561901.7	52347	52435	$1.784 \pm 0.001$		$1.785 \pm 0.002$	10.1	11.6
521	144346.27+564545.8	52347	52435	$2.772 \pm 0.001$		$2.732 \pm 0.020$	7.1	7.3
522	144255.80+563138.5	52347	52435	$2.099 \pm 0.001$		$2.094 \pm 0.002$	6.5	6.3

Table 1—Continued

Number	SDSS J	MJD		HSN	$z$	LSN	$S/N_r$	
		HSN	LSN				HSN	LSN
523	144306.67+563112.7	52347	52435	$2.464 \pm 0.002$		$2.463 \pm 0.001$	14.0	13.4
524	144408.38+570445.8	52347	52435	$1.890 \pm 0.001$		$1.887 \pm 0.001$	4.6	5.6
525	144641.21+571040.6	52347	52435	$2.105 \pm 0.001$		$2.107 \pm 0.002$	9.1	9.4
526	144621.41+570041.6	52347	52435	$1.861 \pm 0.002$		$1.862 \pm 0.002$	13.2	14.5
527	144918.17+574953.6	52347	52435	$1.983 \pm 0.002$		$1.995 \pm 0.002$	10.9	12.9
528	033356.92–003122.9	52672	52326	$1.865 \pm 0.002$		$1.866 \pm 0.002$	19.0	13.3
529	033523.31–002203.9	52672	52326	$1.768 \pm 0.001$		$1.767 \pm 0.002$	25.9	20.2
530	032933.97–004801.1	52672	52326	$1.877 \pm 0.001$		$1.878 \pm 0.001$	12.1	10.4
531	033351.52+002341.6	52672	52326	$1.818 \pm 0.002$		$1.817 \pm 0.002$	15.3	11.9
532	162034.40+441756.0	52443	52355	$1.783 \pm 0.002$		$1.786 \pm 0.002$	9.0	4.2
533	161801.99+441219.0	52443	52355	$2.073 \pm 0.002$		$2.078 \pm 0.001$	12.2	5.3
534	161354.18+444129.0	52443	52355	$1.860 \pm 0.002$		$1.861 \pm 0.003$	6.2	3.0
535	161354.47+445245.6	52443	52355	$2.681 \pm 0.002$		$2.690 \pm 0.001$	12.6	5.7
536	161141.44+443707.3	52443	52355	$1.676 \pm 0.003$		$1.672 \pm 0.002$	10.0	4.7
537	161137.22+443024.5	52443	52355	$1.682 \pm 0.002$		$1.678 \pm 0.000$	7.7	2.9
538	161115.13+443909.6	52443	52355	$2.028 \pm 0.001$		$1.014 \pm 0.001$	4.0	1.4
539	161240.98+435749.3	52443	52355	$1.741 \pm 0.001$		$1.766 \pm 0.001$	4.0	0.7
540	161003.54+442353.7	52443	52355	$2.600 \pm 0.003$		$2.581 \pm 0.006$	18.8	8.5
541	160851.52+460352.5	52443	52355	$1.774 \pm 0.001$		$1.775 \pm 0.001$	13.5	5.3
542	161253.92+451341.5	52443	52355	$2.256 \pm 0.002$		$2.260 \pm 0.001$	10.3	5.5
543	161958.24+452631.2	52443	52355	$2.689 \pm 0.002$		$2.686 \pm 0.001$	5.5	2.3
544	161937.94+453338.4	52443	52355	$1.875 \pm 0.001$		$1.877 \pm 0.001$	4.4	2.0
545	102532.57+474919.7	52347	52674	$1.926 \pm 0.002$		$1.925 \pm 0.002$	8.7	8.5
546	102007.29+473124.1	52347	52674	$2.101 \pm 0.002$		$2.099 \pm 0.002$	8.9	8.8
547	102119.53+474703.7	52347	52674	$1.767 \pm 0.002$		$1.768 \pm 0.002$	11.5	10.8
548	101902.02+473714.5	52347	52674	$2.948 \pm 0.002$		$2.945 \pm 0.001$	9.7	7.7
549	101620.58+474227.3	52347	52674	$2.002 \pm 0.001$		$1.983 \pm 0.003$	9.9	11.1
550	101408.82+473150.6	52347	52674	$1.895 \pm 0.002$		$1.899 \pm 0.002$	9.4	11.1
551	101416.97+484816.1	52347	52674	$1.905 \pm 0.002$		$1.906 \pm 0.002$	12.1	12.3

Table 1—Continued

Number	SDSS J	MJD		HSN	$z$	LSN	$S/N_r$	
		HSN	LSN				HSN	LSN
552	101830.23+485110.2	52347	52674	1.852 ± 0.001	1.855 ± 0.002	12.3	10.3	
553	102048.82+483908.8	52347	52674	1.940 ± 0.002	1.940 ± 0.002	17.5	16.9	
554	102121.78+492059.0	52347	52674	3.415 ± 0.002	3.398 ± 0.001	5.5	4.6	
555	102111.02+491330.3	52347	52674	1.720 ± 0.001	1.720 ± 0.002	10.8	9.3	
556	105813.05+493936.1	52346	52669	2.399 ± 0.002	2.394 ± 0.002	5.6	7.2	
557	105657.54+492957.9	52346	52669	2.160 ± 0.001	2.162 ± 0.003	12.2	16.5	
558	105922.46+494918.2	52346	52669	1.680 ± 0.001	1.691 ± 0.002	2.7	5.9	
559	105820.66+494604.1	52346	52669	1.835 ± 0.002	1.833 ± 0.003	3.3	8.2	
560	105859.13+501000.7	52346	52669	3.269 ± 0.001	3.271 ± 0.001	10.1	11.9	
561	105629.61+494340.6	52346	52669	3.800 ± 0.002	3.801 ± 0.001	5.0	6.1	
562	105027.74+490453.0	52346	52669	1.864 ± 0.001	1.866 ± 0.001	6.2	11.1	
563	104951.09+493156.2	52346	52669	1.791 ± 0.001	1.786 ± 0.002	7.4	9.7	
564	104816.63+492714.1	52346	52669	1.951 ± 0.002	1.952 ± 0.002	10.6	10.4	
565	104810.44+501150.0	52346	52669	2.165 ± 0.002	2.172 ± 0.003	13.2	9.7	
566	104806.47+501021.5	52346	52669	1.784 ± 0.002	1.785 ± 0.002	3.8	3.6	
567	104524.48+492822.0	52346	52669	2.886 ± 0.002	2.895 ± 0.001	7.4	6.1	
568	104620.97+495337.8	52346	52669	1.905 ± 0.000	1.907 ± 0.002	12.9	10.6	
569	104344.95+494516.7	52346	52669	2.421 ± 0.001	2.481 ± 0.002	16.8	10.8	
570	104426.25+510506.2	52346	52669	1.961 ± 0.002	1.959 ± 0.002	11.6	9.5	
571	105002.65+512729.5	52346	52669	1.813 ± 0.001	1.812 ± 0.002	15.9	11.1	
572	105119.30+510544.8	52346	52669	1.778 ± 0.001	1.775 ± 0.002	15.5	10.6	
573	104855.22+504845.5	52346	52669	1.781 ± 0.002	1.778 ± 0.002	12.1	9.9	
574	105213.30+512826.1	52346	52669	1.689 ± 0.001	1.687 ± 0.002	8.5	7.0	
575	105416.46+512724.5	52346	52669	2.371 ± 0.001	2.368 ± 0.001	16.1	12.7	
576	105410.51+505905.1	52346	52669	3.363 ± 0.002	0.637 ± 0.004	9.4	9.1	
577	105427.92+504835.6	52346	52669	1.973 ± 0.002	1.980 ± 0.002	8.5	6.3	
578	105454.16+503123.9	52346	52669	1.874 ± 0.001	1.876 ± 0.003	19.1	12.4	
579	105546.18+503959.7	52346	52669	2.016 ± 0.001	2.017 ± 0.001	17.8	14.7	
580	105526.66+511328.7	52346	52669	1.776 ± 0.001	1.777 ± 0.002	7.0	5.2	

Table 1—Continued

Number	SDSS J	MJD		HSN	$z$	LSN	$S/N_r$	
		HSN	LSN				HSN	LSN
581	105828.00+505700.9	52346	52669	1.669 ± 0.002	1.672 ± 0.002	13.5	9.1	
582	105724.69+502030.3	52346	52669	1.718 ± 0.002	1.715 ± 0.002	7.8	8.3	
583	105844.23+503315.7	52346	52669	2.243 ± 0.001	2.240 ± 0.002	13.2	9.6	
584	074709.64+293756.2	52346	52663	1.953 ± 0.002	1.939 ± 0.002	9.4	8.7	
585	074407.41+294707.4	52346	52663	1.861 ± 0.001	1.862 ± 0.002	10.9	14.0	
586	074254.58+294714.9	52346	52663	2.182 ± 0.002	2.182 ± 0.002	12.8	12.1	
587	074228.13+292123.8	52346	52663	2.178 ± 0.002	2.176 ± 0.002	12.9	12.6	
588	074311.52+302549.1	52346	52663	1.770 ± 0.002	1.769 ± 0.002	10.8	8.2	
589	074357.06+300742.7	52346	52663	2.177 ± 0.002	2.177 ± 0.002	15.6	14.6	
590	074440.17+300241.8	52346	52663	1.667 ± 0.001	1.667 ± 0.002	12.8	11.8	
591	074412.05+295906.7	52346	52663	1.696 ± 0.002	1.703 ± 0.003	22.9	19.0	
592	074625.28+302020.7	52346	52663	1.735 ± 0.001	1.735 ± 0.002	27.8	21.7	
593	074834.86+302550.4	52346	52663	1.743 ± 0.002	1.742 ± 0.003	10.1	11.2	
594	074809.46+300630.5	52346	52663	1.693 ± 0.002	1.694 ± 0.002	18.6	19.2	
595	074914.13+305605.8	52346	52663	3.435 ± 0.002	3.436 ± 0.001	13.1	11.8	
596	074937.74+304021.4	52346	52663	1.729 ± 0.002	1.718 ± 0.002	3.7	4.8	
597	221227.74+005140.6	52813	52525	1.773 ± 0.002	1.770 ± 0.001	13.5	10.9	
598	082443.39+055503.7	52962	52737	2.102 ± 0.003	2.100 ± 0.001	13.3	9.0	
599	082311.10+055643.6	52962	52737	1.761 ± 0.002	1.763 ± 0.002	9.8	5.9	
600	082719.65+061835.3	52962	52737	2.182 ± 0.002	2.185 ± 0.001	6.3	3.9	
601	082807.73+062133.9	52962	52737	2.154 ± 0.001	2.153 ± 0.002	21.4	12.4	
602	082736.89+061812.1	52962	52737	2.195 ± 0.002	2.194 ± 0.001	28.6	18.6	
603	082117.41+054536.4	52962	52737	1.837 ± 0.002	1.837 ± 0.002	13.3	7.5	
604	082328.61+061146.0	52962	52737	2.783 ± 0.002	2.790 ± 0.001	24.8	14.6	
605	082256.01+060528.7	52962	52737	1.983 ± 0.002	1.965 ± 0.008	9.4	4.2	
606	081941.12+054942.6	52962	52737	1.701 ± 0.002	1.697 ± 0.003	2.8	2.3	
607	081931.48+055523.6	52962	52737	1.687 ± 0.002	1.696 ± 0.002	21.1	12.6	
608	081653.90+064307.1	52962	52737	1.824 ± 0.001	1.822 ± 0.002	8.3	5.4	
609	082257.04+070104.3	52962	52737	2.954 ± 0.002	2.956 ± 0.001	17.5	10.2	

Table 1—Continued

Number	SDSS J	MJD		HSN	$z$	LSN	$S/N_r$	
		HSN	LSN				HSN	LSN
610	082503.56+071344.0	52962	52737	$2.524 \pm 0.002$		$2.547 \pm 0.001$	10.0	6.8
611	082305.95+064930.5	52962	52737	$1.665 \pm 0.001$		$1.668 \pm 0.002$	15.5	10.9
612	082404.91+064322.2	52962	52737	$1.865 \pm 0.001$		$1.871 \pm 0.002$	8.5	5.9
613	082645.88+071647.0	52962	52737	$3.137 \pm 0.002$		$3.122 \pm 0.001$	18.3	12.5
614	082628.00+062556.5	52962	52737	$1.983 \pm 0.002$		$1.982 \pm 0.002$	10.7	7.5
615	082710.95+071650.5	52962	52737	$3.151 \pm 0.002$		$3.142 \pm 0.001$	4.2	2.6

Table 2. 1450Å Luminosity, C IV line dispersion, and estimated black hole mass at both epochs for all objects.

Number	$L_{1450}$ $10^{44} \text{ erg s}^{-1}$		$\sigma_{\text{C IV}}$ $\text{km s}^{-1}$		$\log(M_{\text{BH}}/M_{\odot})$	
	HSN	LSN	HSN	LSN	HSN	LSN
1	48 ± 8	57 ± 11	3834 ± 97	3740 ± 159	8.79 ± 0.05	8.81 ± 0.06
2	197 ± 17	212 ± 22	4197 ± 125	4408 ± 122	9.19 ± 0.03	9.25 ± 0.03
3	105 ± 10	193 ± 18	3456 ± 141	3440 ± 261	8.88 ± 0.04	9.01 ± 0.07
4	396 ± 23	315 ± 22	3371 ± 118	3320 ± 119	9.16 ± 0.03	9.10 ± 0.04
5	208 ± 21	164 ± 20	3942 ± 144	3970 ± 159	9.15 ± 0.04	9.10 ± 0.05
6	379 ± 45	268 ± 49	2919 ± 114	2708 ± 174	9.03 ± 0.04	8.88 ± 0.07
7	86 ± 11	73 ± 10	3294 ± 181	2229 ± 475	8.79 ± 0.06	8.41 ± 0.19
8	58 ± 8	48 ± 6	3784 ± 189	3904 ± 155	8.82 ± 0.06	8.81 ± 0.05
9	224 ± 20	235 ± 24	3786 ± 184	3732 ± 218	9.13 ± 0.05	9.13 ± 0.06
10	127 ± 12	117 ± 13	3735 ± 164	3627 ± 174	8.99 ± 0.04	8.95 ± 0.05
11	291 ± 20	321 ± 27	3688 ± 103	3703 ± 161	9.17 ± 0.03	9.20 ± 0.04
12	92 ± 8	122 ± 14	3877 ± 149	3903 ± 292	8.95 ± 0.04	9.02 ± 0.07
13	92 ± 10	106 ± 15	3658 ± 92	3626 ± 112	8.90 ± 0.03	8.92 ± 0.04
14	311 ± 21	312 ± 24	4120 ± 97	4009 ± 131	9.28 ± 0.03	9.26 ± 0.03
15	206 ± 14	207 ± 9	3487 ± 91	4118 ± 61	9.04 ± 0.03	9.19 ± 0.02
16	109 ± 16	128 ± 24	3658 ± 155	3564 ± 209	8.94 ± 0.05	8.95 ± 0.07
17	64 ± 6	79 ± 13	4163 ± 148	3770 ± 427	8.93 ± 0.04	8.89 ± 0.11
18	166 ± 11	197 ± 23	4765 ± 34	4636 ± 62	9.26 ± 0.02	9.28 ± 0.03
19	37 ± 7	53 ± 10	4098 ± 133	3921 ± 189	8.79 ± 0.05	8.83 ± 0.06
20	91 ± 9	123 ± 17	3960 ± 93	3294 ± 245	8.96 ± 0.03	8.87 ± 0.07
21	310 ± 23	373 ± 50	3317 ± 69	3116 ± 138	9.09 ± 0.03	9.08 ± 0.05
22	247 ± 12	340 ± 26	3648 ± 82	3622 ± 145	9.12 ± 0.02	9.19 ± 0.04
23	29 ± 6	20 ± 13	4205 ± 350	4115 ± 556	8.76 ± 0.09	8.65 ± 0.20
24	62 ± 7	58 ± 12	3713 ± 224	4024 ± 319	8.82 ± 0.06	8.88 ± 0.08
25	131 ± 7	122 ± 14	3018 ± 91	2769 ± 215	8.81 ± 0.03	8.72 ± 0.07
26	175 ± 15	189 ± 26	3680 ± 127	3542 ± 241	9.05 ± 0.04	9.04 ± 0.07
27	121 ± 12	167 ± 18	3738 ± 138	3364 ± 263	8.98 ± 0.04	8.96 ± 0.07
28	110 ± 17	109 ± 20	3676 ± 186	2753 ± 603	8.94 ± 0.06	8.69 ± 0.20
29	129 ± 13	78 ± 16	4049 ± 149	3497 ± 406	9.07 ± 0.04	8.82 ± 0.11



Table 2—Continued

Number	$L_{1450}$ $10^{44} \text{ erg s}^{-1}$		$\sigma_{\text{C IV}}$ $\text{km s}^{-1}$		$\log(M_{\text{BH}}/M_{\odot})$	
	HSN	LSN	HSN	LSN	HSN	LSN
30	101 ± 8	84 ± 11	3404 ± 156	3529 ± 224	8.86 ± 0.04	8.85 ± 0.06
31	55 ± 5	55 ± 8	3596 ± 63	3460 ± 119	8.77 ± 0.03	8.73 ± 0.05
32	654 ± 19	588 ± 26	3345 ± 48	3260 ± 81	9.27 ± 0.01	9.22 ± 0.02
33	97 ± 8	91 ± 13	3022 ± 156	3359 ± 225	8.74 ± 0.05	8.82 ± 0.07
34	69 ± 8	82 ± 15	3457 ± 106	3524 ± 179	8.79 ± 0.04	8.84 ± 0.06
35	248 ± 12	261 ± 24	3733 ± 57	4037 ± 82	9.14 ± 0.02	9.22 ± 0.03
36	59 ± 7	88 ± 13	3528 ± 133	3681 ± 182	8.77 ± 0.04	8.89 ± 0.06
37	280 ± 13	264 ± 25	3749 ± 50	3490 ± 135	9.18 ± 0.02	9.10 ± 0.04
38	60 ± 6	66 ± 13	3223 ± 165	2291 ± 617	8.69 ± 0.05	8.42 ± 0.24
39	171 ± 17	142 ± 32	2612 ± 230	2826 ± 461	8.75 ± 0.08	8.77 ± 0.15
40	136 ± 8	112 ± 16	3648 ± 110	3808 ± 217	8.99 ± 0.03	8.98 ± 0.06
41	369 ± 16	313 ± 19	3912 ± 44	3956 ± 52	9.28 ± 0.01	9.25 ± 0.02
42	105 ± 8	100 ± 8	4288 ± 49	4431 ± 45	9.07 ± 0.02	9.09 ± 0.02
43	76 ± 8	54 ± 8	3339 ± 156	3357 ± 170	8.78 ± 0.05	8.70 ± 0.06
44	83 ± 11	76 ± 12	3370 ± 358	4093 ± 176	8.80 ± 0.10	8.95 ± 0.05
45	157 ± 14	126 ± 19	2429 ± 248	3181 ± 173	8.67 ± 0.09	8.85 ± 0.06
46	447 ± 35	548 ± 49	1851 ± 139	1857 ± 159	8.67 ± 0.07	8.72 ± 0.08
47	204 ± 11	216 ± 14	3660 ± 74	3536 ± 99	9.08 ± 0.02	9.07 ± 0.03
48	141 ± 12	122 ± 18	3923 ± 92	3819 ± 138	9.06 ± 0.03	9.00 ± 0.05
49	32 ± 12	14 ± 4	4156 ± 157	4063 ± 479	8.77 ± 0.09	8.56 ± 0.13
50	75 ± 9	59 ± 9	3703 ± 144	3631 ± 169	8.86 ± 0.04	8.79 ± 0.05
51	66 ± 10	58 ± 10	3341 ± 333	3702 ± 272	8.74 ± 0.09	8.80 ± 0.08
52	116 ± 8	134 ± 9	3679 ± 127	3644 ± 130	8.96 ± 0.03	8.98 ± 0.03
53	119 ± 12	108 ± 11	3479 ± 140	3445 ± 124	8.91 ± 0.04	8.88 ± 0.04
54	60 ± 7	35 ± 6	2997 ± 321	3270 ± 222	8.63 ± 0.10	8.58 ± 0.07
55	50 ± 7	51 ± 6	3872 ± 211	3956 ± 183	8.81 ± 0.06	8.83 ± 0.05
56	82 ± 11	67 ± 10	2065 ± 277	2214 ± 230	8.37 ± 0.12	8.39 ± 0.10
57	28 ± 9	30 ± 8	3439 ± 588	3820 ± 356	8.57 ± 0.17	8.68 ± 0.10
58	177 ± 47	158 ± 28	3286 ± 479	3638 ± 352	8.96 ± 0.14	9.02 ± 0.09

Table 2—Continued

Number	$L_{1450}$ $10^{44} \text{ erg s}^{-1}$		$\sigma_{C\ IV}$ $\text{km s}^{-1}$		$\log(M_{BH}/M_{\odot})$	
	HSN	LSN	HSN	LSN	HSN	LSN
59	$24 \pm 14$	$18 \pm 10$	$2911 \pm 348$	$2225 \pm 579$	$8.39 \pm 0.17$	$8.10 \pm 0.26$
60	$238 \pm 13$	$241 \pm 12$	$3721 \pm 118$	$3687 \pm 109$	$9.13 \pm 0.03$	$9.13 \pm 0.03$
61	$96 \pm 9$	$102 \pm 8$	$3338 \pm 132$	$3607 \pm 105$	$8.83 \pm 0.04$	$8.91 \pm 0.03$
62	$24 \pm 11$	$29 \pm 9$	$3512 \pm 353$	$3468 \pm 390$	$8.55 \pm 0.14$	$8.59 \pm 0.12$
63	$167 \pm 11$	$161 \pm 10$	$3307 \pm 142$	$3219 \pm 127$	$8.95 \pm 0.04$	$8.92 \pm 0.04$
64	$145 \pm 10$	$125 \pm 8$	$3581 \pm 145$	$3096 \pm 168$	$8.98 \pm 0.04$	$8.82 \pm 0.05$
65	$35 \pm 7$	$40 \pm 7$	$1550 \pm 454$	$1899 \pm 383$	$7.93 \pm 0.26$	$8.14 \pm 0.18$
66	$69 \pm 12$	$60 \pm 11$	$3608 \pm 143$	$3557 \pm 119$	$8.82 \pm 0.05$	$8.78 \pm 0.05$
67	$88 \pm 14$	$102 \pm 11$	$4255 \pm 101$	$3962 \pm 148$	$9.02 \pm 0.04$	$8.99 \pm 0.04$
68	$159 \pm 97$	$159 \pm 118$	$3501 \pm 152$	$3684 \pm 124$	$8.99 \pm 0.15$	$9.03 \pm 0.17$
69	$337 \pm 36$	$357 \pm 39$	$3397 \pm 119$	$3454 \pm 123$	$9.13 \pm 0.04$	$9.16 \pm 0.04$
70	$140 \pm 17$	$145 \pm 16$	$3382 \pm 140$	$3277 \pm 138$	$8.93 \pm 0.05$	$8.91 \pm 0.05$
71	$85 \pm 10$	$86 \pm 11$	$4136 \pm 105$	$4229 \pm 119$	$8.99 \pm 0.04$	$9.01 \pm 0.04$
72	$344 \pm 29$	$292 \pm 28$	$3173 \pm 77$	$3093 \pm 90$	$9.08 \pm 0.03$	$9.02 \pm 0.03$
73	$56 \pm 7$	$73 \pm 9$	$4145 \pm 104$	$3665 \pm 159$	$8.89 \pm 0.04$	$8.85 \pm 0.05$
74	$63 \pm 8$	$71 \pm 11$	$3536 \pm 155$	$3262 \pm 276$	$8.78 \pm 0.05$	$8.74 \pm 0.08$
75	$91 \pm 8$	$101 \pm 9$	$3175 \pm 98$	$3248 \pm 96$	$8.77 \pm 0.03$	$8.82 \pm 0.03$
76	$85 \pm 12$	$77 \pm 14$	$3507 \pm 143$	$3868 \pm 134$	$8.84 \pm 0.05$	$8.91 \pm 0.05$
77	$246 \pm 13$	$221 \pm 14$	$3682 \pm 98$	$3865 \pm 89$	$9.13 \pm 0.03$	$9.15 \pm 0.03$
78	$131 \pm 16$	$124 \pm 25$	$3697 \pm 116$	$3375 \pm 253$	$8.99 \pm 0.04$	$8.90 \pm 0.08$
79	$80 \pm 9$	$71 \pm 13$	$3645 \pm 143$	$2977 \pm 480$	$8.86 \pm 0.04$	$8.66 \pm 0.15$
80	$60 \pm 10$	$42 \pm 10$	$3374 \pm 103$	$3282 \pm 132$	$8.73 \pm 0.05$	$8.62 \pm 0.07$
81	$232 \pm 15$	$252 \pm 23$	$4046 \pm 87$	$3638 \pm 173$	$9.20 \pm 0.02$	$9.13 \pm 0.05$
82	$63 \pm 9$	$64 \pm 13$	$3923 \pm 68$	$4087 \pm 82$	$8.87 \pm 0.04$	$8.91 \pm 0.05$
83	$185 \pm 12$	$198 \pm 16$	$3331 \pm 81$	$3321 \pm 105$	$8.98 \pm 0.03$	$8.99 \pm 0.03$
84	$79 \pm 13$	$83 \pm 19$	$3452 \pm 658$	$3570 \pm 637$	$8.81 \pm 0.17$	$8.85 \pm 0.16$
85	$209 \pm 17$	$169 \pm 20$	$4183 \pm 79$	$3977 \pm 125$	$9.20 \pm 0.03$	$9.11 \pm 0.04$
86	$570 \pm 30$	$561 \pm 32$	$3977 \pm 69$	$4115 \pm 81$	$9.39 \pm 0.02$	$9.42 \pm 0.02$
87	$302 \pm 24$	$303 \pm 30$	$3433 \pm 81$	$3554 \pm 97$	$9.12 \pm 0.03$	$9.15 \pm 0.03$

Table 2—Continued

Number	$L_{1450}$ $10^{44} \text{ erg s}^{-1}$		$\sigma_{\text{C IV}}$ $\text{km s}^{-1}$		$\log(M_{\text{BH}}/M_{\odot})$	
	HSN	LSN	HSN	LSN	HSN	LSN
88	$136 \pm 13$	$123 \pm 15$	$3170 \pm 360$	$3926 \pm 178$	$8.86 \pm 0.10$	$9.03 \pm 0.05$
89	$111 \pm 10$	$95 \pm 11$	$3401 \pm 269$	$3676 \pm 230$	$8.88 \pm 0.07$	$8.91 \pm 0.06$
90	$261 \pm 21$	$209 \pm 27$	$3185 \pm 159$	$3268 \pm 179$	$9.02 \pm 0.05$	$8.99 \pm 0.06$
91	$93 \pm 20$	$77 \pm 31$	$2633 \pm 363$	$3808 \pm 196$	$8.62 \pm 0.13$	$8.89 \pm 0.10$
92	$31 \pm 7$	$44 \pm 8$	$2853 \pm 749$	$2993 \pm 673$	$8.43 \pm 0.24$	$8.55 \pm 0.20$
93	$60 \pm 71$	$98 \pm 70$	$3645 \pm 356$	$3787 \pm 272$	$8.80 \pm 0.28$	$8.94 \pm 0.18$
94	$207 \pm 13$	$214 \pm 14$	$3099 \pm 308$	$3857 \pm 145$	$8.94 \pm 0.09$	$9.14 \pm 0.04$
95	$60 \pm 8$	$65 \pm 10$	$2261 \pm 545$	$2430 \pm 518$	$8.38 \pm 0.21$	$8.46 \pm 0.19$
96	$57 \pm 7$	$41 \pm 8$	$3254 \pm 271$	$3431 \pm 327$	$8.69 \pm 0.08$	$8.66 \pm 0.10$
97	$585 \pm 28$	$602 \pm 32$	$3594 \pm 51$	$3495 \pm 68$	$9.31 \pm 0.02$	$9.29 \pm 0.02$
98	$241 \pm 27$	$310 \pm 36$	$3848 \pm 162$	$4574 \pm 147$	$9.16 \pm 0.04$	$9.37 \pm 0.04$
99	$150 \pm 12$	$149 \pm 14$	$3800 \pm 111$	$3913 \pm 123$	$9.04 \pm 0.03$	$9.07 \pm 0.04$
100	$211 \pm 9$	$223 \pm 11$	$2873 \pm 100$	$2807 \pm 115$	$8.88 \pm 0.03$	$8.87 \pm 0.04$
101	$131 \pm 11$	$183 \pm 14$	$3920 \pm 150$	$3711 \pm 192$	$9.04 \pm 0.04$	$9.07 \pm 0.05$
102	$123 \pm 10$	$125 \pm 14$	$3000 \pm 123$	$3045 \pm 134$	$8.79 \pm 0.04$	$8.81 \pm 0.05$
103	$86 \pm 8$	$54 \pm 12$	$3353 \pm 334$	$3479 \pm 433$	$8.81 \pm 0.09$	$8.73 \pm 0.12$
104	$53 \pm 6$	$45 \pm 8$	$3244 \pm 234$	$3340 \pm 310$	$8.67 \pm 0.07$	$8.65 \pm 0.09$
105	$27 \pm 5$	$18 \pm 8$	$3532 \pm 360$	$2716 \pm 692$	$8.59 \pm 0.10$	$8.27 \pm 0.25$
106	$86 \pm 9$	$87 \pm 11$	$3638 \pm 70$	$3630 \pm 90$	$8.88 \pm 0.03$	$8.88 \pm 0.04$
107	$613 \pm 31$	$637 \pm 35$	$3597 \pm 122$	$4781 \pm 152$	$9.32 \pm 0.03$	$9.58 \pm 0.03$
108	$122 \pm 9$	$102 \pm 10$	$3661 \pm 128$	$3583 \pm 171$	$8.96 \pm 0.04$	$8.90 \pm 0.05$
109	$204 \pm 12$	$188 \pm 13$	$4275 \pm 97$	$3915 \pm 151$	$9.22 \pm 0.02$	$9.12 \pm 0.04$
110	$206 \pm 70$	$82 \pm 84$	$4411 \pm 121$	$4008 \pm 249$	$9.25 \pm 0.08$	$8.95 \pm 0.24$
111	$79 \pm 9$	$69 \pm 10$	$3823 \pm 203$	$4059 \pm 247$	$8.90 \pm 0.05$	$8.92 \pm 0.06$
112	$254 \pm 19$	$223 \pm 27$	$3420 \pm 125$	$3781 \pm 135$	$9.07 \pm 0.04$	$9.13 \pm 0.04$
113	$327 \pm 36$	$416 \pm 44$	$3172 \pm 206$	$3187 \pm 240$	$9.07 \pm 0.06$	$9.13 \pm 0.07$
114	$63 \pm 11$	$64 \pm 14$	$2953 \pm 355$	$3534 \pm 277$	$8.62 \pm 0.11$	$8.79 \pm 0.08$
115	$56 \pm 15$	$54 \pm 19$	$3285 \pm 201$	$3312 \pm 249$	$8.69 \pm 0.08$	$8.69 \pm 0.10$
116	$180 \pm 13$	$179 \pm 14$	$3246 \pm 266$	$3005 \pm 293$	$8.95 \pm 0.07$	$8.88 \pm 0.09$

Table 2—Continued

Number	$L_{1450}$ $10^{44} \text{ erg s}^{-1}$		$\sigma_{\text{C IV}}$ $\text{km s}^{-1}$		$\log(M_{\text{BH}}/M_{\odot})$	
	HSN	LSN	HSN	LSN	HSN	LSN
117	$75 \pm 7$	$68 \pm 9$	$3785 \pm 129$	$3390 \pm 226$	$8.88 \pm 0.04$	$8.76 \pm 0.07$
118	$110 \pm 13$	$134 \pm 17$	$3669 \pm 146$	$3335 \pm 220$	$8.94 \pm 0.05$	$8.90 \pm 0.06$
119	$105 \pm 16$	$137 \pm 18$	$4010 \pm 274$	$3435 \pm 514$	$9.01 \pm 0.07$	$8.93 \pm 0.13$
120	$108 \pm 9$	$92 \pm 10$	$3162 \pm 157$	$3160 \pm 175$	$8.81 \pm 0.05$	$8.77 \pm 0.06$
121	$111 \pm 16$	$127 \pm 20$	$3316 \pm 131$	$2889 \pm 194$	$8.86 \pm 0.05$	$8.77 \pm 0.07$
122	$225 \pm 16$	$231 \pm 19$	$3643 \pm 105$	$3771 \pm 116$	$9.10 \pm 0.03$	$9.14 \pm 0.03$
123	$354 \pm 17$	$382 \pm 19$	$3016 \pm 63$	$3068 \pm 66$	$9.04 \pm 0.02$	$9.07 \pm 0.02$
124	$143 \pm 15$	$144 \pm 12$	$3731 \pm 129$	$3695 \pm 117$	$9.02 \pm 0.04$	$9.01 \pm 0.03$
125	$160 \pm 14$	$152 \pm 16$	$3605 \pm 139$	$3558 \pm 177$	$9.01 \pm 0.04$	$8.99 \pm 0.05$
126	$78 \pm 9$	$72 \pm 10$	$3552 \pm 93$	$3300 \pm 140$	$8.84 \pm 0.04$	$8.75 \pm 0.05$
127	$62 \pm 8$	$73 \pm 9$	$2674 \pm 269$	$2547 \pm 345$	$8.53 \pm 0.09$	$8.53 \pm 0.12$
128	$243 \pm 24$	$227 \pm 24$	$2847 \pm 104$	$3000 \pm 94$	$8.90 \pm 0.04$	$8.93 \pm 0.04$
129	$140 \pm 16$	$144 \pm 16$	$2931 \pm 153$	$2912 \pm 142$	$8.80 \pm 0.05$	$8.80 \pm 0.05$
130	$157 \pm 8$	$57 \pm 3$	$3609 \pm 374$	$4788 \pm 275$	$9.01 \pm 0.09$	$9.02 \pm 0.05$
131	$262 \pm 30$	$281 \pm 31$	$2903 \pm 189$	$2476 \pm 378$	$8.94 \pm 0.06$	$8.82 \pm 0.14$
132	$85 \pm 12$	$80 \pm 13$	$3514 \pm 395$	$3038 \pm 527$	$8.85 \pm 0.10$	$8.71 \pm 0.16$
133	$534 \pm 23$	$505 \pm 26$	$3519 \pm 92$	$3601 \pm 106$	$9.27 \pm 0.02$	$9.28 \pm 0.03$
134	$29 \pm 6$	$26 \pm 7$	$2790 \pm 505$	$2713 \pm 544$	$8.40 \pm 0.17$	$8.35 \pm 0.19$
135	$68 \pm 9$	$47 \pm 10$	$2856 \pm 437$	$3554 \pm 220$	$8.62 \pm 0.14$	$8.72 \pm 0.07$
136	$232 \pm 9$	$193 \pm 11$	$3548 \pm 62$	$3528 \pm 79$	$9.08 \pm 0.02$	$9.04 \pm 0.02$
137	$181 \pm 14$	$190 \pm 15$	$4020 \pm 60$	$3780 \pm 84$	$9.14 \pm 0.02$	$9.09 \pm 0.03$
138	$31 \pm 17$	$81 \pm 23$	$4018 \pm 288$	$4031 \pm 263$	$8.73 \pm 0.14$	$8.95 \pm 0.09$
139	$101 \pm 10$	$129 \pm 14$	$3437 \pm 90$	$3522 \pm 101$	$8.87 \pm 0.03$	$8.94 \pm 0.04$
140	$179 \pm 13$	$166 \pm 16$	$2759 \pm 170$	$2989 \pm 184$	$8.81 \pm 0.06$	$8.86 \pm 0.06$
141	$72 \pm 7$	$62 \pm 11$	$3518 \pm 108$	$3109 \pm 257$	$8.81 \pm 0.04$	$8.67 \pm 0.08$
142	$251 \pm 23$	$199 \pm 25$	$3070 \pm 123$	$2022 \pm 368$	$8.98 \pm 0.04$	$8.56 \pm 0.16$
143	$95 \pm 8$	$92 \pm 9$	$3284 \pm 138$	$3130 \pm 188$	$8.81 \pm 0.04$	$8.76 \pm 0.06$
144	$44 \pm 7$	$35 \pm 7$	$3125 \pm 342$	$3505 \pm 251$	$8.59 \pm 0.10$	$8.64 \pm 0.08$
145	$88 \pm 10$	$80 \pm 10$	$3541 \pm 182$	$3689 \pm 193$	$8.86 \pm 0.05$	$8.87 \pm 0.05$

Table 2—Continued

Number	$L_{1450}$ $10^{44} \text{ erg s}^{-1}$		$\sigma_{C\ IV}$ $\text{km s}^{-1}$		$\log(M_{BH}/M_{\odot})$	
	HSN	LSN	HSN	LSN	HSN	LSN
146	220 ± 27	254 ± 28	1105 ± 486	2206 ± 447	8.06 ± 0.38	8.69 ± 0.18
147	65 ± 9	50 ± 11	3473 ± 604	3998 ± 396	8.77 ± 0.15	8.83 ± 0.10
148	39 ± 6	51 ± 8	3581 ± 104	3479 ± 148	8.69 ± 0.05	8.72 ± 0.05
149	55 ± 13	45 ± 19	3816 ± 127	3651 ± 235	8.82 ± 0.06	8.74 ± 0.11
150	220 ± 16	248 ± 22	3877 ± 67	3790 ± 85	9.15 ± 0.02	9.16 ± 0.03
151	148 ± 12	178 ± 17	3368 ± 110	3322 ± 148	8.94 ± 0.03	8.97 ± 0.05
152	97 ± 9	125 ± 14	3741 ± 92	3655 ± 129	8.93 ± 0.03	8.97 ± 0.04
153	349 ± 39	393 ± 58	4023 ± 110	3778 ± 185	9.29 ± 0.04	9.26 ± 0.05
154	84 ± 9	103 ± 14	3589 ± 69	3418 ± 117	8.86 ± 0.03	8.87 ± 0.04
155	57 ± 7	54 ± 14	3937 ± 333	2065 ± 2013	8.85 ± 0.08	8.28 ± 0.85
156	233 ± 13	249 ± 17	3307 ± 78	3383 ± 100	9.02 ± 0.02	9.06 ± 0.03
157	282 ± 18	247 ± 21	3786 ± 102	3764 ± 116	9.19 ± 0.03	9.15 ± 0.03
158	102 ± 8	107 ± 12	3960 ± 122	3992 ± 133	8.99 ± 0.03	9.01 ± 0.04
159	335 ± 57	344 ± 73	3474 ± 131	3622 ± 182	9.15 ± 0.05	9.19 ± 0.07
160	168 ± 9	135 ± 10	3942 ± 80	4069 ± 87	9.10 ± 0.02	9.08 ± 0.03
161	279 ± 33	270 ± 42	3917 ± 111	3672 ± 179	9.21 ± 0.04	9.15 ± 0.06
162	138 ± 12	145 ± 16	4288 ± 70	4199 ± 97	9.13 ± 0.03	9.12 ± 0.03
163	191 ± 86	22 ± 6	3914 ± 90	6656 ± 208	9.12 ± 0.11	9.09 ± 0.07
164	172 ± 14	179 ± 14	3716 ± 124	3758 ± 106	9.06 ± 0.04	9.07 ± 0.03
165	171 ± 15	203 ± 17	2828 ± 133	3077 ± 116	8.82 ± 0.05	8.93 ± 0.04
166	60 ± 8	66 ± 7	3460 ± 302	4081 ± 182	8.75 ± 0.08	8.92 ± 0.05
167	329 ± 52	277 ± 42	2428 ± 210	2404 ± 188	8.83 ± 0.08	8.79 ± 0.08
168	140 ± 23	118 ± 17	3810 ± 143	3701 ± 126	9.03 ± 0.05	8.96 ± 0.05
169	48 ± 8	39 ± 7	3708 ± 173	3652 ± 157	8.76 ± 0.06	8.70 ± 0.06
170	68 ± 9	62 ± 9	3617 ± 182	2933 ± 251	8.82 ± 0.06	8.62 ± 0.08
171	132 ± 14	123 ± 14	4057 ± 152	4240 ± 119	9.07 ± 0.04	9.09 ± 0.04
172	70 ± 11	70 ± 10	1761 ± 578	2975 ± 289	8.20 ± 0.29	8.66 ± 0.09
173	116 ± 14	105 ± 16	3534 ± 361	4371 ± 163	8.92 ± 0.09	9.08 ± 0.05
174	135 ± 10	120 ± 11	3512 ± 103	3398 ± 127	8.95 ± 0.03	8.90 ± 0.04

Table 2—Continued

Number	$L_{1450}$ $10^{44} \text{ erg s}^{-1}$		$\sigma_{C\ IV}$ $\text{km s}^{-1}$		$\log(M_{BH}/M_{\odot})$	
	HSN	LSN	HSN	LSN	HSN	LSN
175	475 ± 27	449 ± 29	3337 ± 173	2813 ± 297	9.20 ± 0.05	9.03 ± 0.09
176	374 ± 27	353 ± 36	3333 ± 127	3131 ± 188	9.14 ± 0.04	9.07 ± 0.06
177	394 ± 16	427 ± 19	3774 ± 71	3666 ± 96	9.26 ± 0.02	9.25 ± 0.03
178	54 ± 8	61 ± 9	4722 ± 141	4981 ± 108	9.00 ± 0.04	9.07 ± 0.04
179	70 ± 11	57 ± 9	3068 ± 191	3015 ± 163	8.68 ± 0.07	8.62 ± 0.06
180	51 ± 9	69 ± 9	3591 ± 320	3805 ± 201	8.75 ± 0.09	8.87 ± 0.06
181	162 ± 18	177 ± 16	3663 ± 107	3617 ± 88	9.03 ± 0.04	9.04 ± 0.03
182	109 ± 15	125 ± 14	3531 ± 78	3633 ± 62	8.91 ± 0.04	8.96 ± 0.03
183	64 ± 8	65 ± 8	4340 ± 99	4301 ± 106	8.97 ± 0.04	8.96 ± 0.04
184	71 ± 11	79 ± 12	3914 ± 151	3759 ± 179	8.90 ± 0.05	8.89 ± 0.05
185	238 ± 22	276 ± 26	3374 ± 66	3311 ± 79	9.05 ± 0.03	9.06 ± 0.03
186	269 ± 20	275 ± 25	2943 ± 273	2955 ± 298	8.96 ± 0.08	8.96 ± 0.09
187	171 ± 17	176 ± 24	2247 ± 243	2581 ± 264	8.62 ± 0.10	8.75 ± 0.09
188	107 ± 7	115 ± 14	3576 ± 166	2955 ± 514	8.91 ± 0.04	8.76 ± 0.15
189	135 ± 45	155 ± 82	3018 ± 221	2969 ± 241	8.82 ± 0.10	8.84 ± 0.14
190	254 ± 14	279 ± 24	3408 ± 127	3379 ± 168	9.07 ± 0.04	9.08 ± 0.05
191	64 ± 11	76 ± 15	3568 ± 219	2489 ± 635	8.79 ± 0.07	8.52 ± 0.23
192	336 ± 30	282 ± 36	2777 ± 202	1646 ± 540	8.96 ± 0.07	8.46 ± 0.29
193	74 ± 10	73 ± 8	3528 ± 290	3906 ± 201	8.82 ± 0.08	8.90 ± 0.05
194	156 ± 15	147 ± 15	2544 ± 323	2252 ± 442	8.70 ± 0.11	8.59 ± 0.17
195	201 ± 25	175 ± 33	3484 ± 245	3547 ± 309	9.04 ± 0.07	9.02 ± 0.09
196	136 ± 13	119 ± 22	4112 ± 181	4014 ± 303	9.09 ± 0.04	9.04 ± 0.08
197	189 ± 11	185 ± 18	3317 ± 181	3602 ± 241	8.98 ± 0.05	9.05 ± 0.06
198	280 ± 19	253 ± 33	3445 ± 128	3723 ± 165	9.10 ± 0.04	9.15 ± 0.05
199	109 ± 7	103 ± 13	2840 ± 193	2699 ± 444	8.72 ± 0.06	8.66 ± 0.15
200	36 ± 80	86 ± 154	4547 ± 211	3850 ± 746	8.88 ± 0.51	8.93 ± 0.44
201	75 ± 6	85 ± 12	3361 ± 152	3588 ± 242	8.78 ± 0.04	8.86 ± 0.07
202	82 ± 9	92 ± 14	3205 ± 131	3078 ± 214	8.76 ± 0.04	8.75 ± 0.07
203	319 ± 14	273 ± 11	3887 ± 52	3862 ± 53	9.24 ± 0.02	9.20 ± 0.02

Table 2—Continued

Number	$L_{1450}$ $10^{44} \text{ erg s}^{-1}$		$\sigma_{C\ IV}$ $\text{km s}^{-1}$		$\log(M_{BH}/M_{\odot})$	
	HSN	LSN	HSN	LSN	HSN	LSN
204	105 ± 7	100 ± 9	3535 ± 110	3921 ± 102	8.90 ± 0.03	8.98 ± 0.03
205	52 ± 8	49 ± 8	3148 ± 282	3787 ± 193	8.64 ± 0.09	8.79 ± 0.06
206	415 ± 21	442 ± 24	3551 ± 83	2486 ± 271	9.22 ± 0.02	8.92 ± 0.10
207	165 ± 16	153 ± 18	3054 ± 181	2905 ± 232	8.88 ± 0.06	8.81 ± 0.07
208	346 ± 17	336 ± 19	3770 ± 86	3510 ± 121	9.23 ± 0.02	9.16 ± 0.03
209	134 ± 10	139 ± 13	3281 ± 135	3404 ± 160	8.89 ± 0.04	8.93 ± 0.05
210	184 ± 8	182 ± 11	3462 ± 87	3096 ± 160	9.01 ± 0.02	8.91 ± 0.05
211	50 ± 7	64 ± 9	4131 ± 127	4406 ± 137	8.86 ± 0.04	8.98 ± 0.04
212	274 ± 10	268 ± 12	2805 ± 171	3207 ± 147	8.92 ± 0.05	9.03 ± 0.04
213	956 ± 28	1008 ± 29	3540 ± 49	3279 ± 64	9.41 ± 0.01	9.35 ± 0.02
214	188 ± 18	190 ± 19	3402 ± 195	3123 ± 236	9.00 ± 0.05	8.93 ± 0.07
215	186 ± 16	99 ± 3	3624 ± 192	3443 ± 259	9.05 ± 0.05	8.86 ± 0.07
216	73 ± 6	80 ± 8	3554 ± 162	3395 ± 224	8.82 ± 0.05	8.80 ± 0.06
217	221 ± 16	227 ± 31	2636 ± 208	2688 ± 340	8.82 ± 0.07	8.84 ± 0.11
218	627 ± 19	644 ± 22	3372 ± 50	3496 ± 50	9.27 ± 0.01	9.31 ± 0.01
219	12 ± 6	14 ± 8	3488 ± 262	3630 ± 300	8.40 ± 0.13	8.47 ± 0.14
220	52 ± 7	56 ± 8	3476 ± 325	3389 ± 393	8.72 ± 0.09	8.72 ± 0.11
221	41 ± 6	36 ± 9	3796 ± 128	3651 ± 242	8.74 ± 0.05	8.68 ± 0.08
222	296 ± 28	273 ± 40	3760 ± 115	3794 ± 153	9.19 ± 0.03	9.18 ± 0.05
223	59 ± 6	97 ± 8	3574 ± 414	3784 ± 504	8.78 ± 0.10	8.94 ± 0.12
224	88 ± 10	80 ± 13	3427 ± 182	3061 ± 352	8.83 ± 0.05	8.71 ± 0.11
225	18 ± 6	9 ± 9	3742 ± 362	4286 ± 296	8.55 ± 0.12	8.52 ± 0.24
226	30 ± 6	21 ± 10	3522 ± 223	2899 ± 628	8.61 ± 0.07	8.37 ± 0.22
227	22 ± 7	16 ± 10	3317 ± 507	3412 ± 750	8.49 ± 0.15	8.45 ± 0.24
228	124 ± 28	88 ± 11	3446 ± 267	3617 ± 127	8.92 ± 0.09	8.88 ± 0.04
229	59 ± 8	58 ± 9	4496 ± 74	4085 ± 125	8.97 ± 0.03	8.89 ± 0.05
230	122 ± 13	118 ± 15	3511 ± 204	3654 ± 203	8.93 ± 0.06	8.95 ± 0.06
231	27 ± 6	20 ± 8	3104 ± 313	3010 ± 515	8.48 ± 0.10	8.39 ± 0.17
232	112 ± 15	88 ± 17	3576 ± 175	2911 ± 384	8.92 ± 0.05	8.69 ± 0.12

Table 2—Continued

Number	$L_{1450}$ $10^{44} \text{ erg s}^{-1}$		$\sigma_{C\ IV}$ $\text{km s}^{-1}$		$\log(M_{BH}/M_{\odot})$	
	HSN	LSN	HSN	LSN	HSN	LSN
233	47 ± 8	23 ± 8	3156 ± 420	3607 ± 387	8.62 ± 0.12	8.57 ± 0.13
234	92 ± 11	92 ± 12	3674 ± 202	3619 ± 240	8.90 ± 0.06	8.89 ± 0.07
235	93 ± 8	75 ± 9	3085 ± 132	2853 ± 184	8.75 ± 0.04	8.64 ± 0.06
236	71 ± 12	64 ± 16	3541 ± 166	3566 ± 222	8.81 ± 0.06	8.79 ± 0.08
237	32 ± 8	40 ± 10	3975 ± 298	3495 ± 471	8.73 ± 0.09	8.67 ± 0.13
238	23 ± 8	22 ± 6	3385 ± 695	3202 ± 659	8.52 ± 0.20	8.45 ± 0.19
239	101 ± 10	102 ± 9	3379 ± 114	3464 ± 95	8.85 ± 0.04	8.87 ± 0.03
240	64 ± 11	61 ± 10	3786 ± 113	3530 ± 121	8.84 ± 0.05	8.77 ± 0.05
241	69 ± 14	54 ± 12	3097 ± 305	3057 ± 275	8.69 ± 0.10	8.62 ± 0.09
242	41 ± 6	37 ± 5	3921 ± 348	3731 ± 288	8.78 ± 0.09	8.71 ± 0.08
243	77 ± 12	72 ± 9	3565 ± 164	3606 ± 129	8.83 ± 0.05	8.83 ± 0.04
244	39 ± 7	45 ± 7	3724 ± 103	3720 ± 105	8.72 ± 0.05	8.75 ± 0.04
245	19 ± 7	20 ± 6	4208 ± 406	3047 ± 614	8.66 ± 0.12	8.40 ± 0.19
246	249 ± 26	285 ± 24	3747 ± 117	4107 ± 95	9.15 ± 0.04	9.26 ± 0.03
247	46 ± 12	1 ± 0	3800 ± 184	5847 ± 428	8.78 ± 0.07	8.37 ± 0.09
248	119 ± 8	127 ± 9	4153 ± 71	3907 ± 84	9.07 ± 0.02	9.03 ± 0.02
249	29 ± 13	42 ± 13	3252 ± 195	3123 ± 228	8.53 ± 0.11	8.58 ± 0.10
250	101 ± 11	152 ± 10	4041 ± 136	3707 ± 103	9.01 ± 0.04	9.03 ± 0.03
251	37 ± 8	52 ± 8	3060 ± 275	3409 ± 181	8.53 ± 0.10	8.70 ± 0.06
252	45 ± 12	48 ± 11	3949 ± 157	3865 ± 149	8.80 ± 0.07	8.80 ± 0.06
253	40 ± 11	41 ± 11	3635 ± 225	3116 ± 300	8.70 ± 0.08	8.58 ± 0.10
254	124 ± 14	113 ± 12	3865 ± 145	3635 ± 153	9.01 ± 0.04	8.94 ± 0.04
255	138 ± 34	134 ± 29	4114 ± 91	4250 ± 80	9.09 ± 0.06	9.12 ± 0.05
256	163 ± 79	138 ± 71	3751 ± 113	3259 ± 196	9.05 ± 0.12	8.89 ± 0.13
257	32 ± 14	39 ± 10	3404 ± 656	3345 ± 504	8.60 ± 0.20	8.63 ± 0.14
258	105 ± 15	108 ± 11	3411 ± 237	3635 ± 144	8.87 ± 0.07	8.93 ± 0.04
259	1552 ± 83	1458 ± 77	2674 ± 110	2863 ± 94	9.28 ± 0.04	9.32 ± 0.03
260	968 ± 63	877 ± 58	3713 ± 46	3764 ± 42	9.45 ± 0.02	9.44 ± 0.02
261	107 ± 12	107 ± 11	3446 ± 136	3405 ± 129	8.88 ± 0.04	8.87 ± 0.04



Table 2—Continued

Number	$L_{1450}$ $10^{44} \text{ erg s}^{-1}$		$\sigma_{C\ IV}$ $\text{km s}^{-1}$		$\log(M_{BH}/M_{\odot})$	
	HSN	LSN	HSN	LSN	HSN	LSN
262	534 ± 21	507 ± 19	2887 ± 75	2969 ± 70	9.10 ± 0.02	9.11 ± 0.02
263	66 ± 8	65 ± 7	4179 ± 108	3796 ± 131	8.94 ± 0.04	8.85 ± 0.04
264	1124 ± 78	1025 ± 65	3040 ± 45	3033 ± 47	9.31 ± 0.02	9.29 ± 0.02
265	97 ± 9	85 ± 9	3263 ± 121	3213 ± 134	8.81 ± 0.04	8.77 ± 0.04
266	216 ± 20	142 ± 25	3504 ± 145	3677 ± 175	9.06 ± 0.04	9.00 ± 0.06
267	108 ± 13	88 ± 22	3774 ± 220	3753 ± 376	8.96 ± 0.06	8.91 ± 0.10
268	169 ± 27	175 ± 28	2939 ± 192	3155 ± 171	8.85 ± 0.07	8.92 ± 0.06
269	154 ± 15	167 ± 18	3398 ± 247	3645 ± 212	8.95 ± 0.07	9.03 ± 0.06
270	366 ± 17	345 ± 19	3420 ± 49	3369 ± 54	9.16 ± 0.02	9.13 ± 0.02
271	315 ± 22	342 ± 27	4058 ± 76	3788 ± 114	9.27 ± 0.02	9.23 ± 0.03
272	72 ± 8	59 ± 10	3914 ± 136	3725 ± 192	8.90 ± 0.04	8.81 ± 0.06
273	57 ± 5	43 ± 6	3684 ± 263	3948 ± 190	8.79 ± 0.07	8.79 ± 0.06
274	46 ± 6	47 ± 8	3539 ± 97	3684 ± 107	8.71 ± 0.04	8.75 ± 0.05
275	30 ± 9	28 ± 7	3921 ± 178	3641 ± 219	8.71 ± 0.08	8.62 ± 0.08
276	22 ± 10	29 ± 9	3766 ± 286	3769 ± 241	8.59 ± 0.13	8.66 ± 0.09
277	146 ± 16	159 ± 17	3274 ± 152	3739 ± 111	8.91 ± 0.05	9.04 ± 0.04
278	19 ± 7	17 ± 7	2693 ± 538	2282 ± 716	8.27 ± 0.20	8.11 ± 0.29
279	253 ± 38	291 ± 47	3410 ± 92	3603 ± 86	9.07 ± 0.04	9.15 ± 0.04
280	174 ± 13	152 ± 14	3663 ± 128	3649 ± 135	9.05 ± 0.04	9.01 ± 0.04
281	359 ± 41	305 ± 43	3641 ± 167	3628 ± 186	9.21 ± 0.05	9.17 ± 0.06
282	75 ± 9	61 ± 11	3041 ± 337	3353 ± 306	8.69 ± 0.10	8.73 ± 0.09
283	82 ± 16	71 ± 11	2968 ± 609	3330 ± 379	8.69 ± 0.18	8.76 ± 0.11
284	24 ± 7	32 ± 7	2911 ± 590	3478 ± 316	8.39 ± 0.19	8.62 ± 0.09
285	198 ± 14	176 ± 10	3449 ± 159	3508 ± 120	9.02 ± 0.04	9.01 ± 0.03
286	95 ± 17	106 ± 12	3770 ± 167	4050 ± 106	8.93 ± 0.06	9.02 ± 0.04
287	49 ± 7	52 ± 13	3440 ± 357	2931 ± 767	8.70 ± 0.10	8.58 ± 0.23
288	56 ± 8	59 ± 8	3477 ± 274	2897 ± 424	8.74 ± 0.08	8.59 ± 0.13
289	145 ± 9	129 ± 9	3449 ± 142	3700 ± 122	8.95 ± 0.04	8.99 ± 0.03
290	91 ± 9	80 ± 9	3568 ± 120	3371 ± 141	8.88 ± 0.04	8.80 ± 0.05

Table 2—Continued

Number	$L_{1450}$ $10^{44} \text{ erg s}^{-1}$		$\sigma_{\text{C IV}}$ $\text{km s}^{-1}$		$\log(M_{\text{BH}}/M_{\odot})$	
	HSN	LSN	HSN	LSN	HSN	LSN
291	$26 \pm 7$	$30 \pm 7$	$3264 \pm 312$	$3096 \pm 318$	$8.51 \pm 0.11$	$8.50 \pm 0.11$
292	$38 \pm 7$	$37 \pm 6$	$3609 \pm 291$	$3161 \pm 390$	$8.69 \pm 0.08$	$8.56 \pm 0.11$
293	$90 \pm 8$	$90 \pm 9$	$3366 \pm 114$	$2990 \pm 172$	$8.82 \pm 0.04$	$8.72 \pm 0.06$
294	$90 \pm 10$	$84 \pm 11$	$3302 \pm 146$	$3293 \pm 158$	$8.80 \pm 0.05$	$8.79 \pm 0.05$
295	$67 \pm 21$	$65 \pm 21$	$3193 \pm 514$	$4257 \pm 216$	$8.71 \pm 0.16$	$8.95 \pm 0.09$
296	$61 \pm 8$	$60 \pm 8$	$3069 \pm 192$	$3659 \pm 123$	$8.65 \pm 0.06$	$8.80 \pm 0.04$
297	$68 \pm 9$	$66 \pm 7$	$3357 \pm 146$	$3498 \pm 112$	$8.76 \pm 0.05$	$8.78 \pm 0.04$
298	$18 \pm 6$	$20 \pm 6$	$3501 \pm 309$	$3137 \pm 414$	$8.49 \pm 0.11$	$8.41 \pm 0.14$
299	$57 \pm 15$	$64 \pm 17$	$3433 \pm 282$	$3746 \pm 222$	$8.74 \pm 0.09$	$8.84 \pm 0.08$
300	$374 \pm 21$	$342 \pm 18$	$3295 \pm 92$	$3187 \pm 98$	$9.13 \pm 0.03$	$9.08 \pm 0.03$
301	$39 \pm 7$	$40 \pm 11$	$3773 \pm 162$	$3793 \pm 237$	$8.73 \pm 0.06$	$8.74 \pm 0.08$
302	$159 \pm 16$	$172 \pm 23$	$2705 \pm 163$	$3012 \pm 188$	$8.76 \pm 0.06$	$8.87 \pm 0.06$
303	$83 \pm 6$	$88 \pm 9$	$3748 \pm 129$	$3629 \pm 251$	$8.90 \pm 0.04$	$8.88 \pm 0.06$
304	$12 \pm 5$	$4 \pm 6$	$3885 \pm 223$	$3212 \pm 615$	$8.49 \pm 0.11$	$8.08 \pm 0.36$
305	$60 \pm 12$	$54 \pm 15$	$2755 \pm 373$	$3113 \pm 424$	$8.56 \pm 0.13$	$8.64 \pm 0.14$
306	$125 \pm 13$	$125 \pm 16$	$3553 \pm 109$	$3523 \pm 159$	$8.94 \pm 0.04$	$8.94 \pm 0.05$
307	$28 \pm 5$	$29 \pm 7$	$3230 \pm 187$	$3469 \pm 250$	$8.52 \pm 0.06$	$8.59 \pm 0.08$
308	$313 \pm 44$	$358 \pm 46$	$3671 \pm 120$	$3799 \pm 85$	$9.18 \pm 0.04$	$9.24 \pm 0.04$
309	$50 \pm 5$	$45 \pm 6$	$3440 \pm 168$	$3750 \pm 161$	$8.70 \pm 0.05$	$8.76 \pm 0.05$
310	$33 \pm 5$	$25 \pm 7$	$4266 \pm 165$	$3100 \pm 621$	$8.80 \pm 0.05$	$8.46 \pm 0.19$
311	$72 \pm 10$	$55 \pm 11$	$3307 \pm 209$	$987 \pm 597$	$8.75 \pm 0.06$	$7.64 \pm 0.53$
312	$27 \pm 6$	$21 \pm 6$	$3687 \pm 196$	$3391 \pm 284$	$8.63 \pm 0.07$	$8.50 \pm 0.10$
313	$41 \pm 8$	$40 \pm 11$	$3053 \pm 318$	$3242 \pm 415$	$8.56 \pm 0.10$	$8.61 \pm 0.13$
314	$34 \pm 8$	$13 \pm 5$	$4154 \pm 178$	$3878 \pm 876$	$8.78 \pm 0.07$	$8.51 \pm 0.22$
315	$46 \pm 7$	$42 \pm 9$	$3626 \pm 483$	$2871 \pm 745$	$8.73 \pm 0.12$	$8.51 \pm 0.23$
316	$310 \pm 12$	$301 \pm 12$	$3550 \pm 42$	$3474 \pm 48$	$9.15 \pm 0.01$	$9.13 \pm 0.02$
317	$41 \pm 5$	$43 \pm 8$	$3975 \pm 95$	$3989 \pm 131$	$8.78 \pm 0.04$	$8.80 \pm 0.05$
318	$35 \pm 5$	$36 \pm 8$	$3468 \pm 438$	$3693 \pm 517$	$8.63 \pm 0.12$	$8.69 \pm 0.13$
319	$67 \pm 9$	$64 \pm 13$	$3903 \pm 125$	$4177 \pm 180$	$8.88 \pm 0.04$	$8.93 \pm 0.06$

Table 2—Continued

Number	$L_{1450}$ $10^{44} \text{ erg s}^{-1}$		$\sigma_{\text{C IV}}$ $\text{km s}^{-1}$		$\log(M_{\text{BH}}/M_{\odot})$	
	HSN	LSN	HSN	LSN	HSN	LSN
320	$52 \pm 5$	$50 \pm 8$	$2569 \pm 277$	$3246 \pm 243$	$8.46 \pm 0.10$	$8.66 \pm 0.08$
321	$611 \pm 20$	$682 \pm 18$	$4022 \pm 94$	$3940 \pm 98$	$9.42 \pm 0.02$	$9.42 \pm 0.02$
322	$15 \pm 5$	$16 \pm 5$	$2869 \pm 552$	$3323 \pm 318$	$8.28 \pm 0.18$	$8.41 \pm 0.11$
323	$71 \pm 12$	$74 \pm 12$	$3614 \pm 278$	$4254 \pm 183$	$8.83 \pm 0.08$	$8.98 \pm 0.05$
324	$27 \pm 7$	$26 \pm 7$	$3968 \pm 180$	$3538 \pm 311$	$8.69 \pm 0.07$	$8.58 \pm 0.10$
325	$22 \pm 7$	$22 \pm 8$	$3665 \pm 250$	$3680 \pm 324$	$8.58 \pm 0.10$	$8.58 \pm 0.11$
326	$30 \pm 5$	$26 \pm 6$	$2557 \pm 568$	$1841 \pm 657$	$8.34 \pm 0.20$	$8.02 \pm 0.31$
327	$73 \pm 14$	$74 \pm 17$	$3343 \pm 90$	$3212 \pm 131$	$8.77 \pm 0.05$	$8.74 \pm 0.06$
328	$49 \pm 8$	$46 \pm 10$	$4714 \pm 166$	$4866 \pm 184$	$8.98 \pm 0.05$	$8.99 \pm 0.06$
329	$69 \pm 9$	$66 \pm 10$	$2438 \pm 277$	$2746 \pm 244$	$8.48 \pm 0.10$	$8.57 \pm 0.08$
330	$83 \pm 19$	$89 \pm 19$	$3833 \pm 179$	$3702 \pm 199$	$8.92 \pm 0.07$	$8.90 \pm 0.07$
331	$44 \pm 9$	$39 \pm 10$	$4467 \pm 169$	$3823 \pm 464$	$8.90 \pm 0.06$	$8.74 \pm 0.12$
332	$80 \pm 15$	$90 \pm 17$	$3570 \pm 166$	$3178 \pm 319$	$8.85 \pm 0.06$	$8.77 \pm 0.10$
333	$62 \pm 12$	$67 \pm 14$	$3488 \pm 379$	$3752 \pm 339$	$8.77 \pm 0.11$	$8.85 \pm 0.09$
334	$34 \pm 7$	$32 \pm 9$	$3529 \pm 309$	$3957 \pm 258$	$8.64 \pm 0.09$	$8.73 \pm 0.09$
335	$77 \pm 9$	$83 \pm 11$	$3540 \pm 170$	$3477 \pm 250$	$8.83 \pm 0.05$	$8.83 \pm 0.07$
336	$38 \pm 7$	$38 \pm 8$	$3518 \pm 184$	$3284 \pm 341$	$8.66 \pm 0.06$	$8.60 \pm 0.10$
337	$43 \pm 12$	$28 \pm 13$	$3473 \pm 182$	$2586 \pm 489$	$8.68 \pm 0.08$	$8.32 \pm 0.20$
338	$88 \pm 9$	$98 \pm 11$	$3618 \pm 130$	$3516 \pm 158$	$8.88 \pm 0.04$	$8.88 \pm 0.05$
339	$87 \pm 19$	$89 \pm 27$	$4204 \pm 98$	$3913 \pm 163$	$9.01 \pm 0.06$	$8.95 \pm 0.08$
340	$92 \pm 7$	$97 \pm 8$	$3800 \pm 75$	$3564 \pm 106$	$8.93 \pm 0.03$	$8.89 \pm 0.03$
341	$107 \pm 11$	$108 \pm 12$	$3293 \pm 121$	$3208 \pm 140$	$8.84 \pm 0.04$	$8.82 \pm 0.05$
342	$12 \pm 6$	$17 \pm 7$	$4147 \pm 202$	$4308 \pm 224$	$8.55 \pm 0.13$	$8.66 \pm 0.11$
343	$16 \pm 5$	$19 \pm 6$	$4250 \pm 187$	$3633 \pm 375$	$8.64 \pm 0.09$	$8.53 \pm 0.12$
344	$42 \pm 7$	$46 \pm 8$	$3623 \pm 111$	$3820 \pm 97$	$8.71 \pm 0.05$	$8.78 \pm 0.05$
345	$77 \pm 14$	$81 \pm 14$	$3576 \pm 304$	$3998 \pm 235$	$8.84 \pm 0.09$	$8.95 \pm 0.07$
346	$82 \pm 6$	$93 \pm 7$	$3404 \pm 144$	$2918 \pm 211$	$8.81 \pm 0.04$	$8.71 \pm 0.07$
347	$71 \pm 7$	$82 \pm 7$	$3491 \pm 96$	$3248 \pm 108$	$8.80 \pm 0.03$	$8.77 \pm 0.04$
348	$283 \pm 17$	$306 \pm 19$	$3430 \pm 46$	$3392 \pm 46$	$9.10 \pm 0.02$	$9.11 \pm 0.02$

Table 2—Continued

Number	$L_{1450}$ $10^{44} \text{ erg s}^{-1}$		$\sigma_{C\ IV}$ $\text{km s}^{-1}$		$\log(M_{BH}/M_{\odot})$	
	HSN	LSN	HSN	LSN	HSN	LSN
349	67 ± 6	60 ± 6	3629 ± 140	3323 ± 180	8.82 ± 0.04	8.72 ± 0.05
350	101 ± 7	89 ± 7	3564 ± 140	3470 ± 181	8.90 ± 0.04	8.85 ± 0.05
351	150 ± 12	152 ± 12	3431 ± 183	3277 ± 187	8.95 ± 0.05	8.92 ± 0.05
352	59 ± 6	54 ± 5	2721 ± 144	2926 ± 112	8.54 ± 0.05	8.58 ± 0.04
353	149 ± 9	155 ± 10	2931 ± 70	3154 ± 67	8.82 ± 0.03	8.89 ± 0.02
354	196 ± 26	240 ± 47	3223 ± 200	3720 ± 237	8.96 ± 0.06	9.13 ± 0.07
355	68 ± 14	76 ± 16	2840 ± 355	2478 ± 463	8.61 ± 0.12	8.52 ± 0.17
356	83 ± 15	94 ± 18	3633 ± 238	3156 ± 442	8.87 ± 0.07	8.78 ± 0.13
357	24 ± 9	21 ± 9	2619 ± 702	2868 ± 746	8.30 ± 0.25	8.35 ± 0.25
358	40 ± 7	38 ± 11	3996 ± 309	4463 ± 438	8.79 ± 0.08	8.87 ± 0.11
359	49 ± 44	18 ± 51	3262 ± 361	3280 ± 406	8.65 ± 0.23	8.43 ± 0.66
360	17 ± 9	1 ± 0	2482 ± 744	7573 ± 613	8.18 ± 0.29	8.51 ± 0.11
361	37 ± 7	35 ± 8	3613 ± 290	4215 ± 199	8.68 ± 0.08	8.80 ± 0.07
362	101 ± 12	117 ± 12	3928 ± 134	3639 ± 225	8.98 ± 0.04	8.95 ± 0.06
363	34 ± 9	17 ± 10	3785 ± 277	2924 ± 681	8.70 ± 0.09	8.32 ± 0.25
364	220 ± 30	227 ± 32	3293 ± 177	2930 ± 269	9.01 ± 0.06	8.91 ± 0.09
365	64 ± 9	85 ± 11	3395 ± 106	2950 ± 176	8.75 ± 0.04	8.69 ± 0.06
366	77 ± 14	58 ± 14	3632 ± 277	3048 ± 508	8.85 ± 0.08	8.64 ± 0.16
367	121 ± 11	126 ± 12	3918 ± 115	3900 ± 125	9.02 ± 0.03	9.03 ± 0.04
368	212 ± 18	233 ± 20	3617 ± 182	3458 ± 225	9.08 ± 0.05	9.06 ± 0.06
369	20 ± 7	17 ± 8	3869 ± 303	3259 ± 513	8.60 ± 0.11	8.42 ± 0.18
370	419 ± 81	437 ± 101	3830 ± 136	3585 ± 189	9.29 ± 0.05	9.24 ± 0.07
371	37 ± 6	36 ± 7	4325 ± 190	3910 ± 252	8.83 ± 0.06	8.74 ± 0.07
372	61 ± 11	47 ± 14	3320 ± 499	3532 ± 561	8.72 ± 0.14	8.71 ± 0.15
373	63 ± 13	9 ± 1	3251 ± 864	6640 ± 484	8.71 ± 0.24	8.89 ± 0.08
374	22 ± 10	21 ± 14	3597 ± 363	2884 ± 582	8.56 ± 0.14	8.36 ± 0.24
375	41 ± 7	44 ± 11	3254 ± 201	3110 ± 396	8.61 ± 0.07	8.59 ± 0.13
376	77 ± 12	87 ± 22	1489 ± 623	3461 ± 397	8.08 ± 0.37	8.84 ± 0.12
377	167 ± 15	179 ± 25	4006 ± 177	3143 ± 643	9.11 ± 0.04	8.92 ± 0.18

Table 2—Continued

Number	$L_{1450}$ $10^{44} \text{ erg s}^{-1}$		$\sigma_{C\text{ IV}}$ $\text{km s}^{-1}$		$\log(M_{BH}/M_{\odot})$	
	HSN	LSN	HSN	LSN	HSN	LSN
378	157 ± 10	159 ± 16	4156 ± 58	4019 ± 99	9.13 ± 0.02	9.11 ± 0.03
379	38 ± 6	50 ± 10	3249 ± 241	3634 ± 367	8.59 ± 0.07	8.75 ± 0.10
380	47 ± 4	53 ± 9	3313 ± 121	2386 ± 442	8.66 ± 0.04	8.40 ± 0.17
381	82 ± 7	82 ± 13	3482 ± 60	3488 ± 111	8.83 ± 0.02	8.83 ± 0.05
382	43 ± 7	25 ± 11	3774 ± 170	3751 ± 304	8.75 ± 0.06	8.62 ± 0.13
383	51 ± 5	67 ± 10	3754 ± 134	3780 ± 178	8.79 ± 0.04	8.85 ± 0.05
384	77 ± 10	71 ± 18	3449 ± 81	3432 ± 156	8.81 ± 0.04	8.78 ± 0.07
385	67 ± 6	36 ± 13	3458 ± 296	2949 ± 744	8.78 ± 0.08	8.50 ± 0.23
386	70 ± 8	81 ± 16	3708 ± 109	3897 ± 202	8.85 ± 0.04	8.92 ± 0.07
387	96 ± 8	86 ± 13	2932 ± 275	3724 ± 257	8.72 ± 0.08	8.90 ± 0.07
388	113 ± 17	109 ± 23	4002 ± 197	4848 ± 166	9.02 ± 0.06	9.18 ± 0.06
389	245 ± 17	216 ± 22	3460 ± 99	3375 ± 167	9.07 ± 0.03	9.02 ± 0.05
390	22 ± 5	23 ± 7	1659 ± 562	1904 ± 586	7.89 ± 0.30	8.02 ± 0.28
391	105 ± 11	95 ± 15	2797 ± 337	2788 ± 522	8.70 ± 0.11	8.67 ± 0.17
392	86 ± 11	96 ± 15	3596 ± 273	3752 ± 277	8.87 ± 0.07	8.93 ± 0.07
393	119 ± 10	151 ± 16	3426 ± 139	3106 ± 295	8.90 ± 0.04	8.87 ± 0.09
394	71 ± 78	180 ± 108	3133 ± 208	3275 ± 234	8.70 ± 0.26	8.96 ± 0.15
395	128 ± 9	136 ± 11	3774 ± 76	3996 ± 89	9.00 ± 0.02	9.06 ± 0.03
396	45 ± 4	60 ± 6	4225 ± 314	3408 ± 697	8.86 ± 0.07	8.74 ± 0.18
397	128 ± 48	123 ± 60	3233 ± 215	3684 ± 183	8.87 ± 0.10	8.97 ± 0.12
398	28 ± 6	31 ± 8	3970 ± 317	4026 ± 342	8.70 ± 0.09	8.73 ± 0.10
399	32 ± 4	25 ± 5	3464 ± 175	3635 ± 243	8.61 ± 0.06	8.59 ± 0.08
400	139 ± 9	121 ± 9	3581 ± 121	3792 ± 112	8.98 ± 0.03	8.99 ± 0.03
401	115 ± 11	122 ± 16	4068 ± 106	3617 ± 211	9.04 ± 0.03	8.95 ± 0.06
402	45 ± 5	51 ± 7	3700 ± 92	3987 ± 95	8.75 ± 0.03	8.84 ± 0.04
403	36 ± 5	37 ± 8	3673 ± 247	3270 ± 482	8.68 ± 0.07	8.59 ± 0.14
404	66 ± 5	87 ± 7	3423 ± 112	3413 ± 137	8.76 ± 0.03	8.82 ± 0.04
405	87 ± 9	85 ± 12	4307 ± 131	4434 ± 140	9.03 ± 0.04	9.05 ± 0.04
406	23 ± 3	25 ± 4	2961 ± 545	3044 ± 643	8.40 ± 0.16	8.44 ± 0.19

Table 2—Continued

Number	$L_{1450}$ $10^{44} \text{ erg s}^{-1}$		$\sigma_{C\ IV}$ $\text{km s}^{-1}$		$\log(M_{BH}/M_{\odot})$	
	HSN	LSN	HSN	LSN	HSN	LSN
407	99 ± 8	109 ± 8	3343 ± 133	3002 ± 190	8.84 ± 0.04	8.77 ± 0.06
408	812 ± 52	772 ± 61	3483 ± 94	3000 ± 190	9.36 ± 0.03	9.22 ± 0.06
409	60 ± 7	56 ± 9	3171 ± 312	1622 ± 687	8.68 ± 0.09	8.08 ± 0.37
410	252 ± 24	273 ± 31	3602 ± 110	2944 ± 260	9.12 ± 0.04	8.96 ± 0.08
411	1181 ± 40	1209 ± 49	3961 ± 25	3970 ± 36	9.55 ± 0.01	9.56 ± 0.01
412	441 ± 35	418 ± 41	2621 ± 169	2754 ± 194	8.97 ± 0.06	9.00 ± 0.07
413	91 ± 10	92 ± 12	3801 ± 90	3843 ± 103	8.93 ± 0.03	8.94 ± 0.04
414	42 ± 7	43 ± 12	2817 ± 382	3401 ± 384	8.49 ± 0.12	8.66 ± 0.12
415	409 ± 30	359 ± 44	4417 ± 45	4107 ± 100	9.41 ± 0.02	9.31 ± 0.04
416	94 ± 42	88 ± 62	3392 ± 388	4408 ± 194	8.84 ± 0.14	9.05 ± 0.17
417	26 ± 6	28 ± 8	3673 ± 537	3463 ± 564	8.62 ± 0.14	8.58 ± 0.16
418	159 ± 12	145 ± 13	3849 ± 103	3845 ± 124	9.07 ± 0.03	9.05 ± 0.04
419	99 ± 10	91 ± 15	3345 ± 160	3444 ± 225	8.84 ± 0.05	8.84 ± 0.07
420	121 ± 10	103 ± 12	3959 ± 76	4111 ± 84	9.03 ± 0.03	9.03 ± 0.03
421	95 ± 8	72 ± 9	4522 ± 150	4609 ± 176	9.09 ± 0.04	9.04 ± 0.05
422	163 ± 11	161 ± 17	3074 ± 126	3088 ± 189	8.88 ± 0.04	8.88 ± 0.06
423	236 ± 48	218 ± 65	2712 ± 187	3335 ± 135	8.85 ± 0.08	9.02 ± 0.08
424	33 ± 5	38 ± 8	2988 ± 347	2058 ± 683	8.49 ± 0.11	8.20 ± 0.29
425	67 ± 6	67 ± 8	3201 ± 420	1864 ± 796	8.71 ± 0.12	8.24 ± 0.37
426	133 ± 12	127 ± 14	3683 ± 127	4021 ± 136	8.99 ± 0.04	9.05 ± 0.04
427	141 ± 14	148 ± 20	2464 ± 413	3190 ± 423	8.65 ± 0.15	8.89 ± 0.12
428	151 ± 23	157 ± 48	4007 ± 176	4121 ± 326	9.09 ± 0.05	9.12 ± 0.10
429	201 ± 14	154 ± 23	4075 ± 98	3752 ± 224	9.17 ± 0.03	9.04 ± 0.06
430	41 ± 8	37 ± 15	2950 ± 680	2842 ± 899	8.53 ± 0.21	8.47 ± 0.29
431	122 ± 10	112 ± 17	4068 ± 59	3657 ± 140	9.06 ± 0.02	8.94 ± 0.05
432	46 ± 7	54 ± 14	3821 ± 161	3510 ± 457	8.78 ± 0.05	8.74 ± 0.13
433	86 ± 9	69 ± 18	3904 ± 131	3453 ± 565	8.94 ± 0.04	8.78 ± 0.16
434	246 ± 18	233 ± 40	3308 ± 148	3312 ± 281	9.04 ± 0.04	9.03 ± 0.08
435	124 ± 81	141 ± 145	2365 ± 536	3140 ± 602	8.59 ± 0.25	8.86 ± 0.29

Table 2—Continued

Number	$L_{1450}$ $10^{44} \text{ erg s}^{-1}$		$\sigma_{\text{C IV}}$ $\text{km s}^{-1}$		$\log(M_{\text{BH}}/M_{\odot})$	
	HSN	LSN	HSN	LSN	HSN	LSN
436	$263 \pm 36$	$309 \pm 80$	$3976 \pm 138$	$4298 \pm 209$	$9.21 \pm 0.04$	$9.32 \pm 0.07$
437	$105 \pm 9$	$95 \pm 19$	$2913 \pm 109$	$3234 \pm 169$	$8.73 \pm 0.04$	$8.80 \pm 0.07$
438	$68 \pm 8$	$49 \pm 16$	$2963 \pm 154$	$3027 \pm 270$	$8.65 \pm 0.05$	$8.59 \pm 0.11$
439	$41 \pm 6$	$57 \pm 16$	$3328 \pm 161$	$4005 \pm 200$	$8.63 \pm 0.06$	$8.87 \pm 0.08$
440	$72 \pm 9$	$96 \pm 19$	$4077 \pm 114$	$4058 \pm 225$	$8.94 \pm 0.04$	$9.00 \pm 0.07$
441	$62 \pm 6$	$71 \pm 15$	$3557 \pm 165$	$3186 \pm 468$	$8.78 \pm 0.05$	$8.72 \pm 0.14$
442	$77 \pm 14$	$112 \pm 25$	$3915 \pm 192$	$4212 \pm 287$	$8.92 \pm 0.06$	$9.07 \pm 0.08$
443	$186 \pm 59$	$158 \pm 91$	$3110 \pm 245$	$2354 \pm 573$	$8.92 \pm 0.10$	$8.64 \pm 0.25$
444	$91 \pm 24$	$76 \pm 38$	$3383 \pm 309$	$2994 \pm 585$	$8.83 \pm 0.10$	$8.68 \pm 0.21$
445	$105 \pm 80$	$47 \pm 202$	$3969 \pm 297$	$4158 \pm 349$	$9.00 \pm 0.19$	$8.86 \pm 0.98$
446	$63 \pm 103$	$190 \pm 245$	$2440 \pm 715$	$2779 \pm 617$	$8.46 \pm 0.45$	$8.83 \pm 0.35$
447	$39 \pm 9$	$13 \pm 15$	$3261 \pm 415$	$3290 \pm 781$	$8.61 \pm 0.12$	$8.36 \pm 0.34$
448	$85 \pm 10$	$97 \pm 17$	$4265 \pm 101$	$4425 \pm 158$	$9.01 \pm 0.04$	$9.08 \pm 0.05$
449	$168 \pm 19$	$165 \pm 30$	$3611 \pm 131$	$3972 \pm 158$	$9.03 \pm 0.04$	$9.10 \pm 0.05$
450	$50 \pm 11$	$6 \pm 2$	$3226 \pm 426$	$6213 \pm 574$	$8.65 \pm 0.13$	$8.73 \pm 0.13$
451	$83 \pm 23$	$141 \pm 40$	$3797 \pm 260$	$3853 \pm 423$	$8.91 \pm 0.09$	$9.04 \pm 0.12$
452	$71 \pm 33$	$77 \pm 62$	$3211 \pm 375$	$3703 \pm 321$	$8.72 \pm 0.15$	$8.87 \pm 0.20$
453	$22 \pm 9$	$21 \pm 16$	$3594 \pm 368$	$3732 \pm 679$	$8.56 \pm 0.13$	$8.57 \pm 0.24$
454	$92 \pm 8$	$90 \pm 10$	$3578 \pm 114$	$3874 \pm 117$	$8.88 \pm 0.04$	$8.94 \pm 0.04$
455	$26 \pm 9$	$31 \pm 12$	$3432 \pm 521$	$4069 \pm 415$	$8.55 \pm 0.16$	$8.74 \pm 0.13$
456	$44 \pm 8$	$21 \pm 15$	$3643 \pm 264$	$4107 \pm 276$	$8.73 \pm 0.08$	$8.66 \pm 0.18$
457	$94 \pm 67$	$97 \pm 94$	$3501 \pm 156$	$3784 \pm 183$	$8.86 \pm 0.17$	$8.94 \pm 0.23$
458	$25 \pm 10$	$1 \pm 0$	$4208 \pm 174$	$5840 \pm 1391$	$8.73 \pm 0.10$	$8.35 \pm 0.23$
459	$172 \pm 50$	$147 \pm 93$	$2646 \pm 491$	$3635 \pm 472$	$8.76 \pm 0.17$	$9.00 \pm 0.18$
460	$17 \pm 7$	$22 \pm 10$	$3456 \pm 349$	$4237 \pm 419$	$8.46 \pm 0.13$	$8.70 \pm 0.14$
461	$66 \pm 7$	$65 \pm 11$	$4157 \pm 152$	$4489 \pm 255$	$8.94 \pm 0.04$	$9.00 \pm 0.06$
462	$73 \pm 9$	$71 \pm 14$	$3089 \pm 226$	$3462 \pm 303$	$8.70 \pm 0.07$	$8.79 \pm 0.09$
463	$35 \pm 8$	$35 \pm 13$	$3216 \pm 125$	$3123 \pm 244$	$8.57 \pm 0.06$	$8.54 \pm 0.11$
464	$129 \pm 16$	$125 \pm 23$	$3600 \pm 124$	$3636 \pm 168$	$8.96 \pm 0.04$	$8.96 \pm 0.06$

Table 2—Continued

Number	$L_{1450}$ $10^{44} \text{ erg s}^{-1}$		$\sigma_{\text{C IV}}$ $\text{km s}^{-1}$		$\log(M_{\text{BH}}/M_{\odot})$	
	HSN	LSN	HSN	LSN	HSN	LSN
465	336 ± 24	381 ± 34	3805 ± 120	3683 ± 174	9.23 ± 0.03	9.23 ± 0.05
466	35 ± 9	39 ± 17	3232 ± 322	3798 ± 502	8.57 ± 0.11	8.74 ± 0.15
467	414 ± 44	338 ± 70	3280 ± 155	3276 ± 251	9.15 ± 0.05	9.10 ± 0.08
468	111 ± 13	76 ± 23	4159 ± 158	3769 ± 503	9.05 ± 0.04	8.88 ± 0.14
469	99 ± 10	104 ± 17	3661 ± 78	3446 ± 173	8.92 ± 0.03	8.87 ± 0.06
470	130 ± 11	75 ± 16	3598 ± 192	3278 ± 525	8.96 ± 0.05	8.76 ± 0.15
471	263 ± 23	251 ± 51	4216 ± 80	3123 ± 469	9.26 ± 0.03	8.99 ± 0.14
472	673 ± 39	679 ± 86	3645 ± 101	3403 ± 289	9.35 ± 0.03	9.29 ± 0.08
473	423 ± 55	399 ± 142	3233 ± 157	3847 ± 230	9.14 ± 0.05	9.28 ± 0.10
474	83 ± 13	78 ± 31	3817 ± 185	4221 ± 382	8.91 ± 0.06	8.99 ± 0.12
475	188 ± 17	164 ± 36	3359 ± 219	3995 ± 286	8.99 ± 0.06	9.11 ± 0.08
476	156 ± 16	128 ± 32	2463 ± 378	2727 ± 597	8.68 ± 0.14	8.72 ± 0.20
477	109 ± 11	76 ± 25	3593 ± 142	3513 ± 616	8.92 ± 0.04	8.82 ± 0.17
478	48 ± 52	105 ± 170	3726 ± 185	4274 ± 430	8.76 ± 0.25	9.06 ± 0.38
479	67 ± 6	71 ± 16	4255 ± 101	3009 ± 710	8.96 ± 0.03	8.67 ± 0.21
480	95 ± 10	52 ± 8	3343 ± 334	3250 ± 295	8.83 ± 0.09	8.66 ± 0.09
481	37 ± 7	25 ± 5	3158 ± 450	3257 ± 359	8.56 ± 0.13	8.51 ± 0.11
482	66 ± 8	66 ± 6	3647 ± 157	3771 ± 128	8.82 ± 0.05	8.85 ± 0.04
483	92 ± 14	98 ± 13	3789 ± 206	3904 ± 173	8.93 ± 0.06	8.97 ± 0.05
484	35 ± 12	32 ± 10	2583 ± 706	3545 ± 332	8.38 ± 0.25	8.63 ± 0.11
485	288 ± ***	277 ± 18	3521 ± 6404	3660 ± 113	9.13 ± 1.84	9.15 ± 0.03
486	62 ± 7	52 ± 7	3570 ± 169	3650 ± 158	8.79 ± 0.05	8.77 ± 0.05
487	21 ± 8	37 ± 6	4398 ± 326	4723 ± 136	8.72 ± 0.11	8.92 ± 0.05
488	105 ± 40	170 ± 35	4020 ± 192	3155 ± 494	9.01 ± 0.10	8.91 ± 0.14
489	82 ± 15	83 ± 14	3431 ± 129	3095 ± 148	8.82 ± 0.06	8.73 ± 0.06
490	352 ± 49	365 ± 49	3694 ± 114	3430 ± 134	9.22 ± 0.04	9.16 ± 0.05
491	138 ± 9	146 ± 10	3781 ± 160	4309 ± 99	9.02 ± 0.04	9.15 ± 0.03
492	63 ± 7	64 ± 7	4152 ± 172	4158 ± 183	8.92 ± 0.04	8.93 ± 0.05
493	43 ± 6	53 ± 6	4520 ± 166	3749 ± 346	8.91 ± 0.05	8.80 ± 0.09



Table 2—Continued

Number	$L_{1450}$ $10^{44} \text{ erg s}^{-1}$		$\sigma_{\text{C IV}}$ $\text{km s}^{-1}$		$\log(M_{\text{BH}}/M_{\odot})$	
	HSN	LSN	HSN	LSN	HSN	LSN
494	$27 \pm 8$	$37 \pm 8$	$3680 \pm 401$	$3189 \pm 514$	$8.62 \pm 0.12$	$8.57 \pm 0.15$
495	$426 \pm 16$	$403 \pm 17$	$3406 \pm 62$	$3432 \pm 66$	$9.19 \pm 0.02$	$9.18 \pm 0.02$
496	$59 \pm 6$	$63 \pm 6$	$3603 \pm 95$	$3588 \pm 103$	$8.78 \pm 0.03$	$8.80 \pm 0.04$
497	$214 \pm 17$	$168 \pm 15$	$3859 \pm 130$	$4027 \pm 108$	$9.14 \pm 0.03$	$9.12 \pm 0.03$
498	$52 \pm 11$	$46 \pm 11$	$3271 \pm 238$	$3678 \pm 199$	$8.67 \pm 0.08$	$8.74 \pm 0.07$
499	$158 \pm 14$	$116 \pm 17$	$4060 \pm 96$	$3668 \pm 222$	$9.11 \pm 0.03$	$8.95 \pm 0.06$
500	$75 \pm 14$	$2 \pm 0$	$3372 \pm 281$	$5744 \pm 1145$	$8.78 \pm 0.09$	$8.45 \pm 0.19$
501	$97 \pm 15$	$97 \pm 22$	$3523 \pm 143$	$3380 \pm 279$	$8.88 \pm 0.05$	$8.84 \pm 0.09$
502	$53 \pm 11$	$47 \pm 13$	$3131 \pm 640$	$2911 \pm 720$	$8.64 \pm 0.18$	$8.55 \pm 0.22$
503	$57 \pm 9$	$58 \pm 12$	$3077 \pm 432$	$2359 \pm 686$	$8.64 \pm 0.13$	$8.41 \pm 0.26$
504	$83 \pm 20$	$86 \pm 21$	$4093 \pm 194$	$3285 \pm 384$	$8.97 \pm 0.07$	$8.79 \pm 0.12$
505	$259 \pm 22$	$252 \pm 26$	$3482 \pm 50$	$3521 \pm 57$	$9.09 \pm 0.02$	$9.10 \pm 0.03$
506	$257 \pm 19$	$257 \pm 23$	$3012 \pm 91$	$3033 \pm 106$	$8.97 \pm 0.03$	$8.97 \pm 0.04$
507	$341 \pm 69$	$387 \pm 77$	$3910 \pm 156$	$4223 \pm 124$	$9.26 \pm 0.06$	$9.35 \pm 0.05$
508	$185 \pm 17$	$197 \pm 24$	$4004 \pm 117$	$3618 \pm 236$	$9.14 \pm 0.03$	$9.06 \pm 0.06$
509	$74 \pm 16$	$66 \pm 21$	$4064 \pm 248$	$3470 \pm 593$	$8.94 \pm 0.07$	$8.78 \pm 0.17$
510	$72 \pm 17$	$75 \pm 26$	$3140 \pm 186$	$2554 \pm 404$	$8.71 \pm 0.08$	$8.54 \pm 0.16$
511	$276 \pm 41$	$286 \pm 67$	$3735 \pm 80$	$3338 \pm 182$	$9.17 \pm 0.04$	$9.08 \pm 0.07$
512	$58 \pm 10$	$59 \pm 14$	$3466 \pm 262$	$3485 \pm 339$	$8.75 \pm 0.08$	$8.76 \pm 0.10$
513	$111 \pm 11$	$109 \pm 15$	$4399 \pm 152$	$4119 \pm 277$	$9.10 \pm 0.04$	$9.04 \pm 0.07$
514	$73 \pm 12$	$75 \pm 16$	$3439 \pm 160$	$3490 \pm 212$	$8.79 \pm 0.06$	$8.81 \pm 0.07$
515	$41 \pm 9$	$36 \pm 12$	$3433 \pm 273$	$3072 \pm 599$	$8.66 \pm 0.09$	$8.53 \pm 0.19$
516	$93 \pm 13$	$80 \pm 17$	$3664 \pm 161$	$3626 \pm 195$	$8.90 \pm 0.05$	$8.86 \pm 0.07$
517	$82 \pm 7$	$85 \pm 10$	$3750 \pm 71$	$3884 \pm 88$	$8.89 \pm 0.03$	$8.93 \pm 0.03$
518	$21 \pm 12$	$10 \pm 9$	$2852 \pm 478$	$3183 \pm 280$	$8.34 \pm 0.20$	$8.27 \pm 0.23$
519	$177 \pm 27$	$170 \pm 22$	$3679 \pm 133$	$3643 \pm 114$	$9.05 \pm 0.05$	$9.04 \pm 0.04$
520	$77 \pm 11$	$89 \pm 10$	$3426 \pm 225$	$3217 \pm 223$	$8.80 \pm 0.07$	$8.78 \pm 0.07$
521	$183 \pm 37$	$147 \pm 30$	$3431 \pm 313$	$2766 \pm 488$	$9.00 \pm 0.09$	$8.76 \pm 0.16$
522	$71 \pm 14$	$67 \pm 13$	$4248 \pm 183$	$4139 \pm 246$	$8.97 \pm 0.06$	$8.93 \pm 0.07$

Table 2—Continued

Number	$L_{1450}$ $10^{44} \text{ erg s}^{-1}$		$\sigma_{C IV}$ $\text{km s}^{-1}$		$\log(M_{BH}/M_{\odot})$	
	HSN	LSN	HSN	LSN	HSN	LSN
523	253 ± 26	216 ± 25	3554 ± 135	3231 ± 190	9.11 ± 0.04	8.99 ± 0.06
524	46 ± 11	53 ± 12	3485 ± 323	3265 ± 325	8.70 ± 0.10	8.67 ± 0.10
525	90 ± 16	99 ± 16	4617 ± 247	4487 ± 194	9.10 ± 0.06	9.09 ± 0.05
526	130 ± 13	145 ± 12	3407 ± 81	3448 ± 77	8.92 ± 0.03	8.95 ± 0.03
527	129 ± 16	131 ± 13	2362 ± 524	3785 ± 133	8.60 ± 0.19	9.01 ± 0.04
528	112 ± 7	102 ± 9	3415 ± 108	3455 ± 130	8.88 ± 0.03	8.87 ± 0.04
529	146 ± 8	154 ± 9	3510 ± 114	3478 ± 135	8.97 ± 0.03	8.97 ± 0.04
530	76 ± 7	93 ± 12	3006 ± 139	2780 ± 227	8.68 ± 0.05	8.66 ± 0.08
531	75 ± 6	94 ± 9	3288 ± 92	3203 ± 128	8.76 ± 0.03	8.79 ± 0.04
532	50 ± 9	58 ± 17	4129 ± 183	4052 ± 288	8.87 ± 0.06	8.88 ± 0.09
533	110 ± 14	120 ± 31	4357 ± 167	3350 ± 857	9.09 ± 0.05	8.88 ± 0.23
534	47 ± 9	50 ± 17	3803 ± 173	3930 ± 268	8.78 ± 0.06	8.82 ± 0.10
535	339 ± 33	324 ± 64	3104 ± 186	2859 ± 490	9.06 ± 0.06	8.97 ± 0.16
536	56 ± 7	57 ± 12	3689 ± 178	4288 ± 183	8.79 ± 0.05	8.93 ± 0.06
537	42 ± 7	36 ± 12	4151 ± 63	3942 ± 154	8.83 ± 0.04	8.75 ± 0.09
538	41 ± 12	4 ± 2	3341 ± 498	6197 ± 808	8.64 ± 0.15	8.68 ± 0.17
539	27 ± 7	21 ± 19	4425 ± 222	4462 ± 498	8.78 ± 0.08	8.74 ± 0.23
540	453 ± 36	458 ± 62	3213 ± 94	3690 ± 137	9.15 ± 0.03	9.27 ± 0.05
541	91 ± 8	92 ± 16	3264 ± 143	2934 ± 393	8.80 ± 0.04	8.71 ± 0.12
542	182 ± 18	211 ± 35	3325 ± 233	3724 ± 305	8.97 ± 0.07	9.10 ± 0.08
543	174 ± 26	152 ± 47	3321 ± 230	3518 ± 521	8.96 ± 0.07	8.98 ± 0.15
544	33 ± 8	37 ± 15	3654 ± 119	3861 ± 202	8.67 ± 0.06	8.74 ± 0.10
545	116 ± 20	116 ± 16	2797 ± 297	2413 ± 311	8.72 ± 0.10	8.59 ± 0.12
546	122 ± 19	109 ± 18	3585 ± 141	3468 ± 146	8.95 ± 0.05	8.89 ± 0.05
547	95 ± 12	92 ± 11	3690 ± 112	3683 ± 121	8.91 ± 0.04	8.90 ± 0.04
548	301 ± 56	220 ± 49	4123 ± 252	4013 ± 205	9.27 ± 0.07	9.18 ± 0.07
549	104 ± 15	92 ± 13	4049 ± 166	3445 ± 224	9.02 ± 0.05	8.85 ± 0.07
550	99 ± 14	96 ± 12	4346 ± 161	4809 ± 89	9.06 ± 0.05	9.15 ± 0.03
551	164 ± 16	180 ± 15	3692 ± 99	3372 ± 106	9.04 ± 0.03	8.98 ± 0.03

Table 2—Continued

Number	$L_{1450}$ $10^{44} \text{ erg s}^{-1}$		$\sigma_{\text{C IV}}$ $\text{km s}^{-1}$		$\log(M_{\text{BH}}/M_{\odot})$	
	HSN	LSN	HSN	LSN	HSN	LSN
552	$84 \pm 10$	$102 \pm 11$	$4279 \pm 198$	$4597 \pm 202$	$9.01 \pm 0.05$	$9.12 \pm 0.05$
553	$194 \pm 13$	$239 \pm 15$	$3176 \pm 112$	$3447 \pm 117$	$8.95 \pm 0.03$	$9.07 \pm 0.03$
554	$105 \pm 60$	$185 \pm 71$	$3882 \pm 240$	$3612 \pm 365$	$8.98 \pm 0.14$	$9.05 \pm 0.13$
555	$46 \pm 8$	$55 \pm 9$	$3576 \pm 51$	$3564 \pm 49$	$8.72 \pm 0.04$	$8.76 \pm 0.04$
556	$124 \pm 27$	$148 \pm 30$	$3559 \pm 303$	$3842 \pm 214$	$8.94 \pm 0.09$	$9.05 \pm 0.07$
557	$203 \pm 24$	$267 \pm 27$	$3824 \pm 166$	$3987 \pm 138$	$9.12 \pm 0.05$	$9.22 \pm 0.04$
558	$34 \pm 15$	$36 \pm 9$	$3049 \pm 796$	$3416 \pm 368$	$8.52 \pm 0.25$	$8.62 \pm 0.11$
559	$32 \pm 18$	$76 \pm 12$	$3989 \pm 265$	$3723 \pm 184$	$8.73 \pm 0.14$	$8.87 \pm 0.06$
560	$298 \pm 70$	$296 \pm 61$	$2912 \pm 142$	$2794 \pm 122$	$8.97 \pm 0.07$	$8.93 \pm 0.06$
561	$211 \pm 118$	$127 \pm 97$	$3334 \pm 221$	$3304 \pm 139$	$9.01 \pm 0.14$	$8.88 \pm 0.18$
562	$78 \pm 13$	$120 \pm 12$	$3196 \pm 201$	$3312 \pm 164$	$8.74 \pm 0.07$	$8.87 \pm 0.05$
563	$64 \pm 9$	$76 \pm 9$	$3699 \pm 148$	$3454 \pm 181$	$8.83 \pm 0.05$	$8.81 \pm 0.05$
564	$100 \pm 10$	$131 \pm 13$	$3484 \pm 109$	$3743 \pm 103$	$8.87 \pm 0.04$	$9.00 \pm 0.03$
565	$159 \pm 15$	$127 \pm 18$	$4435 \pm 56$	$4572 \pm 56$	$9.19 \pm 0.02$	$9.17 \pm 0.03$
566	$22 \pm 8$	$33 \pm 10$	$3546 \pm 211$	$3114 \pm 503$	$8.54 \pm 0.10$	$8.52 \pm 0.16$
567	$246 \pm 37$	$317 \pm 48$	$3100 \pm 220$	$2221 \pm 525$	$8.98 \pm 0.07$	$8.75 \pm 0.21$
568	$111 \pm 10$	$101 \pm 11$	$3403 \pm 158$	$3451 \pm 165$	$8.88 \pm 0.05$	$8.87 \pm 0.05$
569	$197 \pm 22$	$189 \pm 31$	$4202 \pm 91$	$3950 \pm 165$	$9.19 \pm 0.03$	$9.13 \pm 0.05$
570	$90 \pm 10$	$104 \pm 14$	$3284 \pm 99$	$3374 \pm 125$	$8.80 \pm 0.04$	$8.86 \pm 0.04$
571	$116 \pm 9$	$88 \pm 10$	$2710 \pm 217$	$3110 \pm 199$	$8.69 \pm 0.07$	$8.75 \pm 0.06$
572	$99 \pm 8$	$90 \pm 10$	$3568 \pm 138$	$3146 \pm 313$	$8.89 \pm 0.04$	$8.76 \pm 0.09$
573	$49 \pm 8$	$54 \pm 9$	$4791 \pm 250$	$4659 \pm 263$	$8.99 \pm 0.06$	$8.99 \pm 0.06$
574	$40 \pm 6$	$47 \pm 7$	$3333 \pm 141$	$3438 \pm 121$	$8.63 \pm 0.05$	$8.69 \pm 0.05$
575	$237 \pm 20$	$222 \pm 5$	$3981 \pm 41$	$3941 \pm 52$	$9.19 \pm 0.02$	$9.16 \pm 0.01$
576	$513 \pm 70$	$2 \pm 0$	$4162 \pm 238$	$10060 \pm 846$	$9.41 \pm 0.06$	$8.97 \pm 0.08$
577	$69 \pm 10$	$57 \pm 12$	$3568 \pm 168$	$2842 \pm 451$	$8.81 \pm 0.05$	$8.57 \pm 0.15$
578	$158 \pm 9$	$133 \pm 12$	$3503 \pm 108$	$3765 \pm 104$	$8.99 \pm 0.03$	$9.01 \pm 0.03$
579	$164 \pm 11$	$203 \pm 16$	$3630 \pm 76$	$3595 \pm 105$	$9.02 \pm 0.02$	$9.07 \pm 0.03$
580	$38 \pm 6$	$46 \pm 8$	$3779 \pm 142$	$3689 \pm 212$	$8.73 \pm 0.05$	$8.75 \pm 0.07$

Table 2—Continued

Number	$L_{1450}$ $10^{44} \text{ erg s}^{-1}$		$\sigma_{\text{C IV}}$ $\text{km s}^{-1}$		$\log(M_{\text{BH}}/M_{\odot})$	
	HSN	LSN	HSN	LSN	HSN	LSN
581	$64 \pm 6$	$68 \pm 8$	$3078 \pm 178$	$3155 \pm 203$	$8.67 \pm 0.05$	$8.70 \pm 0.06$
582	$47 \pm 6$	$53 \pm 7$	$3698 \pm 171$	$3885 \pm 202$	$8.75 \pm 0.05$	$8.83 \pm 0.06$
583	$220 \pm 18$	$217 \pm 24$	$3609 \pm 135$	$3261 \pm 292$	$9.09 \pm 0.04$	$9.00 \pm 0.08$
584	$97 \pm 10$	$82 \pm 12$	$3670 \pm 44$	$3723 \pm 59$	$8.91 \pm 0.03$	$8.89 \pm 0.04$
585	$81 \pm 7$	$112 \pm 10$	$4051 \pm 148$	$3704 \pm 252$	$8.96 \pm 0.04$	$8.96 \pm 0.06$
586	$99 \pm 10$	$107 \pm 14$	$4018 \pm 132$	$3901 \pm 162$	$9.00 \pm 0.04$	$8.99 \pm 0.05$
587	$169 \pm 14$	$159 \pm 16$	$3521 \pm 112$	$3237 \pm 161$	$9.00 \pm 0.03$	$8.92 \pm 0.05$
588	$62 \pm 6$	$57 \pm 6$	$3008 \pm 155$	$3288 \pm 126$	$8.64 \pm 0.05$	$8.69 \pm 0.04$
589	$203 \pm 14$	$157 \pm 13$	$2612 \pm 288$	$3637 \pm 106$	$8.79 \pm 0.10$	$9.02 \pm 0.03$
590	$51 \pm 5$	$47 \pm 5$	$3510 \pm 129$	$3095 \pm 164$	$8.73 \pm 0.04$	$8.60 \pm 0.05$
591	$143 \pm 7$	$116 \pm 7$	$4286 \pm 53$	$3834 \pm 79$	$9.14 \pm 0.02$	$8.99 \pm 0.02$
592	$174 \pm 7$	$141 \pm 8$	$3370 \pm 46$	$3316 \pm 58$	$8.97 \pm 0.02$	$8.91 \pm 0.02$
593	$43 \pm 6$	$49 \pm 5$	$3979 \pm 171$	$3803 \pm 186$	$8.80 \pm 0.05$	$8.79 \pm 0.05$
594	$77 \pm 6$	$80 \pm 6$	$2194 \pm 610$	$3423 \pm 239$	$8.41 \pm 0.24$	$8.81 \pm 0.06$
595	$280 \pm 46$	$303 \pm 50$	$3616 \pm 97$	$3861 \pm 90$	$9.14 \pm 0.04$	$9.22 \pm 0.04$
596	$11 \pm 5$	$19 \pm 5$	$4097 \pm 264$	$4685 \pm 208$	$8.52 \pm 0.12$	$8.75 \pm 0.07$
597	$84 \pm 7$	$76 \pm 8$	$3861 \pm 107$	$3614 \pm 128$	$8.92 \pm 0.03$	$8.84 \pm 0.04$
598	$187 \pm 19$	$127 \pm 23$	$3029 \pm 191$	$3406 \pm 206$	$8.90 \pm 0.06$	$8.91 \pm 0.07$
599	$66 \pm 9$	$57 \pm 14$	$4111 \pm 130$	$3447 \pm 497$	$8.92 \pm 0.04$	$8.74 \pm 0.14$
600	$98 \pm 21$	$73 \pm 32$	$3585 \pm 266$	$4095 \pm 283$	$8.90 \pm 0.08$	$8.94 \pm 0.12$
601	$310 \pm 22$	$315 \pm 40$	$3907 \pm 82$	$3656 \pm 197$	$9.23 \pm 0.02$	$9.18 \pm 0.06$
602	$543 \pm 26$	$494 \pm 41$	$3040 \pm 78$	$3144 \pm 143$	$9.15 \pm 0.03$	$9.15 \pm 0.04$
603	$108 \pm 11$	$90 \pm 19$	$3116 \pm 170$	$3342 \pm 241$	$8.80 \pm 0.05$	$8.82 \pm 0.08$
604	$961 \pm 50$	$764 \pm 80$	$3562 \pm 93$	$3075 \pm 245$	$9.41 \pm 0.03$	$9.23 \pm 0.07$
605	$81 \pm 11$	$44 \pm 18$	$2830 \pm 404$	$3362 \pm 563$	$8.65 \pm 0.13$	$8.66 \pm 0.18$
606	$18 \pm 7$	$29 \pm 11$	$4811 \pm 88$	$4883 \pm 178$	$8.77 \pm 0.10$	$8.89 \pm 0.10$
607	$180 \pm 11$	$105 \pm 12$	$3435 \pm 161$	$3068 \pm 314$	$9.00 \pm 0.04$	$8.78 \pm 0.09$
608	$64 \pm 9$	$69 \pm 16$	$3517 \pm 133$	$3821 \pm 172$	$8.78 \pm 0.05$	$8.87 \pm 0.07$
609	$511 \pm 41$	$432 \pm 64$	$3638 \pm 142$	$3694 \pm 177$	$9.29 \pm 0.04$	$9.26 \pm 0.05$

Table 2—Continued

Number	$L_{1450}$ $10^{44} \text{ erg s}^{-1}$		$\sigma_{C\ IV}$ $\text{km s}^{-1}$		$\log(M_{BH}/M_{\odot})$	
	HSN	LSN	HSN	LSN	HSN	LSN
610	$203 \pm 23$	$243 \pm 47$	$3831 \pm 158$	$3584 \pm 366$	$9.12 \pm 0.04$	$9.10 \pm 0.10$
611	$102 \pm 7$	$96 \pm 11$	$3539 \pm 126$	$3330 \pm 233$	$8.89 \pm 0.04$	$8.83 \pm 0.07$
612	$72 \pm 9$	$85 \pm 17$	$4152 \pm 164$	$3897 \pm 266$	$8.95 \pm 0.05$	$8.94 \pm 0.08$
613	$586 \pm 56$	$567 \pm 84$	$3521 \pm 87$	$3943 \pm 90$	$9.29 \pm 0.03$	$9.38 \pm 0.04$
614	$89 \pm 11$	$97 \pm 18$	$3757 \pm 162$	$3749 \pm 277$	$8.91 \pm 0.05$	$8.93 \pm 0.08$
615	$89 \pm 52$	$82 \pm 77$	$3030 \pm 400$	$3344 \pm 589$	$8.73 \pm 0.18$	$8.80 \pm 0.26$

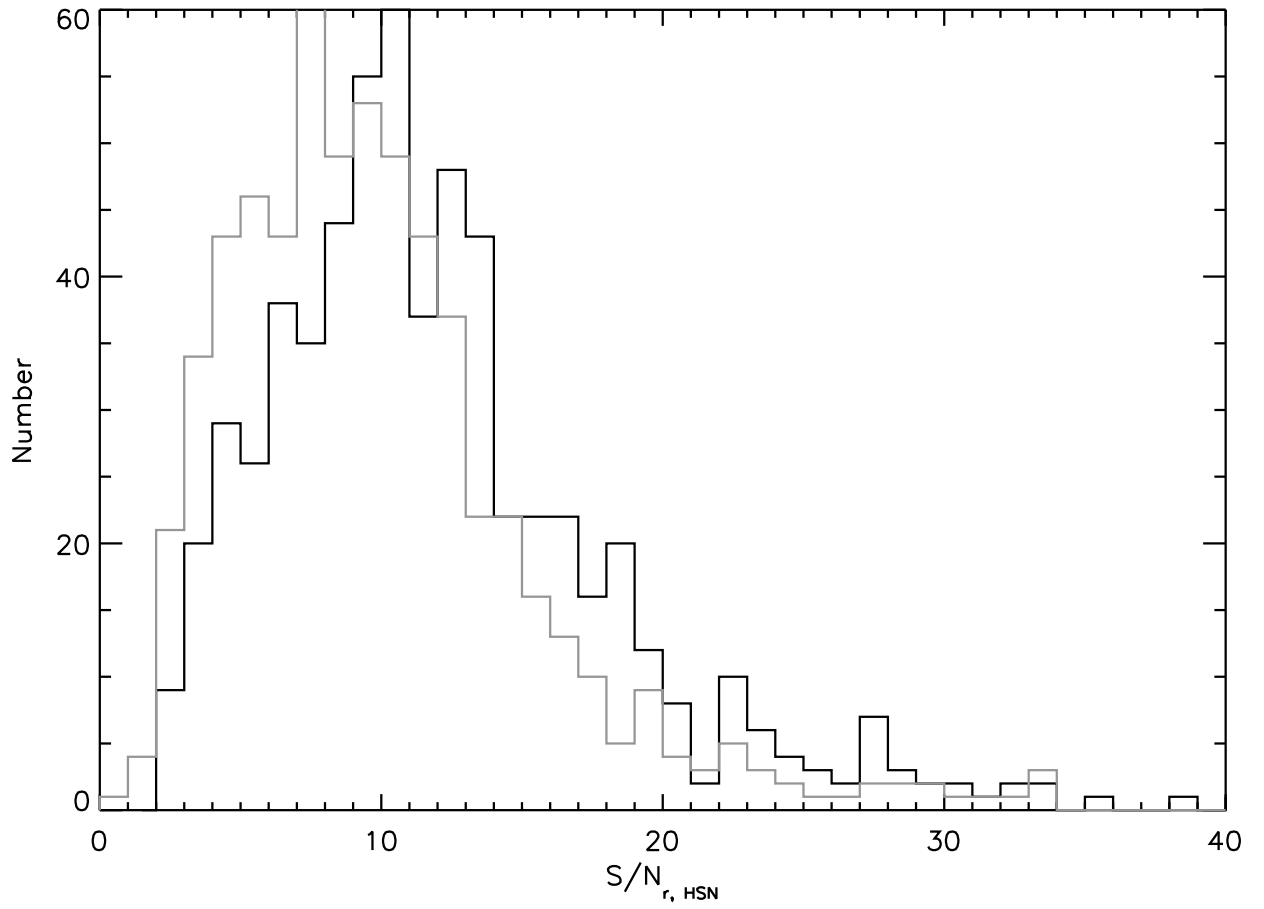


Fig. 1.—  $r$ -band signal-to-noise ratio at the high-S/N (dark histogram) and low-S/N (gray histogram) epochs.

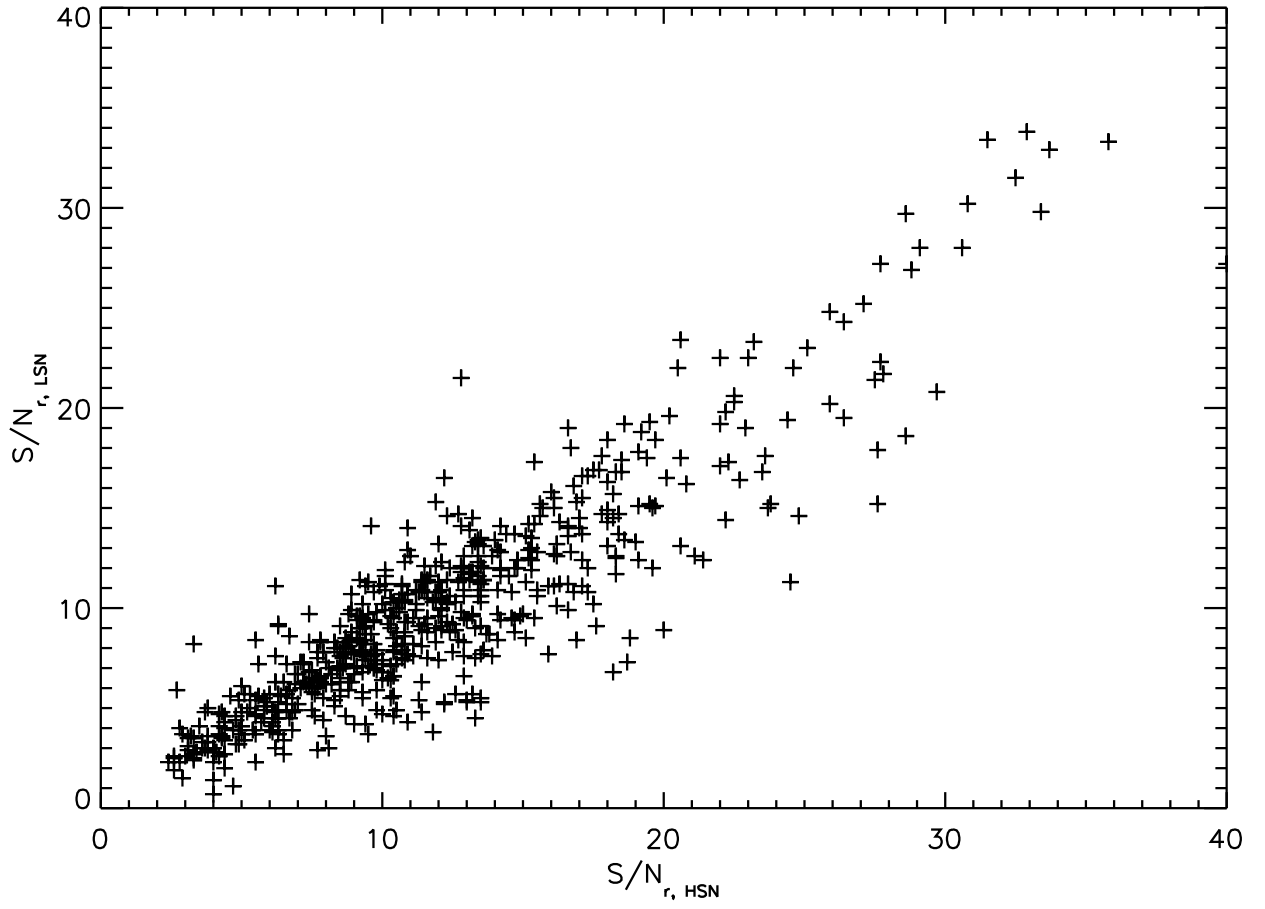


Fig. 2.—  $r$ -band signal-to-noise ratio at the high-S/N epoch versus the same quantity at the low-S/N epoch.

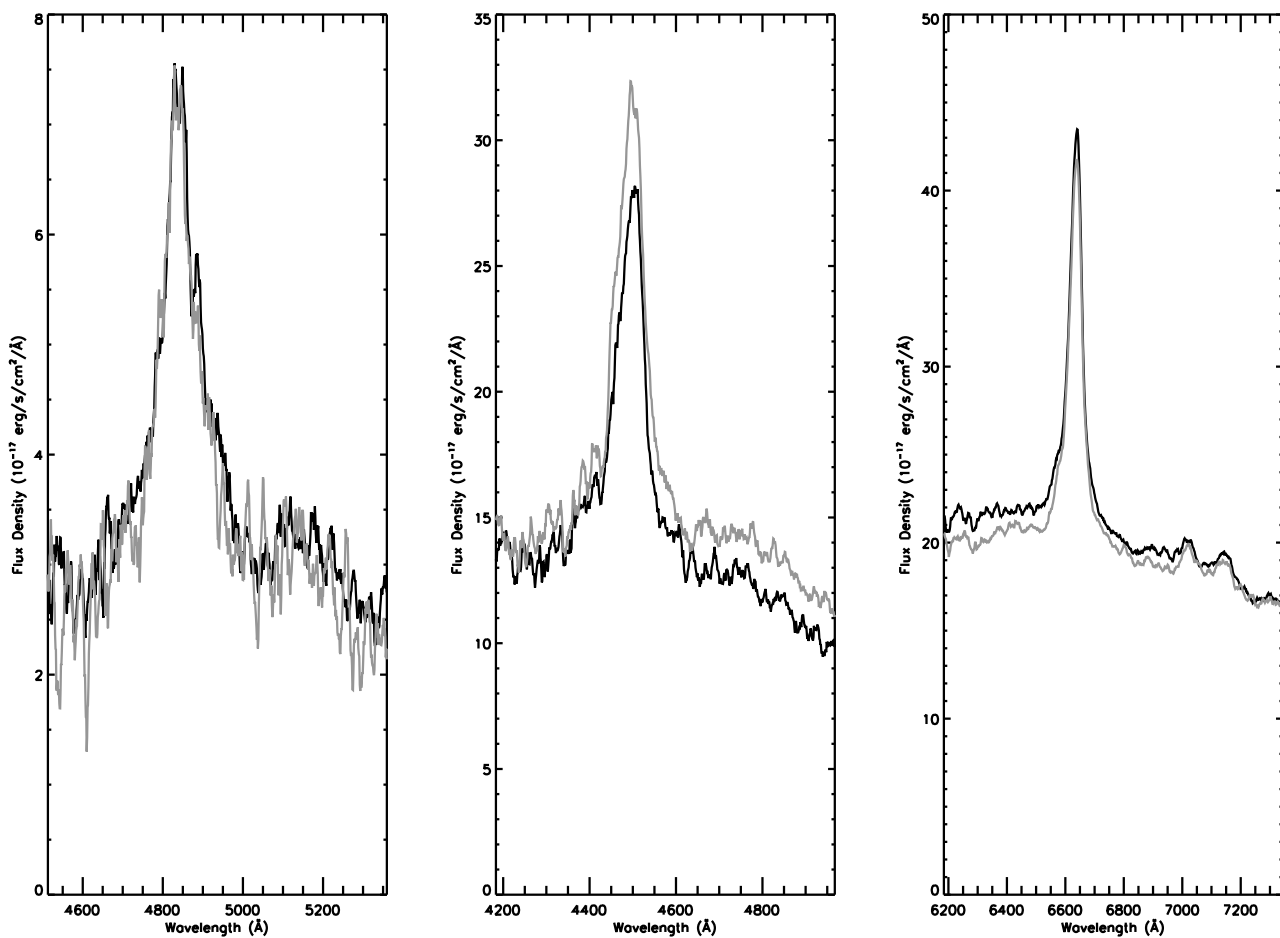


Fig. 3.— Example spectra from the quasars studied in this paper, with objects increasing in spectra signal-to-noise ratio from left to right. Shown in the observed frame are the regions of the spectra used in the estimation of black hole mass. Dark curves represent the spectra from the high-S/N epoch, while grey curves are those spectra for the low-S/N epoch. (Left) SDSS J150104.94–010727.9;  $S/N_{r,\text{HSN}}=4.9$  (Center) SDSS J101416.97+484816.1;  $S/N_{r,\text{HSN}}=12.1$  (Right) SDSS J030449.86–000813.4;  $S/N_{r,\text{HSN}}=30.8$ .



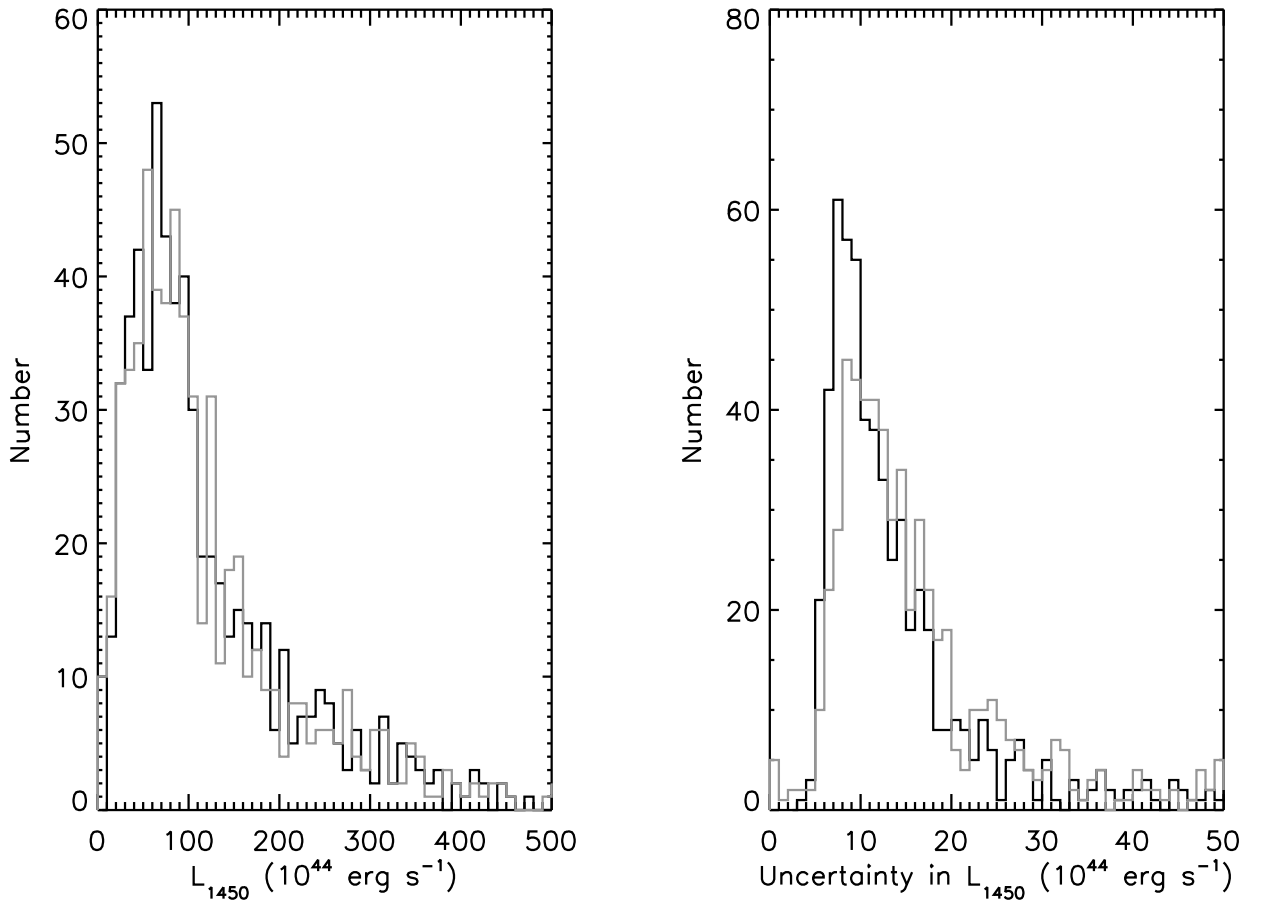


Fig. 4.— (Left) 1450Å luminosity ( $L_{1450}$ ) at the high-S/N (dark histogram) and low-S/N (gray histogram) epochs. (Right) Uncertainty in the 1450Å luminosity at the high-S/N (dark histogram) and low-S/N (gray histogram) epochs.

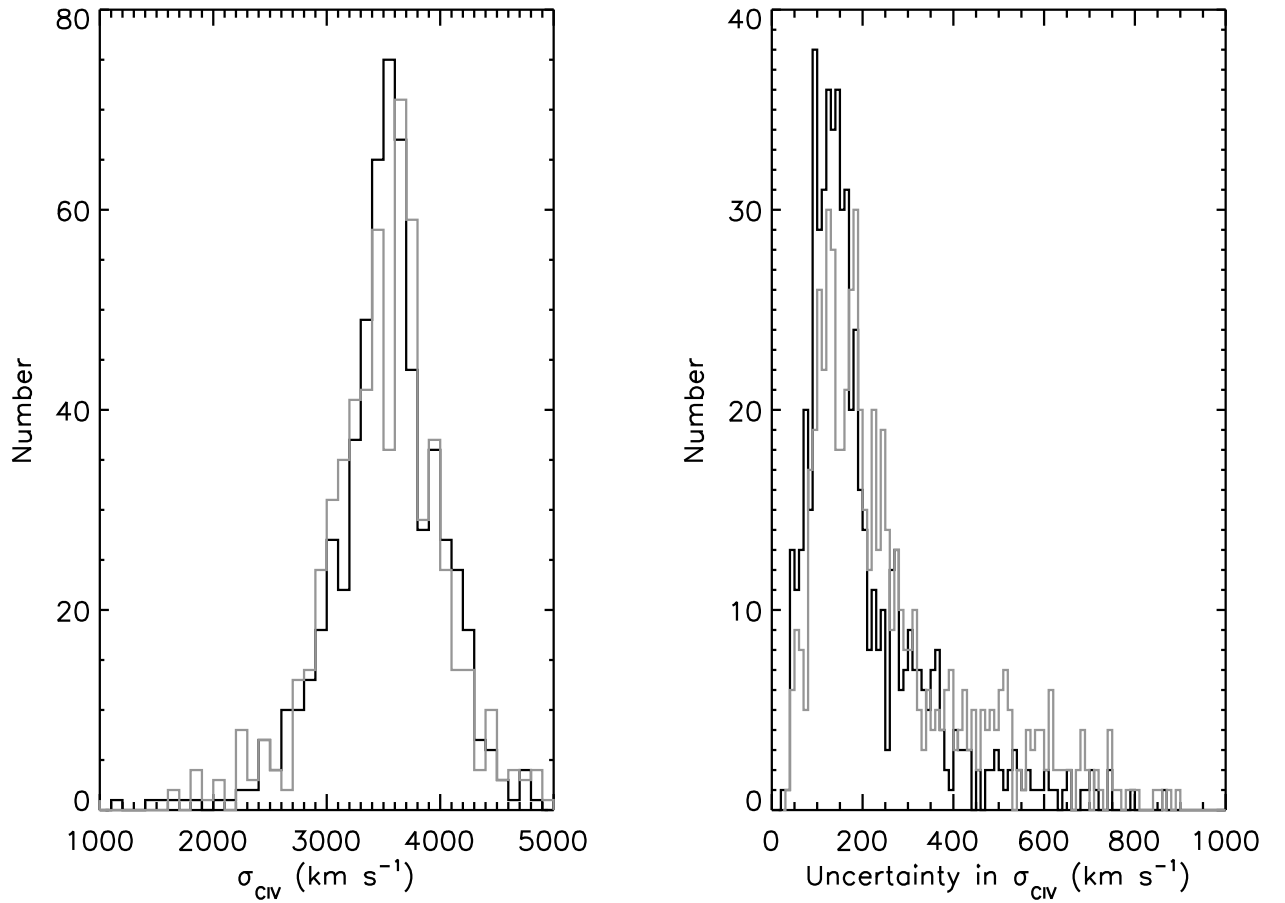


Fig. 5.— (Left) C IV line dispersion ( $\sigma_{CIV}$ ) at the high-S/N (dark histogram) and low-S/N (gray histogram) epochs. (Right) Uncertainty in the C IV line dispersion at the high-S/N (dark histogram) and low-S/N (gray histogram) epochs.

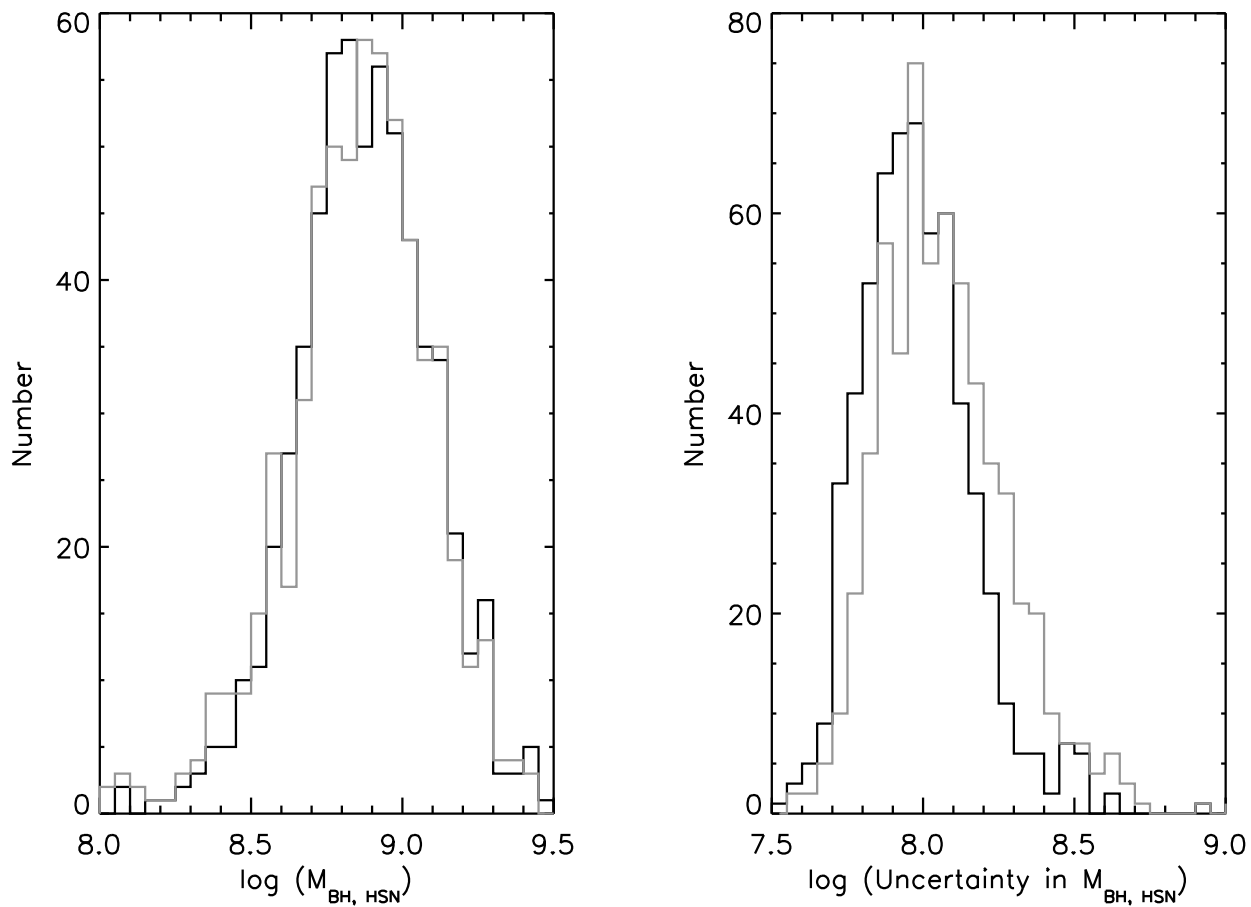


Fig. 6.— (Left) Logarithm of the estimated black hole mass ( $M_{BH}$ ) at high-S/N (dark histogram) and low-S/N (gray histogram) epochs. (Right) Logarithm of the uncertainty ((calculated by propagating measurement errors in  $L_{1450}$  and  $\sigma_{CIV}$ ) in the estimated black hole mass at the high-S/N (dark histogram) and low-S/N (gray histogram) epochs.

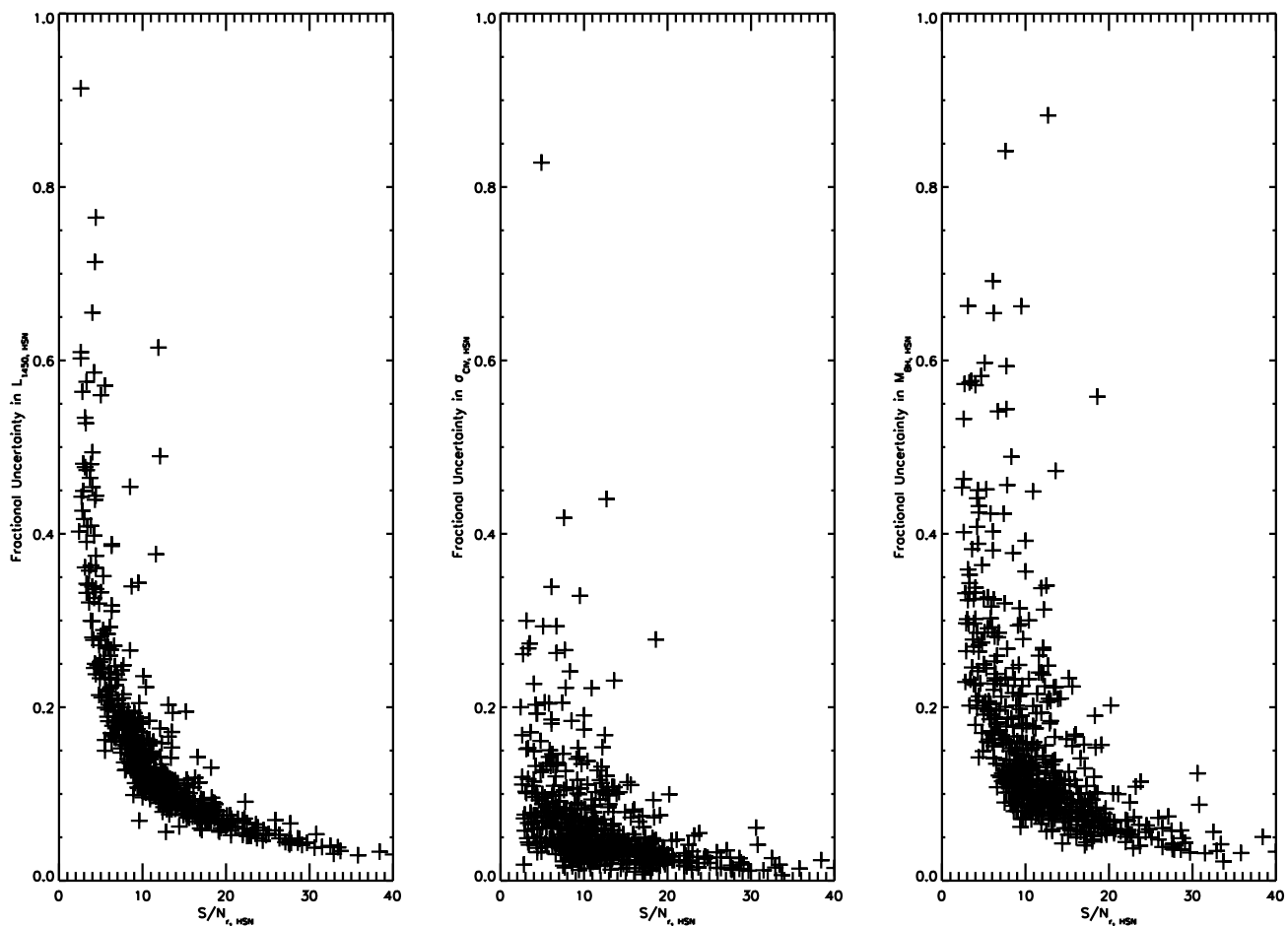


Fig. 7.— (Left) Fractional measurement uncertainty in the 1450Å luminosity ( $\sigma_{L_{1450}}/L_{1450}$ ) as a function of  $r$ -band signal-to-noise ratio ( $S/N_r$ ) at the high- $S/N$  epoch. (Center) The same, but for uncertainty in the C IV line dispersion. (Right) The same, but for uncertainty in the estimated black hole mass.

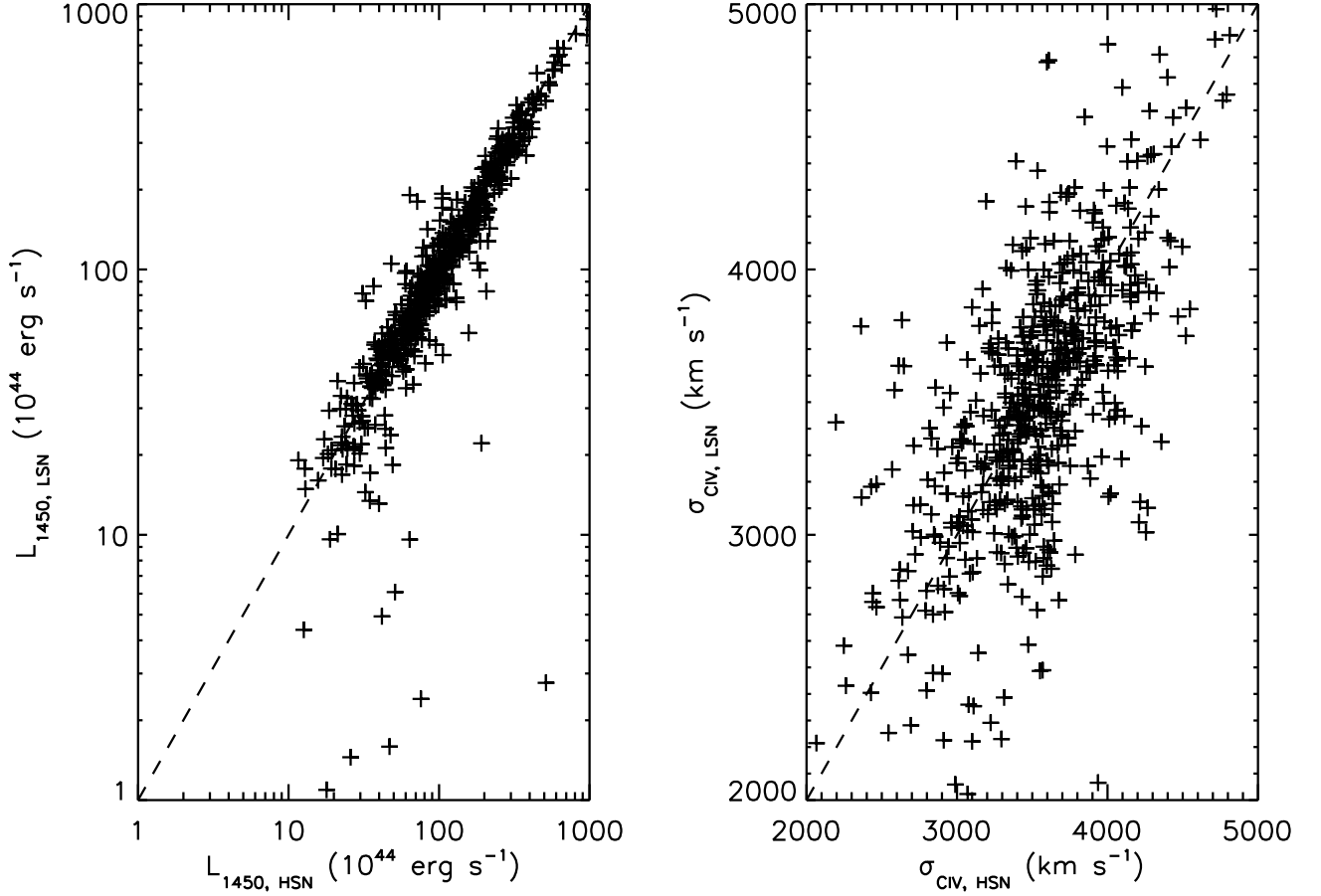


Fig. 8.— (Left) 1450Å luminosity at the high-S/N epoch ( $L_{1450, \text{HSN}}$ ) versus the same quantity at the low-S/N epoch ( $L_{1450, \text{LSN}}$ ). (Right) C IV line dispersion at the high-S/N epoch ( $\sigma_{\text{CIV, HSN}}$ ) versus the same quantity at the low-S/N epoch ( $\sigma_{\text{CIV, LSN}}$ ). The dashed lines indicate zero change in the quantities between epochs.

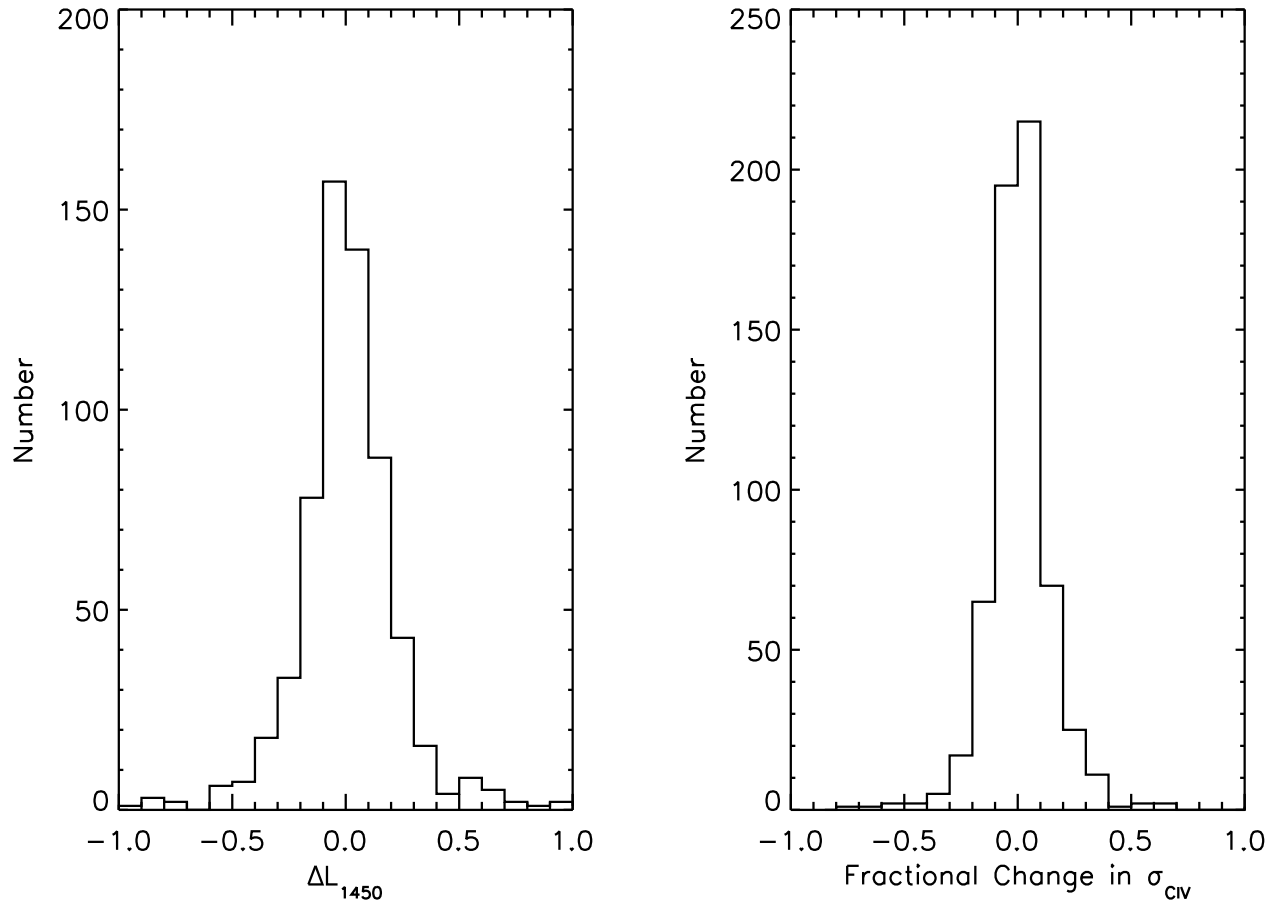


Fig. 9.— (Left) Fractional change in 1450Å luminosity. The standard deviation of the sample is 0.161. (Right) Fractional change in C IV line dispersion. The standard deviation is 0.108.

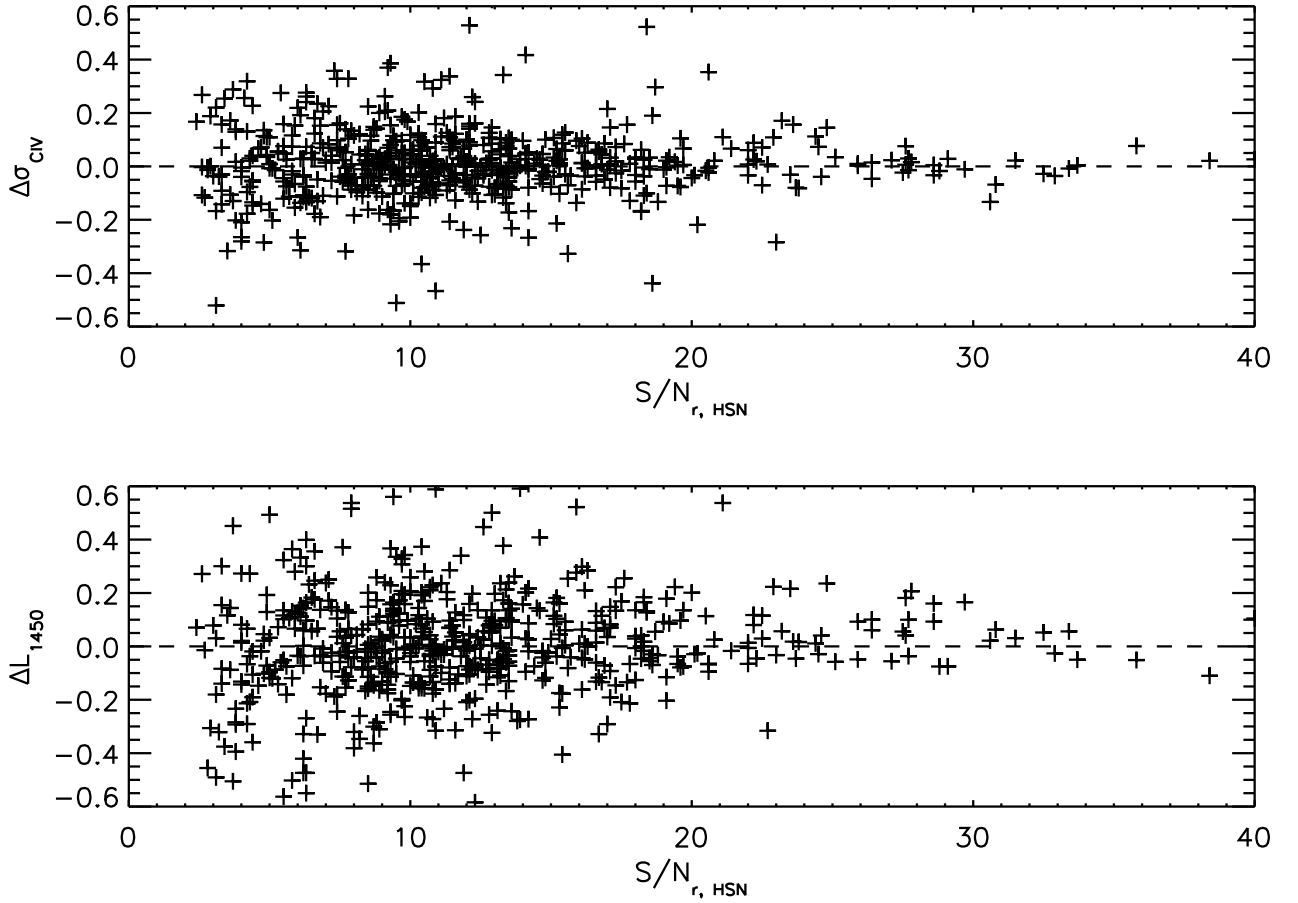


Fig. 10.— (Upper) Fractional change in C IV line dispersion as a function of  $r$ -band signal-to-noise ratio at the high-S/N epoch. (Lower) Fractional change in  $1450\text{\AA}$  luminosity as a function of  $r$ -band signal-to-noise ratio at the high-S/N epoch. The dashed lines indicate zero change in the quantities between epochs.

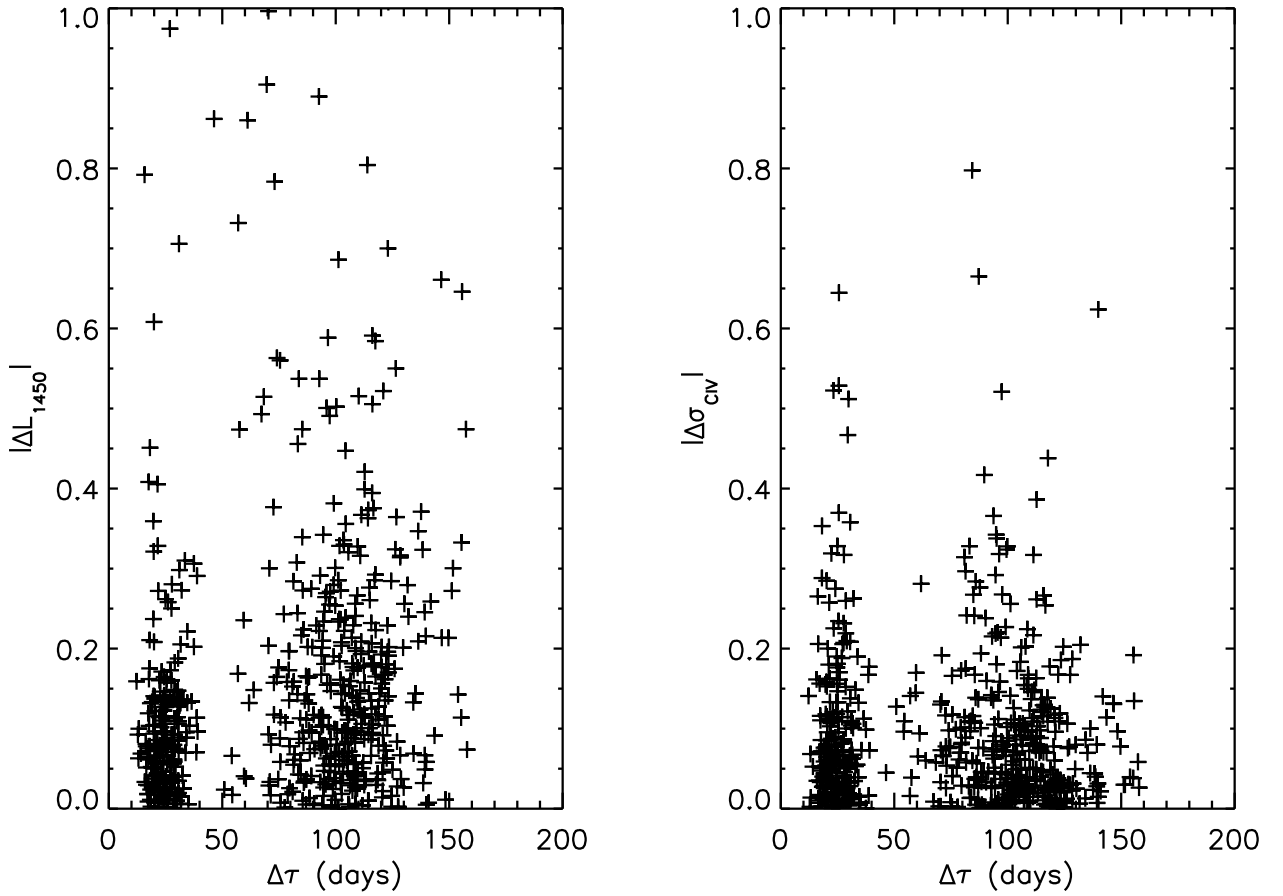


Fig. 11.— (Left) Absolute value of the fractional change in 1450Å luminosity as a function of rest-frame time lag between epochs. (Right) Absolute value of the fractional change in C IV line dispersion as a function of rest-frame time lag between epochs.



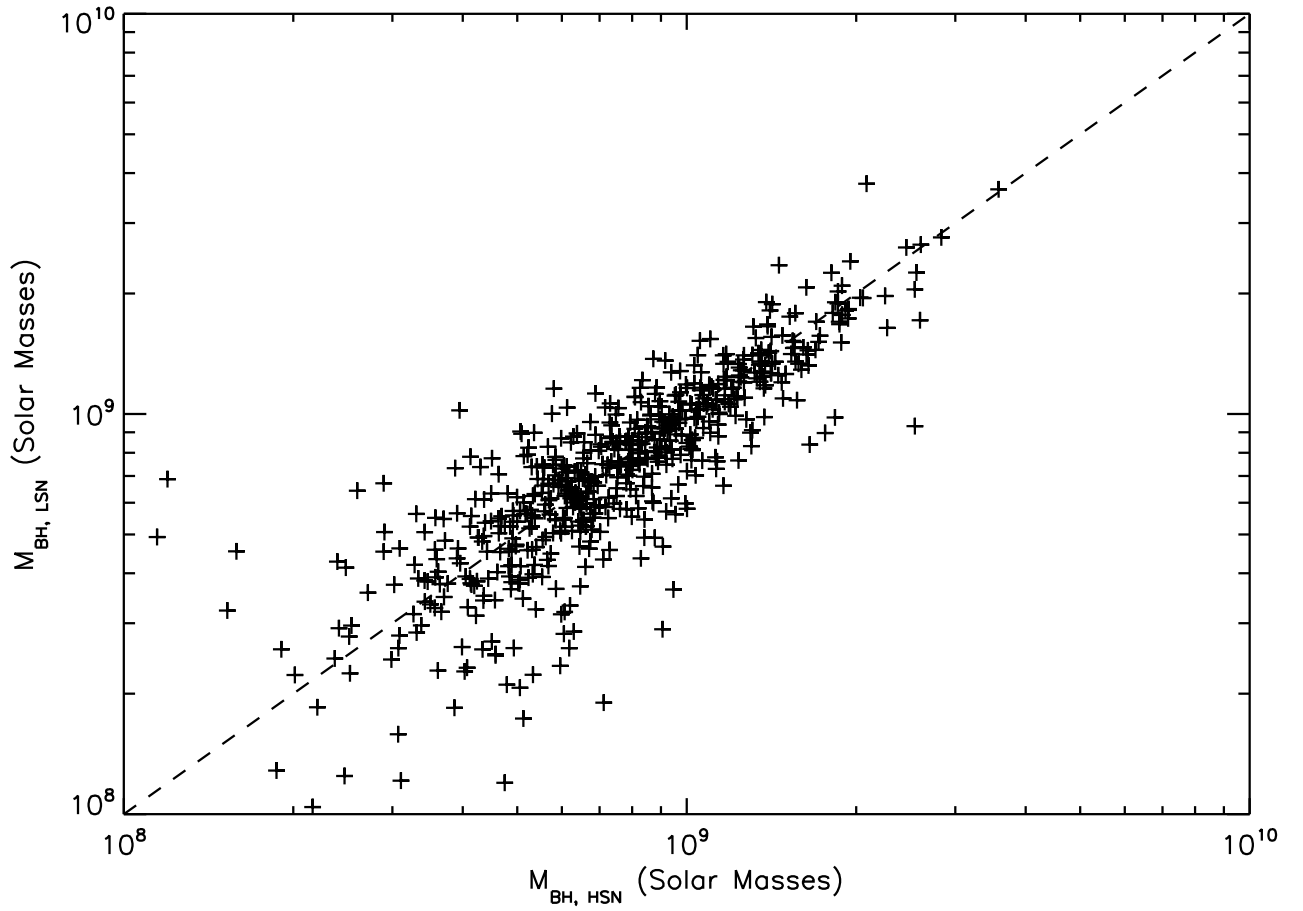


Fig. 12.— Estimated black hole mass at the high-S/N epoch versus the same quantity at the low-S/N epoch. The dashed line indicates zero change in  $M_{\text{BH}}$  between epochs.

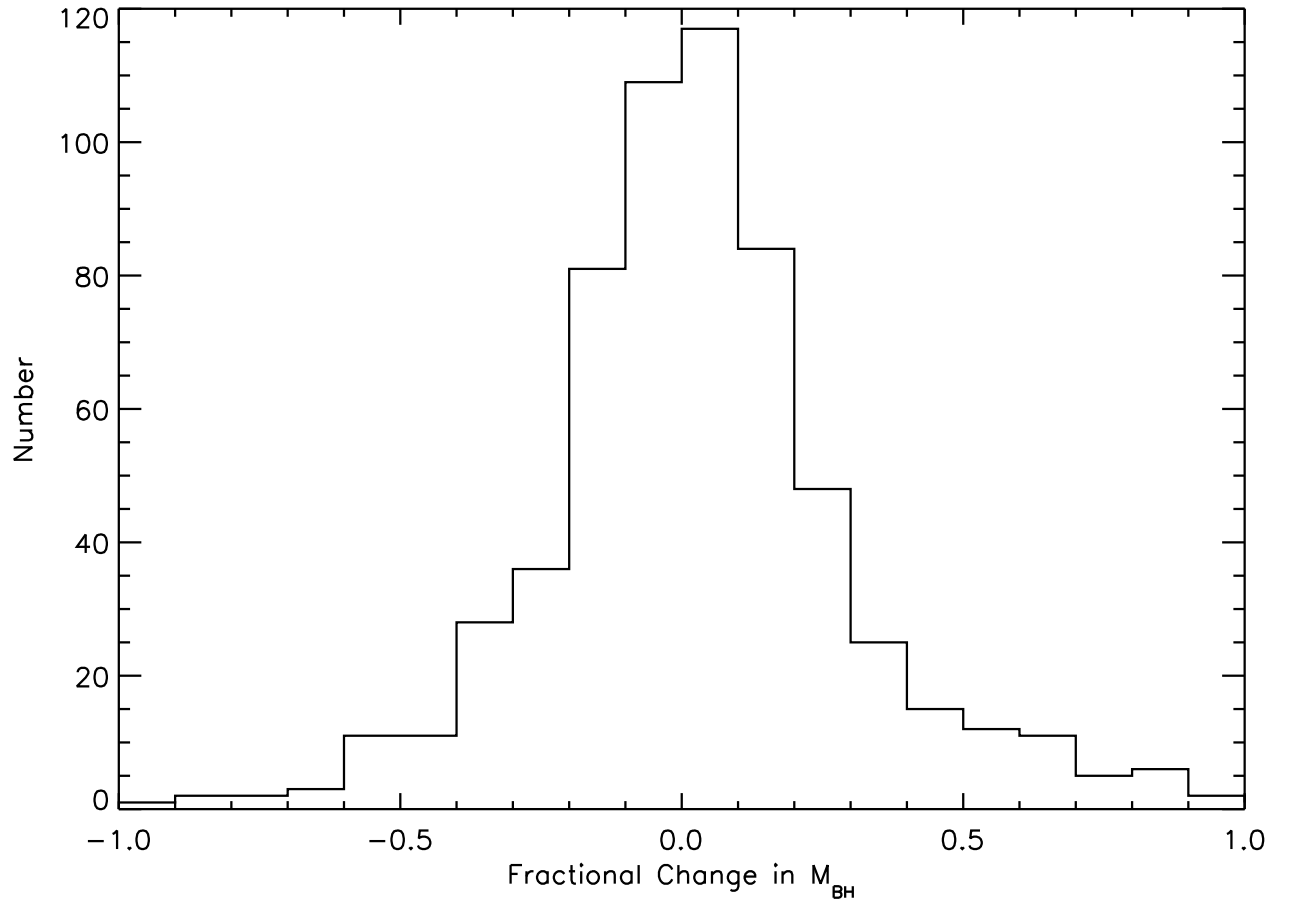


Fig. 13.— Fractional change in estimated black hole mass. The standard deviation of the sample is 0.301.

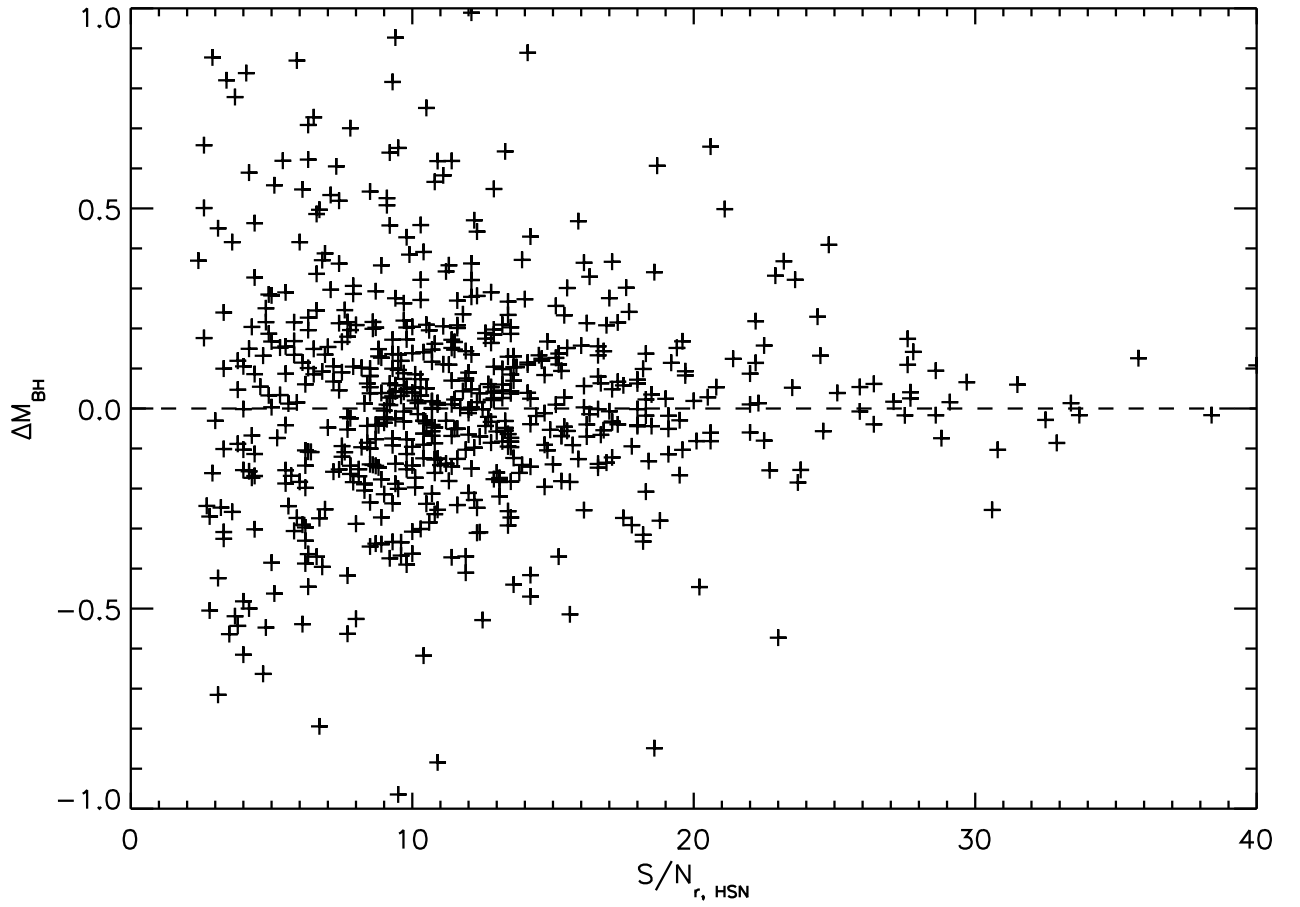


Fig. 14.— Fractional change in estimated black hole mass as a function of  $r$ -band signal-to-noise ratio at the high-S/N epoch. The dashed line indicates zero change in  $M_{\text{BH}}$  between epochs.

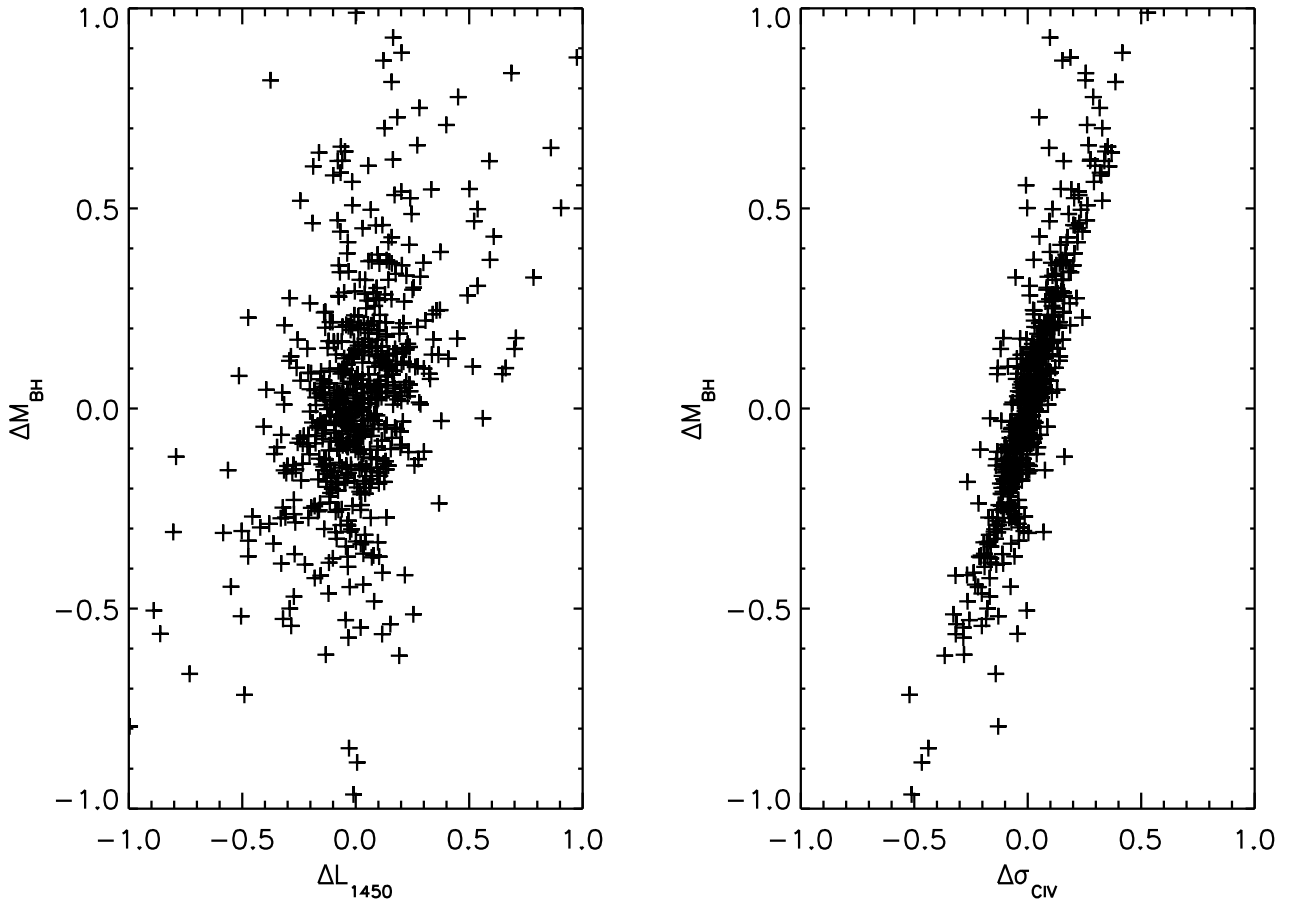


Fig. 15.— (Left) Fractional change in estimated black hole mass as a function of the fractional change in 1450Å luminosity. (Right) Fractional change in estimated black hole mass as a function of the fractional change in the C IV line dispersion.